Understanding the Characteristics of Cut-off Lows over the Western Cape, South Africa

Sabina Abba Omar

Thesis Presented for the Degree of

DOCTOR OF PHILOSOPHY

In the Department of Environmental and Geographical Science

University of Cape Town

Supervisor: Assoc. Prof. Babatunde J. Abiodun

Declaration I

I hereby declare that all the work in this thesis is mine and that information derived from other studies have been properly acknowledged and referenced in an included reference list. I understand the meaning of plagiarism and know that it is wrong.

Signed by candidate

Sabina Abba Omar

Declaration II

Parts of this thesis has been submitted and are under review for publication in the following papers:

- Abba Omar, S. and Abiodun, B.J., 2019a Characteristics of cut-off lows during the 2015–2017 drought in the Western Cape, South Africa. Under Review - *Atmospheric Research.*
- Abba Omar, S. and Abiodun, B.J., 2019b Simulating the characteristics of cut-off low rainfall over the Western Cape using WRF and MPAS models. Under Review - *Climate Dynamics.*
- Abba Omar, S. and Abiodun, B.J., 2019c. Simulating the Influence of Topography on Cut-off Lows over Southern Africa. Submitted - *International Journal of Climatology*.

Abstract

Cut-off lows (COLs) are an important rainfall source in the Western Cape. While several studies have examined the devastating impacts of COLs during extreme rainfall events, little is known about the characteristics of COLs during droughts and how the characteristics are influenced by the South African complex topography. This thesis investigates the interannual variability of COLs and COL precipitation over Western Cape, with a focus on the 2015 - 2017 drought that affected the region and examines how well climate models simulate the variability. It also studies how the complex topography of South Africa influences the COLs characteristics. Four types of datasets (observation, satellite, reanalysis, and simulation) were analysed for the thesis. The observation, satellite and reanalysis data were analysed from the period 1979-2017, while two simulations were performed using a regional climate model (called WRF) and a variable grid model (called MPAS) for the period 2007-2017. A COL tracking algorithm was used to extract all the COLs that occurred in the vicinity of the Western Cape during the study periods. The Self Organising Map (SOM) was used to classify the COLs into groups based on their precipitation patterns. The upper-air data was analysed to study the characteristics of the COLs in each group. To examine the role of topography on COLs, WRF was applied to simulate three COLs over real and three idealised terrains (i.e. “no topography”, “only-west-topography” and “only east topography”).

The results show that, on average, the Western Cape experiences 10 COLs per year and the COLs contribute about 11% of the annual precipitation over the province, although with a large interannual variability. In 2015 and 2016, the COLs occurred more frequently than normal, with more than normal precipitation contribution, thereby reducing the drought severity in the two years. Contrarily, in 2017, the COL frequency and precipitation contribution were less than normal, because COLs were mainly seen further south. Nevertheless, we found that an increase in annual COL frequency does not always lead to an increase in the annual COL precipitation, because the COLs produce different amounts of precipitation. More than 45% of the COLs over the Western Cape produces little or no precipitation. The SOM results reveal that the spatial distribution of COL

precipitation can be grouped into four major patterns. The first pattern indicates precipitation over the entire Western Cape while the second shows little or no precipitation; the third and fourth patterns feature precipitation over south-east coast and south-west coast, respectively. The major difference between the first pattern (i.e. wet cols) and the second pattern (dry COLs) is that while the wet COL is associated with a southward transport of warm and moist tropical air towards the Western Cape, the dry COL is not. Hence, the contrast between the warm and cold air mass is weaker in dry COLs than in its wet counterpart.

The models (WRF and MPAS) capture the seasonal and annual climatologies of COLs and their precipitation. However, they do not always capture the inter-annual variability, with WRF outperforming MPAS in general and during the drought period. Both models represented all the COL precipitation patterns well but under-estimated the frequency of dry COLs throughout the seasons. However, the models were able to simulate the general observed differences between dry and wet COLs. WRF simulation shows that topography influences the precipitation, track, formation and vertical structure of COLs. Topography provides the additional forcing needed for COL formation. The results of this study may be applied to improve monitoring and prediction of extreme rainfall events over the Western Cape.

Acknowledgements

Firstly, I would like to thank my supervisor, A/Prof. Babatunde Abiodun for all his support, encouragement, patience and giving of knowledge. I am truly grateful for all his guidance and help during the thesis. He has taught me so much.

This research was possible through the financial support of the National Research Fund (NRF) and the University of Cape Town (UCT). I would also like to acknowledge the Climate Systems Analysis Group (CSAG) for the computing resources, as well as the Centre for High Performance Computing (CHPC). I also need to acknowledge the various institutes which I was able to gain access to data for this research. For his technical support, patience and unrelenting willingness to help, I would like to thank Phillip Mukwenha.

I would like to thank my colleagues and friends at UCT. A special thanks to the Atmospheric Science peer-review group for reading, analysing, debating our work together - it was both collegiate and helpful. To Stefaan, Teboho, Nadia, Koketso, Temitope, Mariam, Myra, Tich, Linda - thanks for all the laughs, the support and interesting discussions. To my friends outside of UCT thanks for being understanding and for good times along the way.

Lastly, a real big thank you to my family. Some special thanks to my father, Mahomed Saleh Abba Omar, and Inga Niehaus for all the love, support and encouragement. To my uncle, Stef Raubenheimer for believing in me. Most importantly to my homestead for truly being there for me. To Noel Carr - for always being there, to my brother - Thomas Carr for being the fizz to my pop and to my mom, Therese Raubenheimer, for being my rock and for your unconditional love.

Table of Contents

List of Figures

List of Tables

List of Abbreviations

AORP	All over rainfall pattern
ARA	All-year rainfall area
CFSR	Climate Forecast System Reanalysis
CHIRPS	Climate Hazards Group InfraRed Precipitation with Station
COL	Cut-Off Low
COLs	Cut-Off Lows
CONTROL	Simulation experiments with real topography
CPC	Climate Prediction Center
CRU	Climatic Research Unit
DJF	December-January-February
ETOPO	Simulation experiments with east topography only
GCMs	Global climate models
GDAS	Global Data Assimilation System
GDP	Gross domestic product
GFS	Global Forecasting System
ITCZ	Intertropical convergence zone
JJA	June–July–August
MAM	March–April–May
MPAS	Model for Prediction across Scales
MSE	Moist static energy
NCAR	National Centre for Atmospheric Research
NORP	No rainfall pattern
NoTOPO	Simulation experiments with no topography
PFJ	Polar front jet
RCM	Regional climate model
RMSE	Root Mean Square Error
RRTMG	Rapid Radiative Transfer Model–GCM applications
SALLJ	South American Low Level Jet
SAO	Semi-annual oscillation

SAWS	South African Weather Service
SERP	South east coast rainfall pattern
SOM	Self-Organising Map
SON	September–October–November
SRA	Summer rainfall area
SST	Sea surface temperature
TTT	Tropical temperate troughs
VGCM	Variable (or stretched) grid GCM
WCP	Western Cape Province
WCRP	West coast rainfall pattern
WRA	Winter rainfall area
WRF	Weather Research and Forecasting
WSM3	WRF Single-moment 3-class microphysics scheme
WSM6	WRF Single-moment 6-class microphysics scheme
WTOPO	Simulation experiments with east topography only
YSU	Yonsei University

Chapter 1 : Introduction

1.1 What are Cut-off Lows?

A Cut-off low (COL) is a closed, cold-cored low in the upper troposphere. These systems start as troughs in the upper atmosphere Rossby wave. The troughs become unstable, extend equatorward and therefore, become cut-off from the wave. Their life-cycle can be generally described by four stages as depicted in Fig. 1.1. The first stage starts with a high-amplitude upper level trough which advects colder, polar air equatorward (Nieto et al., 2005). The trough becomes unstable as the wave increases in amplitude and sometimes decreases in wavelength. During the second stage, the tear-off stage, the trough's instability increases and it begins to become separated from the wave, along with the cold air being advected with it (Porcù et al., 2007). Once the tear-off stage is completed, a closed low-pressure system with a pool of cold, polar air is formed and this is the stage called the cut-off stage.

At this point the system can be identified as a closed low within geopotential height and temperature fields between the 200hPa - 500hPa pressure level. Depending on the system, the low may extend to the surface, however some COLs are shallower than others (Porcù, et al. 2007) and some may even have an anticyclone at the surface. Strictly speaking at this stage the system is completely cut-off from the meridional flow, although this isn't always entirely true. However, because of this separation from the general flow, COLs tracks can often be erratic and difficult to predict (Nieto et al., 2008), as their motion, unlike mid-latitude cyclones, is no longer driven by the jet-stream. To add to this, since they are no longer influenced by the general flow, COLs can remain quasi-stationary over an area for several days thus giving them the capacity to considerably influence the weather over that area (Gimeno et al., 2007).

The last stage in a COL's lifecycle is the final stage or the dissipation stage. This stage is dependent on the surface conditions and convection. Since COLs are colder than the surrounding environment they lead to unstable conditions, which, depending on the surface conditions, can lead to considerable convection. Thus, COLs have the potential to cause severe precipitation events. However, the precipitation is often dependent on the moisture availability and temperature of the surface, as different surface conditions may permit or inhibit convection. This adds to the challenges that come with COL prediction. When instability occurs, convection and release of latent heat (due to precipitation) results in the decay of the COL as the cold-core can no longer be maintained. This is especially effective over warmer surfaces whereas colder surfaces help to prolong the lifespan of COLs and thus COLs over colder surfaces will be maintained until they become subsumed into a westerly trough or they track over a warmer surface (Nieto et al., 2008). Therefore, COLs are weather systems that are dependent both on the westerly flow in the upper-mid troposphere as well as the conditions at the surface. Once they become disconnected from the westerlies, their tracks become less predictable and the amount of precipitation they produce and their lifespan is dependent on the surface conditions. Under the right conditions they can produce substantial precipitation.

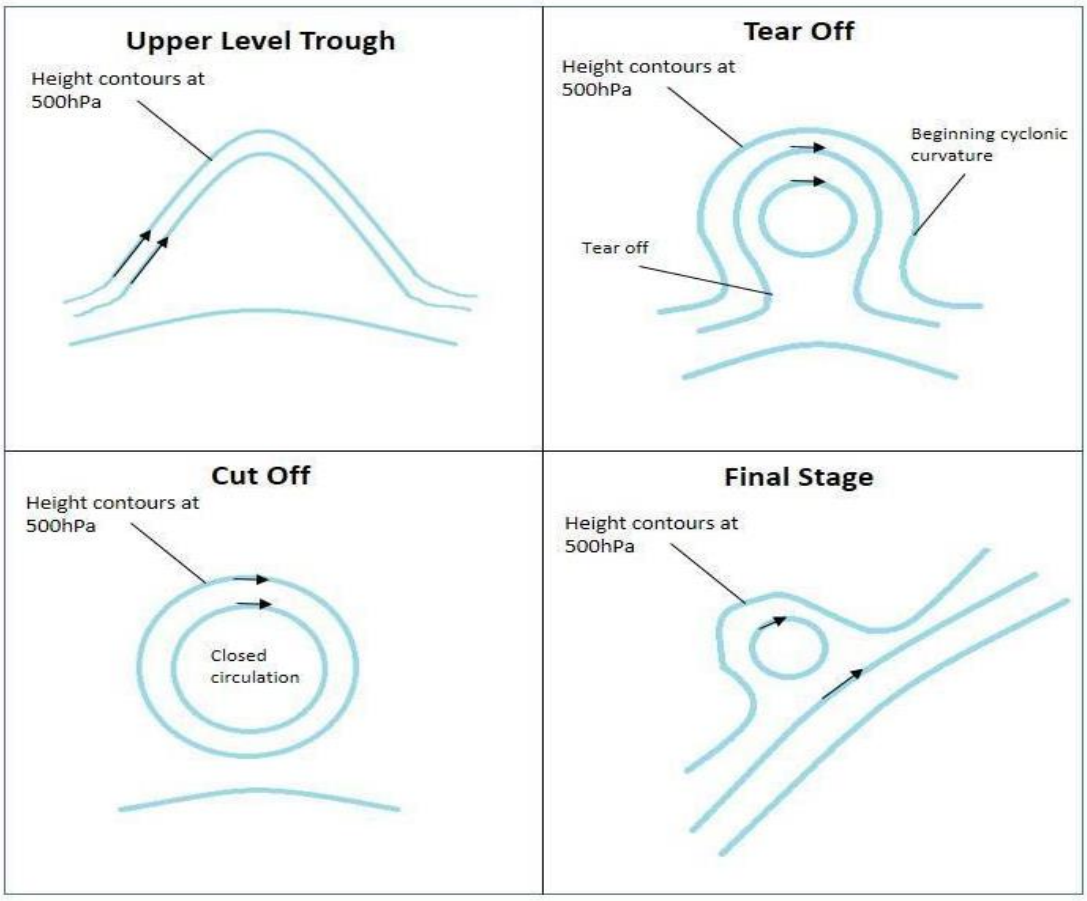

Figure 1.1: An idealized diagram showing the typical stages of a cut-off low in the southern hemisphere. Adapted from Nieto et al (2005)

1.2 South African Climate

1.2.1 South Africa's Geographic Position and Topography

South Africa is situated at the southern tip of Africa. Owing to its position, South Africa is influenced by tropical, subtropical, and mid-latitude weather systems. The country is also influenced by the Indian Ocean to the east and the Atlantic Ocean to the west, along with two ocean currents that play a major role in South African climate. The warm Agulhas current flows along the east and south coast of South Africa, and in contrast, the cold Benguela current flows along the west coast. This sea surface temperature (SST)

difference helps to set up a precipitation gradient across the country, with drier conditions over the west of the country and wetter conditions to the east. South Africa's topography adds another layer of complexity to the country's climate which not only sets up spatial gradients in precipitation and temperature, but also sets up areas which exhibit different intra-annual signals. South Africa's topography consists of steep escarpments along the east, south and west coasts. These escarpments make up the slopes of the central plateau which sits over the interior of most of South Africa. The central plateau slopes gently, with higher elevations over the eastern parts and lower in the west and northern parts. The Drakensberg Mountains make up part of the eastern escarpment and some of their highest peaks rise up beyond 3000m. The Cape Fold Mountain Belt consists of the well-known mountains that lie along the south and west coast of South Africa, and along with the western and southern escarpment affect the climate of the region. The topography also generally leads to a west-east as well as a north-south gradient in precipitation over South Africa (Pohl et al., 2014).

1.2.2 The Weather Systems that Influence South Africa

Several weather systems contribute to precipitation over South Africa. As indicated earlier, due to South Africa's geographical position, the country is influenced by tropical, sub-tropical, and mid-latitude systems. During summer, the Intertropical Convergence Zone (ITCZ) shifts southwards, along with easterly waves and lows that bring summer precipitation to most parts of South Africa. With the shift of the ITCZ, the semi-permanent sub-tropical systems, which include the Atlantic and Indian anticyclones, are also shifted further south, allowing for rainy conditions to dominate most of the country. During winter, the ITCZ shifts further north and the sub-tropical highs move over the country, leading to dry conditions over parts of the country. However, along with this shift, the jet stream and westerly waves are shifted northward, bringing with them mid-latitude cyclones and cold fronts. As discussed previously, these also bring COLs, but COLs are less dependent on the position of the jet. The northward shift of the jet shifts the tracks of these cold fronts, which allows for these systems to track along the south-west and south coasts of South Africa. The fronts bring precipitation over the escarpment areas and sometimes further

inland through organised squall lines (Tyson and Preston-Whyte, 2000), bringing winter precipitation to these regions. During the shoulder seasons, precipitation is mostly caused by the transport of warm moist air from the Agulhas current over the escarpment. This produces precipitation, mostly over the eastern and south coast regions, during the summer and shoulder seasons (Engelbrecht and Landman, 2016). The combination of the different weather systems, the topography and the country's geographic position lead to regions of different rainfall regimes. The summer rainfall region is dominated by tropical and sub-tropical systems, the winter rainfall region is mainly influenced by weather systems brought by the westerlies, and the all-year round rainfall region which is influenced by both.

1.2.3 Western Cape and it's Precipitation

The Western Cape is the only part of South Africa that receives most of its precipitation during winter (Mahlalela et al., 2018). On average it receives its highest precipitation during the winter months of June-July-August (JJA). However, the precipitation signal is a bit more complicated as the province can actually be divided into three different rainfall regions. Fig. 1.2 shows these different rainfall regimes, the winter rainfall region is situated over the western parts of the province, where precipitation varies from less than 200 mm in the north to over 1000 mm per year over the mountainous regions (Mahlalela et al. 2018). The all-year rainfall region occurs along the south coast and sees similar precipitation amounts throughout the year, with yearly precipitation totals ranging from 400 to above 100 mm. The north-east part of the province is called the late summer rainfall region, where precipitation falls mainly during January-February. This area receives less precipitation than the other regions, i.e. between 200 and 400 mm per year (Mahlalela et al., 2018).

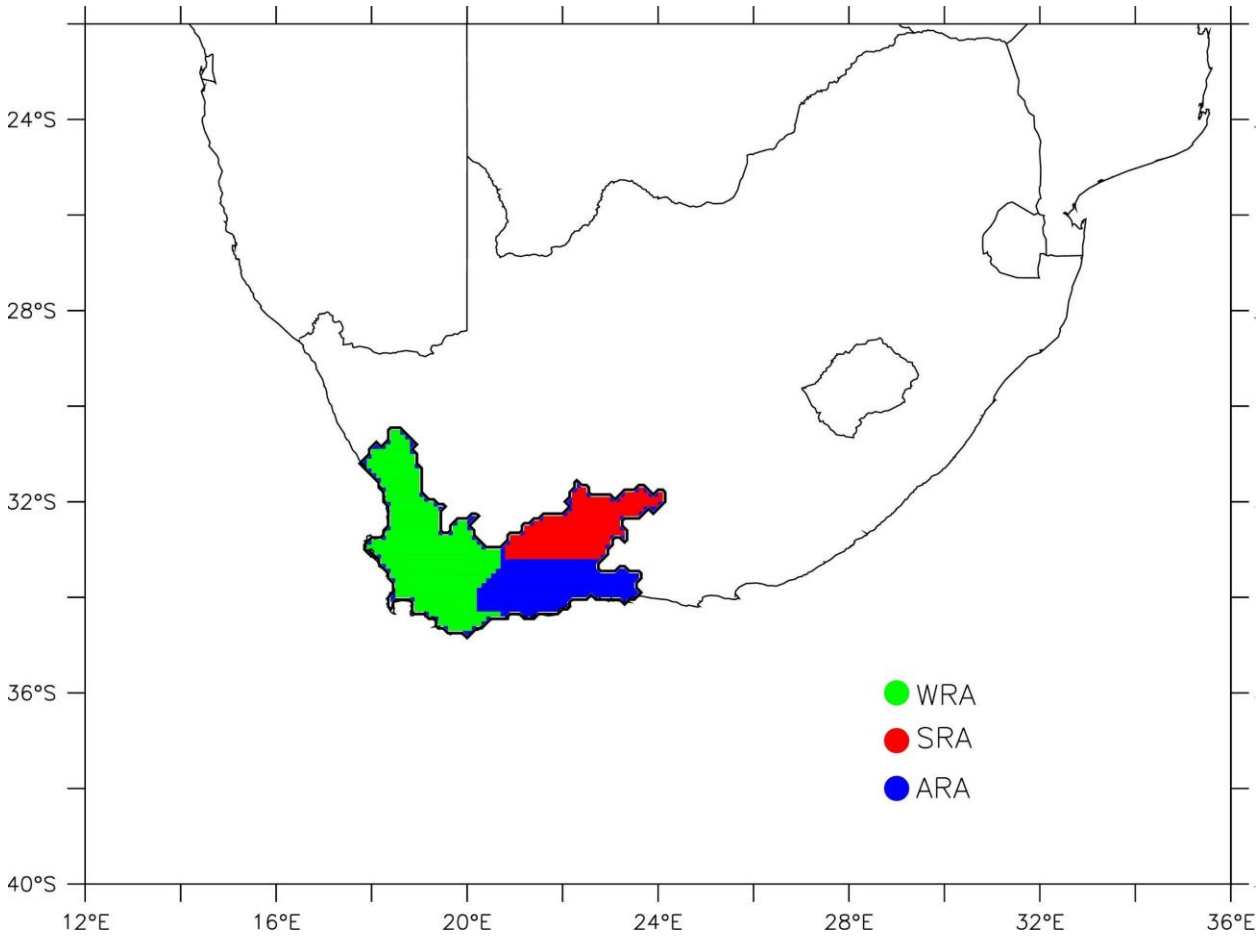

Figure 1.2: A map of South Africa with the Western Cape highlighted. The Western Cape rainfall regions are designated as WRA (i.e. the winter rainfall region), ARA (i.e. the all year rainfall region) and SRA (i.e. the late summer rainfall region).

1.2.4 Factors Influencing Western Cape Precipitation

Most of the south coast is influenced by both mid-latitude and tropical weather systems (Engelbrecht et al., 2015). The mid-latitude systems that affect the area are cold fronts, ridging highs, and COLs, and the tropical influence is generally from Tropical Temperate Troughs (TTT) (Engelbrecht et al., 2015). The warm Agulhas current allows for moisture to be brought into the region and it is one of the reasons why ridging highs lead to precipitation over the region (Taljaard, 1985). Since this area is influenced both by the winter precipitation-bearing mid-latitude systems, the summer tropical systems and ridging highs, it receives precipitation all year round and thus the south coast designated as the All-year Rainfall Area (ARA). Unlike the south coast, the north-eastern region of the Western Cape is dominated by summer precipitation systems and forms the Summer

Rainfall Area (SRA). This is because the Cape Fold Mountain belt acts as a barrier to the penetration of moisture from the Agulhas current (Du Plessis and Schloms, 2017) and of cold fronts into the SRA.

The Winter Rainfall Area (WRA) dominates the overall precipitation signal of the province, but it is actually confined to the western parts of the region (Mahlalela et al., 2018), where the main precipitation influences are mid-latitude weather systems i.e. cold fronts and associated mid-latitude cyclones and COLs (Lennard and Hegerl, 2015; Otto et al., 2018; Weber et al., 2018). Atmospheric rivers are also important to winter precipitation as they transport moisture into the region and therefore fuel cold fronts. Extreme precipitation days over the winter rainfall region are often associated with atmospheric rivers (Blamey et al., 2018). The main moisture sources for atmospheric rivers seem to be from the south east Atlantic Ocean and South America (Ramos et al., 2019). There is a link between the phase of the South American Low Level Jet (SALLJ) and moisture transport to Southern Africa. During what is called the no Chaco jet event the winds do not deviate as far south and thus are able to transport moisture zonally (Ramos et al., 2019). The continental areas north of Southern Africa are also a moisture source for Western Cape winter rainfall. However, the mechanism behind this transport is still not clear (Ramos et al., 2019).

1.3 Impacts of COLs

Cut-off lows (COLs) are known for intense rainfall. COLs form due to unstable Rossby waves (Porcù et al., 2007; Favre et al., 2012), where troughs in the Rossby wave extend equatorward and become cut-off (Campetella and Possia, 2007; Favre et al., 2013). The air within the COL is thus colder than the surrounding atmosphere. This produces an unstable atmosphere which leads to deep convection and can cause extreme precipitation (Singleton and Reason, 2007b). Cut-off lows have been reported to cause floods and disaster events in different parts of the world (Porcù et al., 2007; Hu et al., 2010; Stucki et al., 2012; Abatzoglou, 2016).

COLs have been known to cause floods over mid-latitude and sub-tropical regions in both the northern and southern hemispheres. For example, COLs bring extreme precipitation to the Mediterranean region (Porcù et al., 2007), United States (Abatzoglou, 2016), north-east China (Hu et al., 2010), South America (Godoy et al., 2011), Australia (McInnes and Hubbert, 2001), and Southern Africa (Singleton and Reason, 2007b). In 2008 a COL led to extreme precipitation over Lisbon, Portugal (Fragoso et al., 2010). The event was the heaviest precipitation event on record and led to flash-flooding, land-slides, displacement of people, and even loss of lives. In Hiroshima, Japan, on the 19 August 2014, a COL resulted in extreme precipitation of 100 $mm.hour^{-1}$ which led to flash flooding, the destruction of 330 houses and 75 deaths (Hirota et al., 2016). Heavy rain, hurricane force winds, and sea swell from a COL event on the 7-9 June 2007 in Australia, led to one of the most expensive natural disasters in the country's history (Dowdy et al., 2011). These examples indicate the destructive impact these systems can have across the world.

South Africa is no exception, as COLs have led to some major natural disasters over the country. One of the most famous of these was the Laingsburg flood which led to the loss of 104 lives (Estie, 1981). Another COL event in 1987, in KwaZulu Natal, led to severe flooding with precipitation amounts exceeding 900 mm in three days (Singleton and Reason, 2007a). While in August 2002, a COL event led to flooding in East London resulting in R2 million in damages, 14 deaths, and 3000 people left homeless (Singleton and Reason, 2007b; E DeJager 2013, personal communication, 13 December). The Western Cape Province of South Africa seems particularly vulnerable to COLs, as more than half (7 out of 12) of the flooding events in the province, during 2003-2008, were caused by these weather systems (Holloway et al., 2010). Here are some examples of the damages caused by COL events in the Western Cape:

1. In 2003 a COL led to floods over the Western Cape, which cost the province R212.4 million in damages, required the evacuation of 200 people and led to the loss of three lives (Holloway et al., 2010; Pharoah et al., 2016).

2. In 2006 heavy floods from two COLs cost the province R600 million in damages, the displacement of 1600 people and five deaths (Pharoah et al., 2016).

3. Heavy precipitation from a COL in November 2013 affected 19000 people living in low-cost housing and informal settlements. To add to this, 121 patients had to be evacuated from a clinic and the overall damage totaled R167 million (Pharoah et al., 2016).

4. In January 2014 a strong COL, seen in Fig. 1.3, led to a flood and 33 people had to be rescued by helicopter. The flood also led to 4 fatalities and over R450 million in damages (Pharoah et al., 2016).

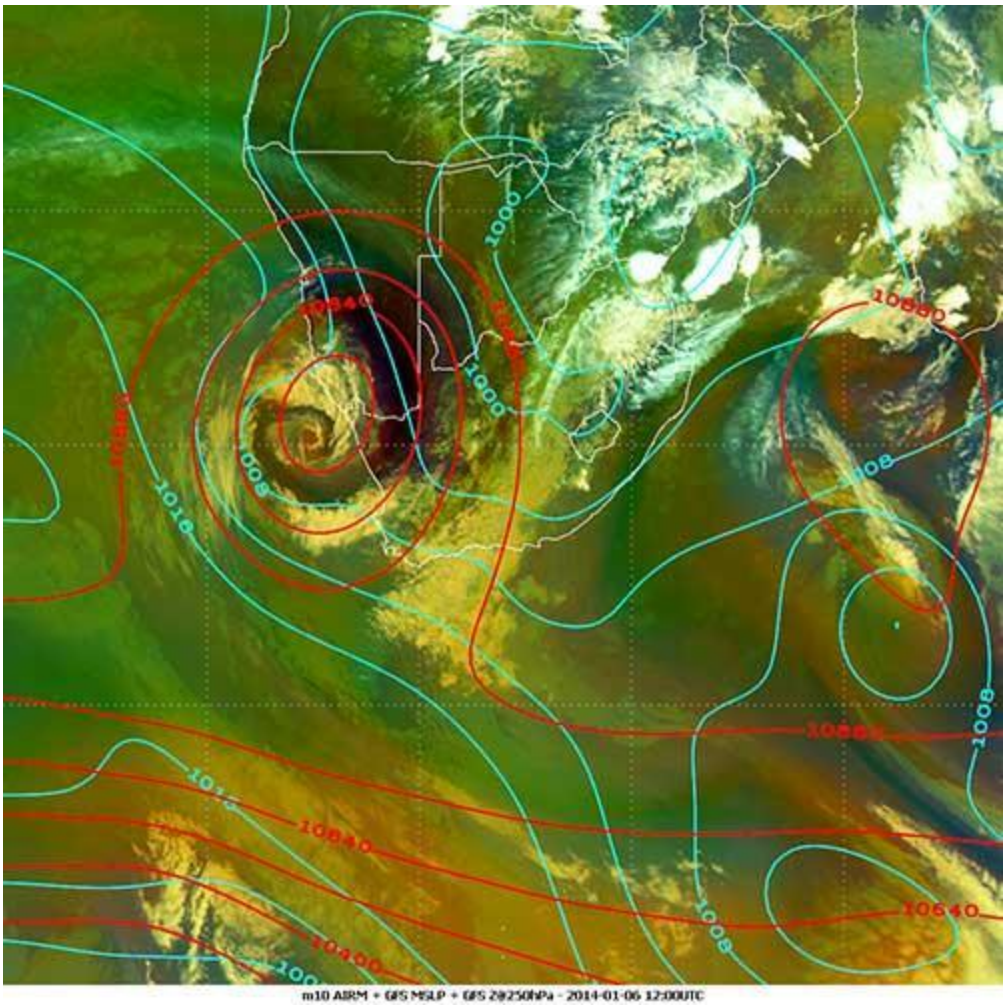

Figure 1.3: Airmass RGB overlaid with GFS analyses of geopotential height at 250hPa and mean sea level pressure during a COL event on the 9 January 2014 (source: Eumetsat, 2014).

1.4 The Western Cape Drought

Droughts can exert a heavy toll on the socio-economic activities of any community, especially in the Western Cape, where human resilience to climate extremes is very low (Nath and Behera, 2011). In 2015–2017, a severe drought reduced water availability in the Western Cape (South Africa), placing enormous stress on the community. During this period, the annual precipitation over the province decreased by more than 50% of the normal levels (consecutively over the three years). In 2017, the levels of the dams, which provide water for all activities in the province, dropped to 32% (with the last 10% of dam water being unusable). This led to the most severe drought since 1904 (Otto et al., 2018) and the worst water shortage in the province in the last 113 years (Botai et al., 2017). As

a result, severe water restrictions were imposed, limiting each resident to 50 litres per day. The Western Cape drought was declared a national disaster (Visser, 2018) and the economic impact was enormous. For example, between 28,000 and 35,000 agricultural jobs were lost (Pienaar and Boonzaaier, 2018), water-reliant businesses (such as nurseries, car washes, and construction companies) were closed down, and many hospitality industries were unable to provide enough water for their clients, as they were running on minimum water capacity. There is concern that with ongoing global warming this type of drought may become more frequent in the future. This may have devastating impacts on South Africa's economy, because the Western Cape provides 14% of South Africa's gross domestic product (GDP) and it is home to the City of Cape Town, Africa's most popular tourist destination, with approximately 3.7 million inhabitants (StatsSA, 2011). Hence, for better drought management and effective planning in the future, there is a need to understand how different precipitation bearing systems over the Western Cape changed during the period.

1.5 Motivation of Study

While COLs bring destructive extreme events, they are also important water sources. For example, a COL event over North-west Africa, while causing heavy precipitation, also filled the reservoirs providing better irrigation (Knippertz and Martin, 2007). In Australia, COLs play an important role when the southern annular mode is in its positive phase. During the positive phase precipitation decreases due to storm tracks occurring further south, however COLs, which are more frequent during this phase, make up for some of this loss in precipitation. Heavy precipitation from COLs are also known to mask the drying caused by El Niño years over Australia. Thus, in the context of the recent Western Cape drought, COLs could have provided some much-needed relief. While other precipitation-bearing systems have been examined in relation to the drought (Sousa et al., 2018), COLs have not.

Despite the economic damage COLs can cause and their importance as a precipitation source little is known about the contribution of COLs to the Western Cape's precipitation. There is a dearth of information on why COLs produce certain precipitation patterns and

amounts. In other words, why do some COLs produce heavy precipitation while others produce little or no precipitation? Since the Western Cape's precipitation is known for its high precipitation variability it is important to understand better how COL precipitation contributes to this region. To add to this, according to Pharoah et al. (2016) there is an identifiable increase in the frequency of COL-induced extreme precipitation days and that flood events associated with COLs occur almost annually in the Western Cape. Therefore, understanding the characteristics of COLs over the Western Cape is important to aid better planning of both extreme precipitation events and droughts.

However, the skill and accuracy of COL precipitation forecasts over the Western Cape are still very low (Pharoah et al., 2016). To minimise COL-related disasters in the Western Cape, there is a need for more studies on how to improve the prediction of COL precipitation over the province. With an increase in the frequency of drought and extreme precipitation events over the Western Cape, accurately representing COL precipitation in climate models is essential to further understand and predict Western Cape precipitation. However, little is known about how well models are able to capture the characteristics of COLs over this area. To add to this, one of the issues with simulating or forecasting COLs and their precipitation accurately is due to complicated relationships with the terrain below (Nieto et al., 2008). Therefore, exploring how topography influences COLs and their precipitation over the Western Cape could improve understanding and prediction of these systems.

To understand these systems we would like to test certain hypotheses. Firstly, that COLs are important to Western Cape precipitation and that different precipitation patterns are associated with different COL dynamics. Secondly, the drought over the Western Cape presumably meant less COL precipitation over the area too - or was this not necessarily the case? And lastly that topography plays a major role in influencing the formation, track, precipitation and dynamics of COLs over the Western Cape.

1.6 Aim and Objectives

The aim of this study is to examine the characteristics of Cut-off lows and of the associated precipitation pattern over the complex terrain of the Western Cape and investigate the capability of climate models to simulate them. To achieve this aim the following objectives are addressed:

- Investigate the interannual variability of COLs and COL precipitation over the Western Cape and understand whether COL occurrence and precipitation changed during the 2015-2017 drought.
- Identify the different precipitation patterns of COLs over the Western Cape and explore their dynamics.
- Explore how well a variable resolution (or stretched grid) Global Climate Model (VGCM) and Regional Climate Model (RCM) can simulate the variability of COLs and COL precipitation, whether they are able to capture the drought signal as well as the different precipitation patterns and their dynamics.
- Examine the role topography plays in COLs in terms of formation, track, precipitation and dynamics by doing model sensitivity experiments on case studies of COLs over South Africa using different topographic configurations.

These aims and objectives inform the following three hypotheses of the study.

Hypothesis 1: Changes in characteristics of COLs (i.e. tracks frequency and the associated precipitation) over the Western Cape contributes to the 2015-2017 drought in the province.

Hypothesis 2: The characteristics of COLs over the Western Cape can be reproduced by the Weather Research and Forecasting (WRF) and the Model Prediction across Scales (MPAS) models.

Hypothesis 3: The characteristics of COLs over South Africa is influenced by the complex topography of southern Africa.

1.7 Thesis Outline

This work is organised into seven chapters; the present chapter introduces COLs and the different precipitation systems that affect the Western Cape, explains why COLs are important to study over this region, and motivates why a focus on the Western Cape 2015-2017 drought is important.

Chapter 2 provides an overview of the different ways of identifying COLs. The chapter also discusses what other studies have found about COLs and their precipitation over South Africa and the Western Cape. What is known about the Western Cape drought is explored and previous studies about COL behaviour during drought is drawn upon. The Chapter also goes on to examine what is known about the effects of topography on COLs over other regions as well as in South Africa.

Chapter 3 describes the datasets used in the study and model set-ups. It outlines how the COLs were identified and tracked for this work, explains how COL precipitation is characterised and describes how the role of topography is examined.

Chapter 4 reports the characteristics of COLs over the Western Cape. It describes the spatial and temporal characteristics of their occurrence and associated precipitation. The chapter also explores whether these signals changed during the 2015-2017 drought. The chapter identifies the main precipitation patterns associated with COLs over the Western Cape, explores the dynamics associated with these patterns, and further examines the main differences between the wettest precipitation pattern and the driest precipitation pattern.

Chapter 5 explores whether the climate models are able to capture the COL characteristics identified in chapter 4 and whether they were able to simulate the nature of these characteristics during the 2015-2017 drought. It also examines whether the models simulate the same precipitation patterns associated with COLs and if the models are able to capture the differences, identified in chapter 4, between dry and wet COLs.

Chapter 6 presents the results of the topography sensitivity experiments and describes how different parts of the South African topography may influence the formation, track, and precipitation of the COLs examined. It also examines how topography influences the vertical structure of a chosen COL.

Chapter 7 outlines and summarises the findings of this study. The chapter also points out the shortcomings of this study and provides suggestions to improve the work.

Chapter 2 : Literature Review

This chapter provides a comprehensive review of COL studies. It starts by reviewing the differences in the definition of COLs in the literature and how the differences influence the COL identifications in the studies. Then, it reviews previous studies on characteristics of COLs and the associated precipitation over the Western Cape. It also summarises findings of previous studies on COL simulations and the influence of topography on COL characteristics over South Africa.

2.1 Definition and Identification of Cut-off Lows

COLs are often defined or called using different names in the literature. This usually causes confusion in terms of providing good definitions of these systems. The first reference to these systems seems to have been by Koppen (1886) in which the author referred to them as cold air pools (Llasat and Puigcerver, 1989). The authors defined cold air pools as marked depressions in the mid-upper troposphere with cold centers. However, this term became used too commonly for many different upper level cold core lows (Llasat et al., 2007) and thus the term cut-off low was born to indicate that they were systems that had been separated from their original air mass through the strangulation of troughs in the westerly wave (Palmén, 1949; Llasat et al., 2007).

Despite the refining of the system's name there are several ways in which COLs have been identified. Some studies have used subjective approaches to identify COLs. Both Price and Vaughan (1993) and Kentarchos and Davies (1998) manually inspected geopotential height and wind vectors at the 200hPa level and defined a COL as a system which exhibited a closed geopotential height contour or closed circulation. However, subjective identification of COLs is labor intensive and often not plausible for analyses longer than a couple of years. Therefore, studies have also made use of objective algorithms to identify COLs. Some studies have used algorithms that identify COLs from

geopotential height and temperature minima on a specific pressure level (Singleton and Reason, 2007b; Favre et al., 2012; Engelbrecht et al., 2013). Other studies use potential vorticity data (Pinheiro et al., 2017) and still others use several variables based on a conceptual model of a COL (Reboita et al., 2010; Ndarana and Waugh, 2010). Nieto et al. (2008) compared two different COL climatologies using different identification techniques. The one technique used different variables based on a conceptual model of COL which was used previously by Nieto et al. (2005), and the second technique used PV values to identify COLs on different isentropes. Nieto et al. (2008) concluded that the results from each method agreed well but that bigger differences are seen when different atmospheric levels are used.

Pinheiro et al (2019) also compared different methods, the authors compared single and multiple variable schemes. Looking at just geopotential height and relative vorticity anomalies they found that the relative vorticity method picked up more COL tracks than using geopotential height especially for lower latitude regions and summer COLs, more early stage developing COLs were identified. However, when the cut-off criterion was put in place the two methods showed more similar values and also showed similar seasonal and intensity distributions. The authors added variables to the two methods and explored how adding wind, wind and potential vorticity, wind and temperature and finally all three variables influenced the identification of these COLs. The authors concluded that the simpler method, with just adding wind, was able to identify more COLs. This was concluded by manually comparing identified COLs to a visual inspection of the 300hPa geopotential height fields. The authors were not able to explore all methods such as using just temperature alone without wind and also stated that individual regions needed to be explored in more detail and that different levels and datasets will influence the performance of a specific method. This indicates that simpler methods may provide better results but that for specific regions, levels and datasets the method chosen needs to be manually verified.

This issue with different levels was examined by Reboita et al. (2010), who identified COLs using 200hPa, 300hPa and 500hPa geopotential heights and found that using

different levels yielded different results such as seasonal frequency and location. The results motivated Ndarana and Waugh (2010) to explore the differences further. They concluded that COLs are more likely to occur at different levels over the southern hemisphere depending on the season and the strength of the sub-tropical and polar jets. This suggests that, as long as a method is validated correctly, the most important consideration should be the choice of level used in identifying the COLs. Results from Ndarana and Waugh (2010) indicate that over the Western Cape and South Africa 500hPa COLs have higher annual occurrences than at the 250hPa level. However, the present study shall explore this further by testing COLs at both the 300hPa level and 500hPa level as this has not yet been compared over the Western Cape.

2.2 Characteristics of Cut-off lows over South Africa and the Western Cape

Several studies have explored COL characteristics over the Southern hemisphere and have provided some general information on COLs over South Africa (Fuenzalida et al., 2005; Reboita et al., 2010; Pinheiro et al., 2017). All the studies found that preferential areas of COL occurrence are located around the continental regions of South America, Southern Africa and Australia. Pinheiro et al. (2017) analyzed COL track density for 1979-2014 at the 300hPa level over the Southern Hemisphere and found that, in autumn and spring, COLs mostly occur over the south and south west coast of South Africa. During winter this maximum is seen mainly over the south west coast and in summer the track density is comparatively less, and the maximum is seen just off the south coast. Fuenzalida et al. (2005) analyzed the period 1969-1999, also at the 300hPa level, and found similar results except during summer where the area of maximum COL occurrence was over the south west coast and the number of COLs per season was less than that of Pienheiro et al. (2017). The difference in number of COLs per season could be attributed to the change in satellite data after 1979. Reboita et al. (2010) found that pre-1979 COL climatologies showed fewer COLs. The authors compared the period 1950-1978 and 1979-1999 and found that the later period shows more COLs over South Africa than the earlier period. Off the coast of the Western Cape is one of the areas which shows the

largest difference over South Africa, where up to 40 more COLs are seen in the later period. These climatological studies show that there is a preferential region for COLs off the south and west coast of the Western Cape. However, there are some disagreements between the frequency and seasonality of occurrence and very little information on how these COLs over the coasts affect the Western Cape.

While the COL studies over South Africa provide some insights into COL characteristics over the Western Cape, no study looks at COL behaviour specifically over the Western Cape. For instance, studying the contribution of COLs to precipitation over South Africa, Favre et al. (2013) found that COLs, identified at the 500hPa level, contribute less to the precipitation of the south west compared to the south coast and eastern regions of South Africa. The authors' results show that COLs contribute less than 15% to the annual precipitation of the Western Cape region, with some higher percentages seen on the eastern border of the Western Cape. However, their results only show the percentage of seasonal contribution and indicate that some areas of the Western Cape exceed 15% especially during the summer and spring months. These results suggest that the contribution of precipitation by a COL event over the Western Cape is overshadowed by the cold fronts that bring precipitation during the winter season. This study focused on the whole of South Africa and therefore information about what types of tracks of COLs influence Western Cape precipitation, as well as finer details that can only be gauged from a more area-focused study, are not available. This study also used data from 1979-2010 which does not cover the present drought years and therefore it does not provide an idea of whether COLs over the Western Cape were more or less frequent during this drought event.

Singleton and Reason (2007) studied the variability of COL characteristics over Southern Africa for the period 1973-2002. The authors divided Southern Africa into regions and presented seasonal and annual frequency distributions. One of the areas included the Western Cape and south coast regions. This area had the highest frequency of COLs, it showed its highest frequencies occurring during spring and the least during winter. The author also found that the yearly frequencies of COLs suggested a relationship between

semi-annual oscillation (SAO) and wave 3 index. Clearly the Western Cape region has a high frequency of COLs and therefore understanding specifically how these systems influence the Western Cape precipitation and how their occurrences might change is important. Furthermore, the authors identified the COLs at the 300hPa level and as mentioned in section 2.1 this may not be the best choice of level. Engelbrecht et al. (2013) also found a local maximum occurrence of closed lows (which include COLs), at the 500hPa level, off the south west coast, but they also found that this region would experience fewer closed lows in the future (2070-2100). A better understanding of how these lows influence the regional precipitation will help us understand what this could mean for the future. The Western Cape coast is one of the hot spots for COL occurrence, however no study has focused on how COLs influence the Western Cape. Therefore, the present study will improve knowledge on the climatology of COLs lows influencing the Western Cape region, with specific interest in understanding if there are any differences in COLs seen during the region's recent drought.

2.3 COLs and Precipitation

Many studies have investigated COL precipitation from region to region (e.g. Porcù et al. 2007; Hu et al., 2010; Abatzoglou, 2016; Portmann et al., 2018). Since COL precipitation is dependent on many factors such as the terrain, the moisture sources, and the seasonality of the systems, regional studies are necessary in understanding COL precipitation characteristics over a particular area. The previous studies on COL precipitation generally fall into two main types: regional climatological studies and case studies. Regional climatological studies mainly focus on the precipitation statistics, such as seasonality and percentage contribution to that specific region which means that these studies are very specific to that region. For example, Hu et al. (2010) studied the contribution of COL precipitation over Northeast China and Abatzoglou (2016) studied the contribution and correlation of COL precipitation to the overall precipitation in the United States. In a regional climatological study, Porcù et al. (2007) studied the relationships between COL precipitation and vertical structure over the Mediterranean and found that vertical structure was important for precipitation. Their results showed that COLs with a well-developed vertical structure produced more intense precipitation. In a case study,

Portmann et al. (2018) examined the vertical structure of potential vorticity in two COLs and found that under the right baroclinic conditions and low level moisture COLs can produce large-scale ascent similar to that seen in mid-latitude cyclones. Over the Andes, Garreaud and Fuenzalida (2006) found that in a case study of a COL, the Andes helped to maintain the vertical ascent seen within the COL. Along with their climatology study, Hu et al. (2010) also examined three COL case studies and found that the main reason for more rainy COLs was the moisture source from the summer monsoon current. While these case studies provide some information about what is favourable for rain there is still a dearth of information on why COLs produce certain precipitation patterns and amounts. In other words, why do some COLs produce heavy precipitation while others produce little or no precipitation? The present study will improve knowledge in that area.

Few studies have explored COL precipitation over the Western Cape. Singleton and Reason (2007) explored characteristics of COLs over different regions of South Africa, focusing on COL size, duration, location, and frequency but not the associated precipitation. The authors found that generally the region around the Western Cape experiences 4-5 COLs a year. However, how many COLs actually bring precipitation and the type of precipitation they generally bring to the Western Cape is unknown. Favre et al. (2013) studied the contribution of COLs to South African precipitation and found that COLs contribute about 15% to the annual precipitation of the Western Cape, with higher percentages experienced over the eastern part of the province, and during the summer and spring months. However, the study did not explore the different types of precipitation patterns that COLs may bring to the Western Cape and the dynamics of these COLs. Molekwa et al. (2014) examined low, medium, to high precipitation producing COL systems over the Eastern Cape province of South Africa. This area lies to the east of the Western Cape and is generally seen as an all-year rainfall region and therefore is not always the best representation of the winter rainfall dominated province. The authors found that the precipitation type was influenced by the depth of the COL and certain surface conditions. However, they only considered low, medium, and high precipitation as three different precipitation patterns and did not explore the variations in precipitation

patterns within these three categories. Therefore, there is a need for more studies on COL precipitation patterns and the frequency and dynamics of the precipitation patterns.

2.4 The Western Cape Droughts and COLs

Previous studies have investigated the cause of droughts over the Western Cape (e.g. Reason and Rouault, 2005; Sousa et al., 2018; Mahlalela et al., 2018; Otto et al., 2018). Some studies (Sousa et al., 2018; Mahlalela et al., 2018) showed that the 2015-2017 drought, in particular, was caused by a southward shift of the mid-latitude jet and storm tracks that controls the Western Cape precipitation. The southward shift was due to an expansion of the subtropical anticyclones to the mid-latitudes and a southward shift in atmospheric rivers, leading to a decrease in important moisture transport (Sousa et al., 2018). Some studies projected more frequent and more intense droughts over the Western Cape, because global warming would also lead to the expansion of the Hadley cell and a southward shift in storm tracks (Engelbrecht et al., 2009; Abiodun et al., 2018; Naik and Abiodun, 2019). However, Western Cape precipitation is a product of many atmospheric processes. Since the Hadley Cell expansion (or southward shift of the mid-latitude jet) may have different influences on processes, there is a need to study the relative contribution of each process to the Western Cape annual precipitation and understand the factors influencing the contribution.

How these processes influence COLs during the drought over the Western Cape is still unclear. However, studies have shown that changes in jet position can affect the occurrence of COLs (Nieto et al., 2007; Ndarana and Waugh, 2010; Favre et al., 2012). COLs are associated with weaker jets and higher amplitude Rossby waves (Ndarana and Waugh, 2010; Francis and Vavrus, 2012). This process can be explained through wave breaking. Stronger polar and subtropical jets restrict the growth of waves into higher amplitudes which thus reduces wave breaking (Ndarana and Waugh, 2010). Ndarana and Waugh (2010) studied the link between Rossby wave breaking and COLs over the southern hemisphere and found that 89% of COLs over the southern hemisphere are associated with Rossby wave breaking events. Through this lens the seasonal variability in COLs can be explained over the southern hemisphere. Ndarana and Waugh (2010)

found that the sub-tropical jet is less effective at inhibiting COLs at the 250hPa level than the 500hPa level whilst the polar front jet effects 500hPa COLs more than 250hPa level COLs. Sousa et al. (2018) showed that during the 2015-2017 drought the polar front jet was displaced southward which indicates that this would have a positive impact on COL formation. Previous studies have shown that the abundance of precipitation from COLs can provide much-needed relief during droughts. For example, Risbey et al. (2009) found that, during the positive phase of the southern annular mode, there is a decrease in precipitation over southeastern Australia because of the southward shift in storm tracks over the region, but COL precipitation fortunately minimises the impact of such reduction in precipitation. Brown et al. (2009) showed that the heavy precipitation from COL events could mask the drying signal associated with El Niño years over Australia. However, no study has explored whether COLs were in fact more numerous during this drought period or whether there were other signals at play as well. The present study aims to answer this question.

To add to this, little is known about the moisture sources for COLs over the Western Cape. Sousa et al. (2018) found that the southward expansion of the sub-tropical anticyclones weakened the remote moisture sources and atmospheric rivers which led to a southward shift of moisture transport. Therefore, it is unclear whether an increase in COL formation would even have led to more COL precipitation. The present study explores whether COL precipitation was in fact greater than normal during this period as well as what moisture sources are important for COL precipitation over the Western Cape.

2.5 Simulating COLs over South Africa

Most studies on COL simulations over the Western Cape are based on analysis of global climate models (GCMs) or reanalysis datasets (Singleton and Reason, 2007b; Favre et al., 2013). While resolution of the GCM simulations can resolve the spatial structure of COLs, it may not capture the influence of the Western Cape's complex topography (i.e., the mountains, coastlines, and sharp gradients between the warm Agulhas current and the cold Benguela current on COLs (Engelbrecht et al., 2013; Mahlalela et al., 2018). For example, Abiodun et al. (2016) showed that the warm Agulhas current (the width of which

is less than 100 km) plays a crucial role in the precipitation intensity of COLs. However, running GCMs (in climate mode) at a high simulation to resolve the complex topography is too computationally expensive, especially for developing countries. Hence, RCMs and VGCMs offer alternative methods of incorporating the influence of complex topography on simulated COLs. While the capability of RCMs in reproducing the characteristics of COLs have been well documented (Singleton and Reason, 2007a; Abiodun et al., 2016), little is known on how well VGCMs can reproduce them. Engelbrecht et al. (2013) applied a VGCM to study closed lows over Southern Africa, but the study makes no distinction between warm core lows and COLs (which are cold). Maoyi et al. (2018) also applied VGCMs over Southern Africa, but their focus was on simulating tropical cyclones over the south-western Indian Ocean. However, despite the above, there is still a dearth of information on how well climate models, especially RCMs and VGCMs, can simulate the characteristics of COLs and their associated precipitation patterns over the Western Cape. The present study intends to fill this gap, evaluating the capability of two climate models (an RCM and a VGCM) in simulating the characteristics of COLs over the Western Cape.

2.6 The Effects of Topography on COLs

Studies have shown that the formation, track, intensity, and precipitation of COLs are influenced by topography (Boyer and Chen 1988; Fuenzalida et al., 2005; Garreaud and Fuenzalida, 2006; Reboita et al., 2010; Pinheiro et al., 2017). In climatological studies of COLs over the southern hemisphere, Reboita et al. (2010) and Fuenzalida et al. (2005) found a regional maximum in the occurrence of COL over the continental regions of Australia, South America and Africa. This is in contrast with the formation of mid-latitude cyclones which form more evenly across the southern hemisphere (Fuenzalida et al., 2005). This indicates that the terrain of the continental regions influences the formation of COLs. The authors suggest that the reason for this is that the jet streams are stronger over oceanic regions and thus inhibit wave breaking. However, the role of topography in the formation of COLs has not been thoroughly explored. Garreaud and Fuenzalida (2006), performed a case study model sensitivity experiment where topography was removed in the model. The authors found that by removing the topography the formation

of the COL was unaffected. However, a single case study may not be sufficient to conclude this result and this study aims to explore this further.

On the other hand, several studies have shown that the change in intensity and dissipation of COLs can be linked to topography (Boyer and Chen, 1988; Smith et al., 2002; Fuenzalida et al., 2005; Garreaud and Fuenzalida, 2006; Pinheiro et al., 2017). Studying the climatology of COLs at the 500hPa level, Fuenzalida et al. (2005) found regional minima in COLs frequency over the Andes summits, over regions of South Africa's plateau, the southern regions of the Australian Great Divide as well as during some seasons over the New Zealand Alps. Smith et al. (2002) studying COLs over the northern hemisphere at the 500hPa level also found a regional minimum in COL formation over the Rocky Mountains. In a laboratory experiment Boyer and Chen (1988) modeled cut-off low-like systems interacting with model mountains of the northern hemisphere and found that COLs approaching the Rocky and Tibetan mountains were weakened as they passed over the topography and then intensified in the lee of the mountains. This is similar to what Pinheiro et al. (2017) found over the Andes. They found, in a southern hemispheric 300hPa COL climatology study, that COLs during summer and autumn dissipate over the Andes, whereas this is less evident during winter. The authors suggest that COLs decay near the Andes due to the interaction between the COL and the mountain wave. A weak COL will dissipate over the Andes but if the COL is strong it will cross the Andes and can intensify. However, to add to this, Garreaud and Fuenzalida (2006) found that the Andes did play a role in blocking warm, moist air from the interior, and when the mountains were removed the COL decayed earlier and further west.

The influence of topography on the tracks of COLs is less studied. Climatological studies have found that COL tracks are more likely to move easterly, with the background flow. This has been found in southern hemispheric studies (Fuenzalida and Garreaud, 2005; Pinheiro et al., 2017) as well as over different regions such as Australia (Qi et al., 1999) and north-east China (Lu and Wang, 2010). While climatologically it is possible to find some patterns in COL tracks, individual COL tracks can be erratic and often difficult to forecast, and fewer studies have explored the effects topography may have on these.

While Boyer and Chen (1988) in their laboratory experiment showed that different mountains may induce different tracks as the movement of the COLs passing the Rocky Mountains differ to those passing across the Tibetan Plateau, no study has looked at different COL case studies and explored how their tracks may differ with different topographic configurations. Therefore, the present study will fill the gap.

Only few studies have documented the relative influence of topography on COLs over Southern Africa (Taljaard, 1985; Tennant, 1994; Singleton and Reason, 2006; Singleton and Reason, 2007a; Favre et al., 2013). In a climatological study of COLs over South Africa, Taljaard (1985) suggested that Southern African coastal mountains often cause extreme precipitation when onshore winds from COLs advect moist air over them. In a spatial distribution of COLs over Southern Africa, Favre et al. (2013) also found a local maximum over the Orange River basin and attributed it to the lower altitudes. Tennant (1994) performed a numerical modelling study of a COL event off the east coast of South Africa. The COL was simulated with normal topography and removed topography. Removing topography led to less intense precipitation associated with the COL. This was due to the anticyclone being able to ridge further inland which pushed the surface low further to the north east. The combined effect led to less surface convergence and therefore a lack of extreme precipitation. In a similar study over East London, Singleton and Reason (2006) attributed an inland extension of surface depression and precipitation associated with a COL to the Drakensberg Mountains. They argued that the mountains enhanced the extreme precipitation from COLs. In another study, Singleton and Reason (2007a) simulated a COL off the south coast. In the simulation the surface heat fluxes led to the low level depression associated with the COL whilst the topography blocked the depression from moving further inland and led to orographic uplift. However, while all numerical studies removed topography in their sensitivity experiment, none of the studies looked at the different roles the eastern or western escarpment play on the COLs. Since topography has the potential to weaken or intensify cyclolysis and influence precipitation patterns as well as the tracks of the COL, it is important to understand how different parts of Southern Africa's topography may influence the COLs

Chapter 3 : Data and Methodology

This chapter describes the methodology used for this study. It starts by describing the data and models used and the simulations produced. The chapter goes on to explain how the cut-off lows were identified, how their associated precipitation patterns were characterised, how the models were assessed and how the influence of topography was examined

3.1 Data

3.1.1 Observations

The observation precipitation data used in this study was obtained from three gridded precipitation datasets, namely: the Climatic Research Unit (CRU TS4.20; Harris et al., 2019), the Climate Prediction Center's (CPC) Gauge-Based Analysis of Global Daily Precipitation (Xie et al., 2009) and the Climate Hazards Group InfraRed Precipitation with Station data (CHIRPS; Funk et al., 2014). CRU interpolates monthly precipitation anomalies from meteorological stations across the world onto a 0.5° X 0.5° grid and uses an existing climatology to obtain monthly precipitation values for the period 1901–2017 (Harris et al., 2019). This dataset is generally considered to be one of the most reliable observed gridded datasets for precipitation over South Africa because it is solely interpolated from station data. However, its monthly temporal resolution is too low for this study, which requires daily precipitation. CRU was used as a reference for evaluating other datasets at monthly and annual scales. CPC interpolates daily precipitation values from stations onto a 0.125° X 0.125° grid over all land areas. The daily precipitation dataset is released on a 0.5° X 0.5° grid over the globe and is available from 1979 to the present. CHIRPS combines *in-situ* station data with satellite data to create gridded precipitation data from 1981 to 2007 with a 0.25° resolution. Zwart et al. (2018) showed

that CHIRPS is one of the most reliable satellite datasets over Africa. To facilitate comparison, all the precipitation datasets were regridded to a common horizontal resolution (0.25° x 0.25°).

3.1.2 Reanalysis

The reanalysis data used for the study is the Climate Forecast System Reanalysis (CFSR; Saha et al., 2010) data. CFSR is a coupled atmosphere-ocean-land surface-sea ice system that produces precipitation data (among other variables) at a resolution of 0.5°, from 1979 to the present at 6-hourly intervals, but we used daily mean CFSR precipitation data in our study. Zhang et al. (2013) showed that CFSR is one of the best reanalysis precipitation datasets over southern Africa; they attributed the good performance to the high resolution and coupled ocean assimilation of the reanalysis.

The upper-air meteorological data was also obtained from CFSR. The data consists of daily geopotential height, temperature, specific humidity, and wind (zonal and meridional components), at standard pressure levels. Moist static energy and potential temperature data were generated from the geopotential height, temperature and specific humidity. The geopotential height and temperature variables, at 500 hPa and 300 hPa, were used to identify the COLs, while all the upper-air data was used to describe the spatial and vertical structure of the COLs as well as the atmosphere that induced the COLs.

3.1.3 Models

3.1.3.1 The Weather Research and Forecasting (WRF) model

The RCM used in this study is the Weather Research and Forecasting (WRF) model with ARW core version 3.8.1 (Skamarock et al., 2008). The model uses a Eulerian mass dynamical core with a terrain-following vertical coordinate. WRF is able to downscale coarser models to high resolutions with fully compressible non-hydrostatic dynamics. For further information refer to Skamarock et al. (2005). The Model was simulated using a 30km resolution. The parameterization schemes used were chosen because they have shown merit in WRF simulations over Southern Africa in previous studies (Ratnam et al.,

2012; Cretat et al., 2012; Ratna et al., 2014; Ratnam et al., 2016). The schemes used are the Dudhia shortwave radiation scheme (Dudhia, 1989), the RRTM scheme for longwave radiation (Mlawer et al. 1997), the WRF single-moment 3-class (WSM3) microphysics scheme (Hong et al. 2004), the Yonsei University (YSU) planetary boundary layer scheme (Hong et al. 2006), and the Betts-Miller-–Janjic´ cumulus parameterization scheme (Betts and Miller 1986; Janjic´ 1994).

Two different simulation sets were run using WRF. A long simulation and shorter topographical sensitivity experiments.

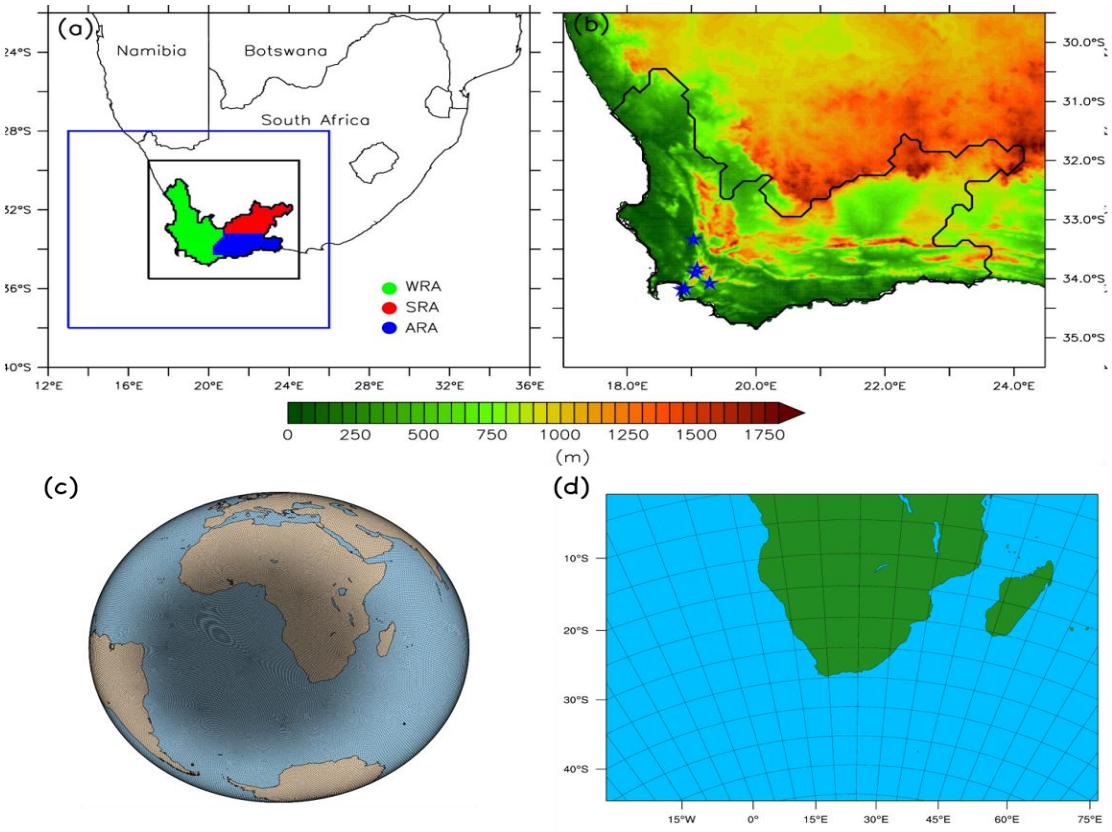

Figure 3.1: The study domain showing (a) a map of South Africa with the Western Cape highlighted and (b) the topography (m) of the Western Cape. The blue box in panel (a) shows the area used in identifying COLs that may influence the Western Cape. The Western Cape rainfall regions are designated as WRA (i.e., the winter rainfall region), ARA (i.e., the all year rainfall region) and SRA (i.e., the late summer rainfall region). The location of the main dams in the Western Cape are indicated with blue stars in panel (b). The domain and grid used in the MPAS simulation is shown in panel (c) and the WRF domain in panel (d).

The long simulation was run and analysed to test how well WRF could simulate the characteristics of COLs over the Western Cape and to compare its performance to the VGCM, WRF was run for the period 2007 – 2017, using a 30 km resolution over the Southern African domain (indicated in Fig. 3.1d). 30 km was chosen for comparison with the finer scale of the VGCM simulation. The model was initialised and forced at the boundaries with the same initial condition data as the VGCM i.e. using CFSR. The CFSR sea surface temperature (SST) data was also used to update the SSTs every six hours in WRF.

Short sensitivity experiments were run to examine the sensitivity of COLs to topography. The same configuration for the long run was used for these experiments, with the exception of the forcing data and the terrain. The terrain was changed for the sensitivity experiments and the changes are detailed in section 3.2.5. For each experiment, an ensemble of 20 simulations were performed with perturbed initial conditions. The simulation domain is the same as in the long WRF simulation. All the simulations cover a period of four months (March-June 2015). Three months of the simulations were discarded for spin-up while the simulations for the last month (June 2015) were analysed in this study. This month was chosen because it is the period COLs are most frequent over the west coast.

An analysis dataset was used to force WRF in these short sensitivity experiments. The analysis dataset is from the NCEP FNL (Final) Operational Global Analysis data (Hereafter referred to as FNL). The analysis dataset uses the same model as the NCEP Global Forecast System (GFS) but is updated an hour later to include more observed data. FNL is updated with data from the Global Data Assimilation System (GDAS), which continuously collects observational data from the Global Telecommunications System (GTS) and other sources. The FNL dataset has a spatial resolution of a 1° x 1° degree grid and a temporal resolution of 6 hours. We used this dataset to provide the initial and boundary conditions for the model simulations. We used the standard surface data

distributed with WRF, which uses the global digital elevation (GMTED2010, USGS (2010)) dataset to represent topography, with a resolution of 30 arc-second.

3.1.3.2 The Model for Prediction across Scales (MPAS)

The VGCM used for this study was the Model for Prediction across Scales (MPAS) version 6.1 (Heinzeller et al., 2016). MPAS was developed at the National Centre for Atmospheric Research (NCAR). MPAS extends the techniques used to solve the non-hydrostatic equations in WRF to a voronoi mesh grid, which includes C-staggering (Skamarock et al., 2012). MPAS has also inherited a subset of the WRF's parameterisation schemes that are appropriate for a GCM (Heinzeller et al., 2016). MPAS uses a hybrid vertical coordinate system, whilst WRF uses terrain following vertical coordinates. The hybrid system reduces errors around steep topography (Heinzeller et al., 2016; Kramer et al., 2018; Park et al., 2019); however, it is less easily coupled to the boundary and surface layer parameterisation schemes (Kramer et al., 2018).

We ran MPAS from 2007 to 2017, using a variable grid of 100-25 km resolution with the finest resolution centered to the west of Southern Africa (as shown in Fig. 3.1c). The simulation was initialised with the CFSR dataset. The CFSR SST data was also used to update the SST conditions at 6-hourly intervals. The physics options used in the MPAS simulation were the MPAS mesoscale reference suite, which are the reference parameterisation schemes for simulations with resolutions greater than 10 km. These include the WRF single-moment 6-class microphysics scheme (WSM6), New Tiedtke convective parameterisation, YSU PBL parameterisation, Monin-Obukhov surface layer parameterisation, the Noah land surface model, and the Rapid Radiative Transfer Model – GCM applications (RRTMG) longwave and shortwave radiation parameterisations.

3.2 Methods

Table 3.1 summarises the experimental design and methodology used in the analysis for each hypothesis, the following sections describe these methods in more detail.

Table 3.1: The experimental design for the study.

Hypothesis	Data Used	Period used	Analysis
Hypothesis 1: Changes in characteristics of COLs (i.e. tracks frequency and the associated rainfall) over the Western Cape contributes to the 2015-2017 drought in the province.	Observed Satellite rainfall data and CFSR Reanalysis data	1981-2017	● Identified the inter-annual and spatial variability in COL occurrence over the Western Cape ● Identified different COL rainfall patterns and associated dynamics ● Based on this examined the differences seen during the drought
Hypothesis 2: The characteristics of COLs over the Western Cape can be reproduced by the Weather Research and Forecasting (WRF) and the Model Prediction Across Scales (MPAS) models.	CFSR Reanalysis, WRF simulation and MPAS simulation	2007-2017	● Explored whether the models were able to capture the mean climate of Southern Africa ● Explored whether the models were able to simulate the characteristics identified from the hypothesis 1 results
Hypothesis 3: The characteristic of COLs over South Africa is influenced by the complex topography of southern Africa.	GDAS Reanalysis, and multi-simulation ensemble from WRF, using different topographic configurations	June - August 2015	● Compared the formation, tracks, rainfall and dynamics of three COLs for the different topographic experiments

3.2.1 Identification and Tracking of Cut-off Lows

We used an algorithm developed by Favre et al. (2012) to identify COLs over Southern Africa, but with some modifications. Using daily upper-level geopotential height and temperature data from CFSR as input, we identified COLs in two steps. First, we identified potential COL centers by extracting all the local minima of geopotential height and temperature at the upper level (i.e. 500 or 300 hPa level) over the domain. A local minimum occurs in a grid point when the geopotential height or temperature values at that point are lower than those at its surrounding eight grid points. The temperature minima must be less than 265 K at the 500 hPa level (or 242 K at the 300 hPa). These temperature thresholds were chosen based on looking at the temperature mean for the entire period at the specific level, the mean temperatures of the tropics was used as a threshold for each level so as to avoid identifying tropical lows. A center of minimum geopotential height was retained as a possible COL center, if there was a temperature minimum within an approximate radius of about 600 km from the center. This is because, at 500 hPa, the temperature minima isotherms are not usually as well defined as the minimum geopotential height isohypse (Favre et al., 2012).

Second, we refined the selected COL centers by ensuring that a COL center did not have any weaker COL center within a radius of about 1450 km. Hence, for each potential COL center, the algorithm eliminated all the weaker potential COL centers (i.e. with higher pressure) within a 1450 km radius. This was done because small-scale variations in pressure might be interpreted as several different COLs, although they belong to the same COL. The remaining COL centers were retained and analysed for the study. Note that we increased the radius for eliminating other weaker COL centers from 1200 km (used in Favre et al., 2012) to 1450 km, because Singleton and Reason (2007b) showed that some COLs can in fact have a larger radius than 1000 km. The choice of the 1450 km radius was based on our manual inspection of two years of CFSR analysis, which also confirmed the results of Singleton and Reason (2007b).

For the topography sensitivity experiments we tracked the COLs. Once the lows were identified we analysed each centre and if the centre the next day was within the COL travel radius (150 km), then the centre was regarded as the same COL. This travel radius was chosen as COLs are known to travel at speeds less than about 42-43km.h^{-1} (Fuenzalida et al., 2005; Favre et al., 2012). And since the tracking was done with the WRF simulations the grid resolution was 30km and the output time was 3 hours therefore we used a rounded off travel distance of 150km per 3 hours. Any identified centre that did not track for at least one day was not considered as a COL.

We tested the sensitivity of our COL statistics to the pressure level, by using the 300 hPa and 500 hPa levels to identify the COLs. The results (Fig. 3.2) indicate that the spatial distribution of COLs varies according to the atmospheric levels. For instance, the number of COLs over the Western Cape is lower at the 300 hPa than at the 500 hPa level. In addition, the distribution of COLs at 300 hPa does not feature the same COL peaks as seen at the 500 hPa level. The peaks off the west coast, over the Western Cape and to the north of the Western Cape have moved further south and east and show fewer COLs than was identified at the 500 hPa level. This is consistent with the findings of Ndarana and Waugh (2010) who studied COLs over the southern hemisphere and found that between 0°E and 60°E, which includes the Western Cape, COLs occur more frequently at the 500hPa level during winter and at the 250hPa level during summer. However, over this region more winter COLs occur. This suggests that 500 hPa COLs are generally more frequent over the Western Cape. Therefore, since we will be focusing on the Western Cape, we will be using the 500 hPa level to identify the number of COL days.

Once we identified COL days over Southern Africa, we extracted only the COL days in which the COL centers fell within a defined region around the Western Cape (shown in Fig. 3.1 - the blue box). This region was used as it provided the best results for characterising Western Cape precipitation, sensitivity to the area chosen was analysed (see Fig. A1-A12) and this area was chosen based on these results. COLs that fell within this region were then referred to as Western Cape COLs. Throughout our paper we refer

to COL days as COLs. Therefore, in our analysis the results include all COL days of which some may be part of the same COL.

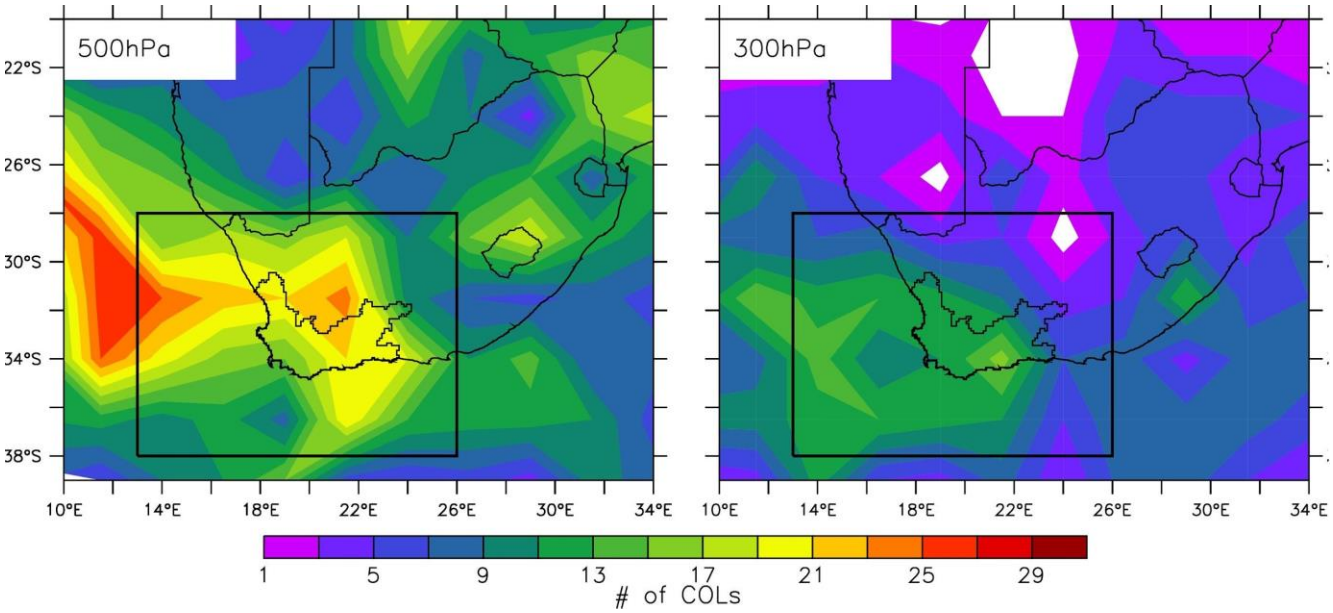

Figure 3.2: The spatial distribution of number of COL days over South Africa summed over the period 1981-2017 summed over 2.5° X 2.5° grid boxes for COLs identified at the 500hPa and those at the 300hPa level. The black square shows the region for which we identified Western Cape COLs. The black outline shows the Western Cape Province.

3.2.2 COL Precipitation

We defined COL precipitation as the precipitation experienced over the Western Cape for each COL day. While this assumes that all the precipitation is caused by the COL and does not take into account other systems that may be influencing the precipitation on that day, this assumption is not unfounded as COLs are synoptic scale systems and therefore it is not a stretch to assume that on COL days the COL system will dominate the conditions over the Western Cape. Therefore, COL precipitation is defined as the precipitation experienced on the day of the COL over the Western Cape. The COL precipitation contribution per year is calculated by summing the precipitation for each COL day within that year and calculating what the percentage this precipitation makes up from the overall precipitation for that year.

3.2.3 Identifying Precipitation Patterns using SOMs

We used a self-organising Map (SOM) to group the spatial distribution of COL precipitation into similar patterns. The SOM, a type of artificial neural network, allows for the dimension reduction and clustering of data (Kohonen, 1990; Lennard and Hergerl, 2015). The data is reduced to archetypical points, called nodes, which are representative of the multi-dimensional data space and its variance. In the context of weather data, these nodes can be visualised and interpreted as the main distinct weather patterns or synoptic types in the data (Lennard et al., 2013; Wolski et al., 2018). This is different to principal component analysis which outputs patterns of variance which cannot be directly related to physical synoptic types or patterns (Dyson, 2015). Liu et al (2006) compared the ability of a SOM with an empirical orthogonal function in extracting four known pattern types in a dataset. The authors found that SOMs was able to extract these four patterns whereas EOF was not. The SOM groups similar patterns together and dissimilar patterns further apart, which also helps to classify the underlying systems represented in the data. Since one of our objectives is to understand the different types of precipitation patterns COLs bring to the Western Cape, using a SOM is an appropriate method as it allows for direct physical interpretation and has been shown to be proficient in identifying different pattern types.

In our study, we used the SOM to classify our COL precipitation days into nine (3 X 3) different patterns (nodes). Nine nodes were used because less than nine seemed to leave out some of the important patterns and ended up grouping most of the patterns into a no precipitation node. Using more than nine nodes leads to more nodes with the same patterns. Hence nine nodes provide enough detail in the types of patterns. For our 3 X 3 SOM the overall frequency and the seasonal frequency of the occurrence of these nodes were analysed, along with the average amount of precipitation per season for each node. The change in frequency and amounts of precipitation during the drought years was explored to understand whether certain types of COL precipitation patterns occurred less frequently or produced less precipitation during those years.

The dynamics associated with the different precipitation patterns were examined by extracting a smaller set of COL days from each node and analysing composites of CFSR geopotential height at the 500 hPa and 850 hPa level, wind at the 850 hPa level, and integrated moisture flux convergence. The smaller set of COL days was selected to consist of those days when all the COLs had centers within a defined region (13 – 17°E; 31 – 34.5°S). This was done to ensure that the composite signal would be clearer and not clouded by a wider range of COL positions that might cause the averaging of the dynamics to be difficult to interpret.

3.2.4 Evaluating the Ability of Models to Capture COL Characteristics

We evaluated the ability of the models in capturing COL characteristics by how well the models were able to capture the general annual and seasonal climatology of the Western Cape by comparing MPAS and WRF to CFSR and CHIRPS data. We then compared the simulated and observed precipitation signals over the Western Cape and during the drought years. Once we had examined the simulated precipitation signals we compared the simulated spatial and temporal COL frequencies, during the 2007-2017 period as well as specifically during the drought years, with observed.

To evaluate how well the models captured the frequency of the COL precipitation patterns a second SOM was performed. The dataset for the SOM analysis consisted of a combination of COL precipitation data from the CHIRPS, CFSR, WRF and MPAS datasets. The results of the SOM classifications were further analysed to study the contribution of each dataset to each SOM node, and the seasonal frequency of each node was also examined.

To explore whether the models could capture the same differences between wet and dry COLs as found for the reanalysis data. The horizontal and vertical structure of a wet and dry COL for each dataset is compared. Each wet COL is extracted from the wettest node in the SOMs and the dry COL from the driest node. It was difficult for us to find the same date in each dataset for each wet and dry COL, but each COL has its center within the

same defined region, (i.e., 32^{o} – 36^{o} S and 14^{o} – 16^{o} E). The horizontal structure of each COL was explored by looking at the geopotential heights and wind vectors at 500hPa, along with the geopotential height at 700hPa and vertically integrated moisture flux and moisture flux convergence. The vertical structure of the dry and wet COLs was compared by plotting zonal temperature and geopotential height anomalies as well as zonal and vertical wind vectors, moist static energy and specific humidity values.

3.2.5 Examining the Influence of Topography

We used WRF to perform four experiments over Southern Africa. The model set-ups for the four experiments are the same, except for the terrain configuration. The model used real southern African topography in the first experiment (hereafter, CONTROL; Fig. 3.3a), flat terrain (i.e. no topography) in the second experiment (hereafter, NoTOPO; Fig. 3.3b), real western topography (i.e. flat terrain east of 24°E) in the third experiment (hereafter, WTOPO; Fig. 3.3c) and real eastern topography (i.e. flat terrain west of 24°E) in the fourth experiment (hereafter, ETOPO; Fig. 3.3d). The eastern topography in the WTOPO experiment was removed by doing the following across each latitude: Firstly testing if the topography between 26°E and 40°E is greater than the 10th percentile of Southern Africa topography, if it is then the topography is reduced by 90% and between 24°E and 26°E is reduced by 50%. This creates flat-like terrain after 26°E and a slope area between 24°E and 26°E where the topography is reduced less. To make the progression between the real topography and the flattened topography smooth and more realistic the slope zone is altered by reducing the topography by increasing percentages. This method created satisfactory and realistic slopes between the flattened and existing terrain, this was tested by visually looking at the height of the topography at each latitude. The same method was used for the WTOPO experiment, only topography between 14°E and 22°E was flattened and a slope was created between 22°E and 24°E. For the NOTOPO experiment the topography was flattened to the 10th percentile if it was greater than the percentile value.

As stated in section 3.1.3.1, for each experiment, an ensemble of 20 simulations were performed with perturbed initial conditions. In each simulation, three COLs (called COL1,

COL2 and COL3) were identified and studied. To examine the influence of topography, the COL characteristics in the four experiments are compared. The comparison focused on COL initiation, track, precipitation and vertical structure.

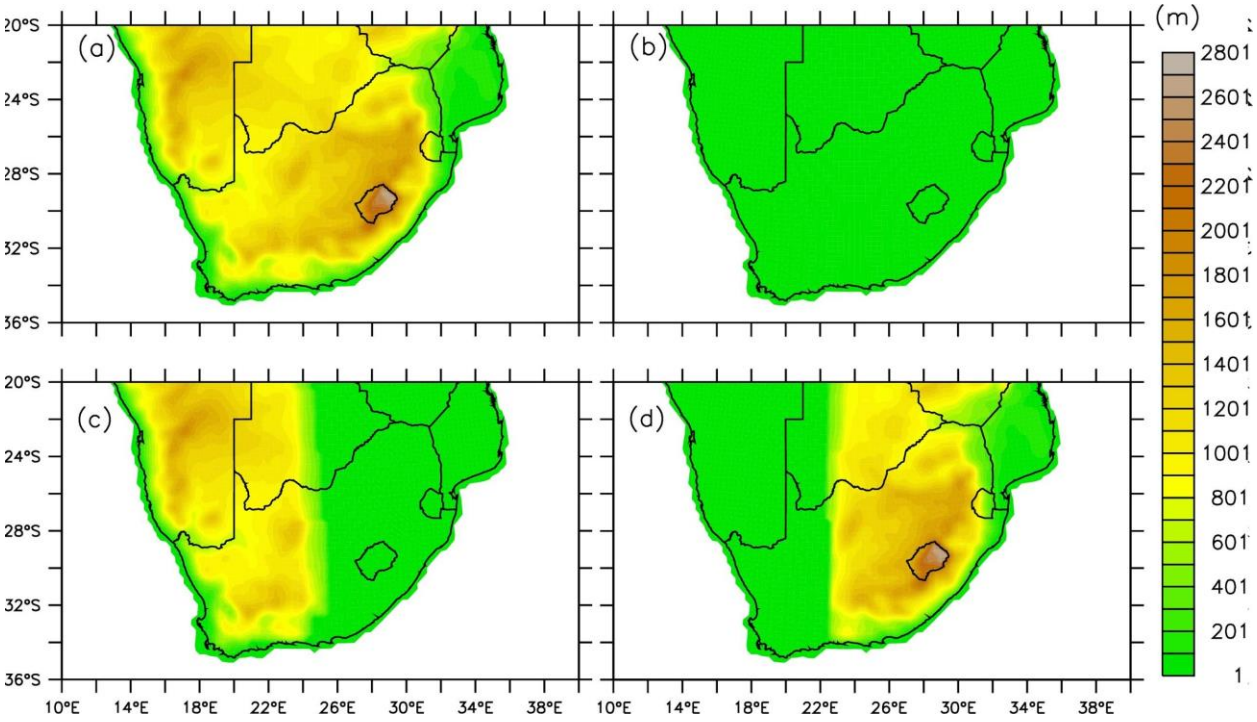

Figure 3.3: The topography (shaded; m) in each topography sensitivity experiment: a) the control experiment (CONTROL; default topography); b) No topography experiment (NoTOPO), c) West topography experiment (WTOPO), and d) East topography experiment (ETOPO).

Chapter 4 : Characteristics of cut-off lows over the Western Cape

This chapter presents and discusses the results of our analysis on understanding the characteristics of COLs over the Western Cape. In this chapter the discrepancies between the observed data is discussed. The spatial and temporal variation in COL frequency is analysed along with the associated precipitation. The different COL precipitation patterns are discussed and the frequency and dynamics of these patterns is explored.

4.1 The Spatio-temporal Variation of Precipitation over the Western Cape

There is good agreement among the four datasets regarding the spatio-temporal variation of precipitation in the Western Cape (Fig. 4.1). In terms of the spatial variation (Fig. 4.1 a - d), the correlation between the datasets is very high ($r > 0.8$). All the datasets feature dry conditions in the interior and wet conditions along the south coast, with precipitation peaks over the west coast and over the Cape Fold Mountains, where most of the Western Cape's dams are located (Fig. 3.1; Blamey et al., 2018). However, the magnitude of the precipitation peaks varies among the datasets. While the peaks are more than 980 mm $year^{-1}$ in the CRU observations, they are less than 500 mm $year^{-1}$ in the CPC dataset. Among the satellite and reanalysis products, CHIRPS features the best agreement with the CRU observations. With the temporal variation (Fig. 4.1e – h), all the datasets agree that the province can be divided into three areas, based on the annual precipitation cycle. While the first area (the winter rainfall area; WRA) receives the maximum precipitation (45–50 mm $month^{-1}$) during the winter, the second area (the summer rainfall area; SRA) experiences the maximum precipitation (25–30 mm $month^{-1}$) in the summer, and the third

area (the all-year rainfall area; ARA) receives almost the same amount of precipitation (35–40 mm month^{-1}) throughout the year. However, the average precipitation over the Western Cape shows the maximum precipitation in winter, because WRA precipitation is higher than ARA and SRA precipitation. The inter-annual variability of precipitation over the province is high (Fig. 4.1i), with the standard deviation ranging from 41 mm year^{-1} (in CHIRPS) to 53 mm year^{-1} (in CPC), 58 mm year^{-1} (in CRU), and 59 mm year^{-1} (in CFSR). The correlation between the CRU observations and the precipitation products on the inter-annual variability is up to 0.89 in CHIRPS but less than 0.5 in CFSR.

All the datasets agree that drought was a prominent feature in 2015–2017. They show that during the drought years the driest conditions throughout the study period occurred (Fig. 4.1). While this study period is limited to 1981-2017, Otto et al., (2018) state that the drought has an occurrence probability of 1 in about 150 years, which shows the long-term extremeness of the drought that extends beyond the restrictions of our study period. The datasets furthermore indicate that the intensity and spatial coverage of the drought increased over the three years (Figs. 4.2 and 4.3). For instance, in the CRU observations, the maximum precipitation deficit (about 100 mm) was limited to the WRA in 2015 (Fig. 4.2a) but covered the entire Western Cape in 2017 (Fig. 4.2i), when the province as a whole experienced the lowest precipitation (within the study period of 1981–2017). In addition, the drought did not affect the winter rainfall in 2015 but did affect it in 2017 (Fig. 4.3a and 4.3i). The major discrepancy between CRU and the other datasets is with CFSR in 2016 ($r = -0.26$; Fig. 4.2h), when CFSR indicates a precipitation surplus over the south-western tip of the province, whereas CRU indicates a precipitation deficit. The best agreement is with CHIRPS in 2017 ($r = 0.74$; Fig. 4.2j). The discrepancy between the precipitation products and CRU can be attributed to many factors. It may be due to deficiencies in the CRU dataset. For instance, Dieppois et al. (2016) show that the number of rain gauges in the Western Cape that are used in generating the CRU dataset has dropped to four since 2000. Mahlalela et al. (2018) reported a precipitation surplus over the south coast in 2015, which agrees with the annual drought severity map for 2015 that was published by the Agricultural Research Council in their December monthly UMLINDI newsletter (UMLINDI, 2015). While this can also be seen in the results of the other

observation and reanalysis products (Fig. 4.2b – d), it contradicts the CRU results which shows a precipitation deficit over this region. The discrepancy may also be due to the differences in resolution (spatial and temporal) of the precipitation products, or due to inadequacies in the precipitation parameterisation schemes in CFSR. However, given that the CHIRPS results have the best correlation with CRU, and shows comparable drought results with Mahlalela et al. (2018) and the UMLINDI newsletter over the province, we will be using CHIRPS precipitation for the rest of the study.

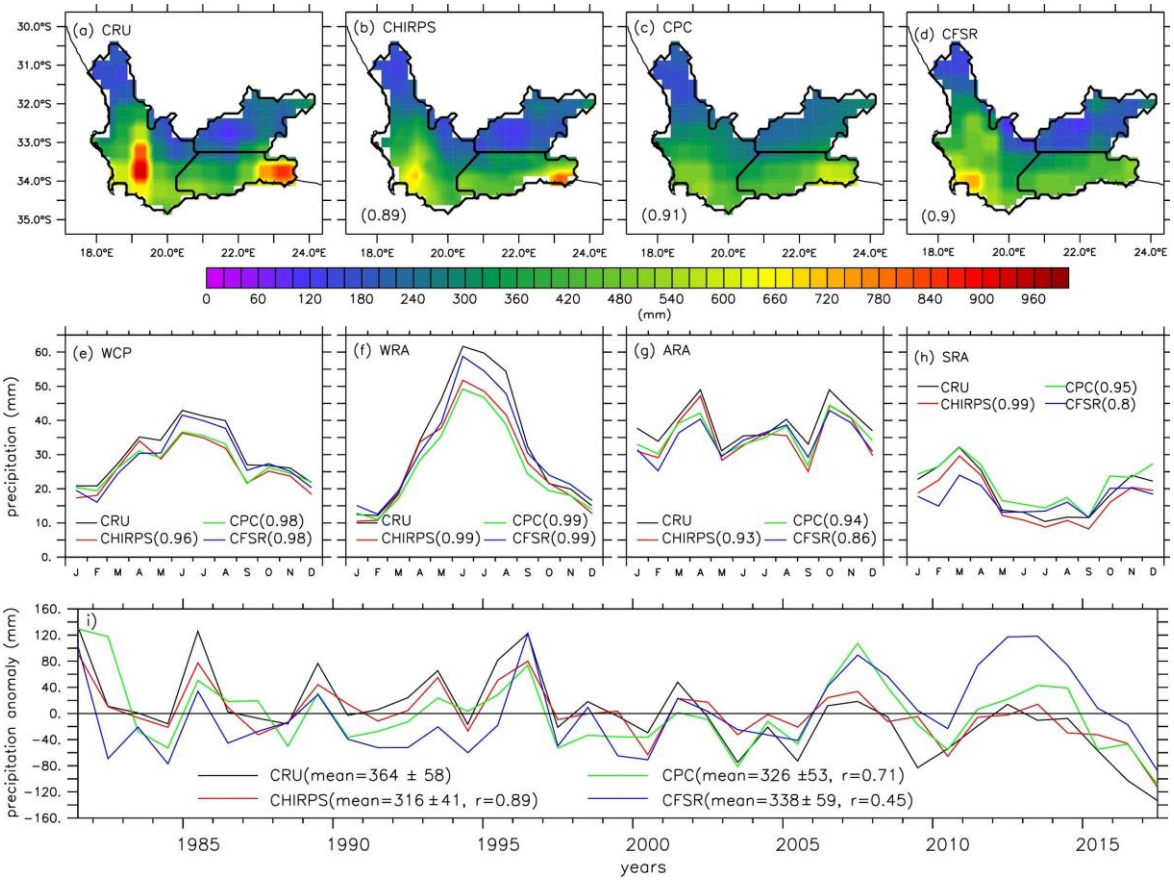

Figure 4.1: The spatial-temporal variation of precipitation over the Western Cape, as depicted by observations (CRU, CHIRPS and CPC) and reanalysis (CFSR) datasets. The top panels (a-d) show the annual precipitation amount (mm.year-1), the middle panels present the annual cycle of the precipitation (mm.month^{-1}) for the whole Western Cape Province (WCP), the winter rainfall area (WRA), the all-year rainfall area (ARA) and the late-summer rainfall area (SRA), while the bottom panel (i) shows the inter-annual variability of the annual precipitation anomalies. The correlation between each dataset and the CRU is indicated in the brackets.

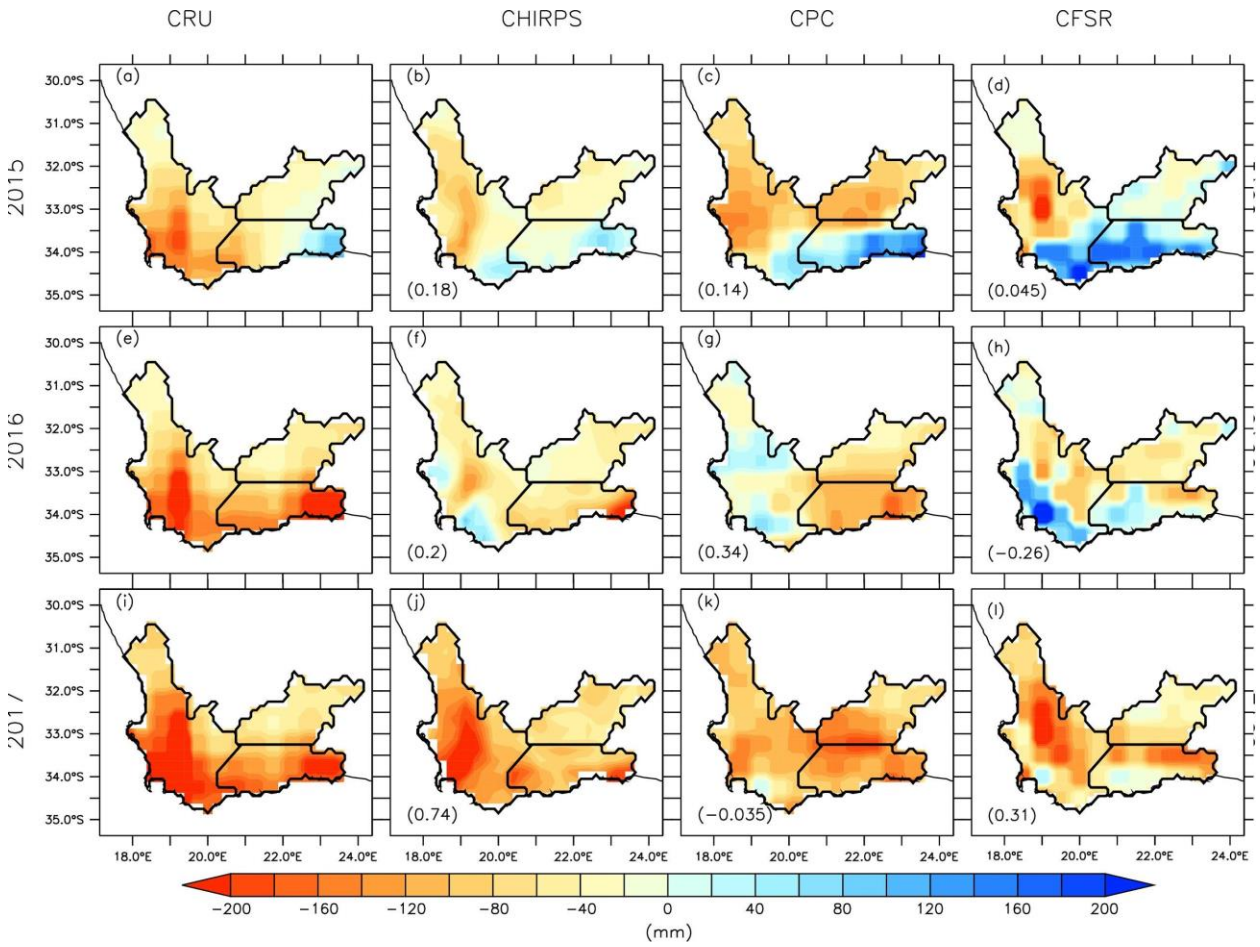

Figure 4.2: The spatial distribution of precipitation anomalies during the three years of drought (2015, 2016 and 2017) as in the observation datasets (CHIRPS, CPC, CRU) and reanalysis dataset (CFSR). The spatial correlation between each dataset and CRU is indicated in the brackets.

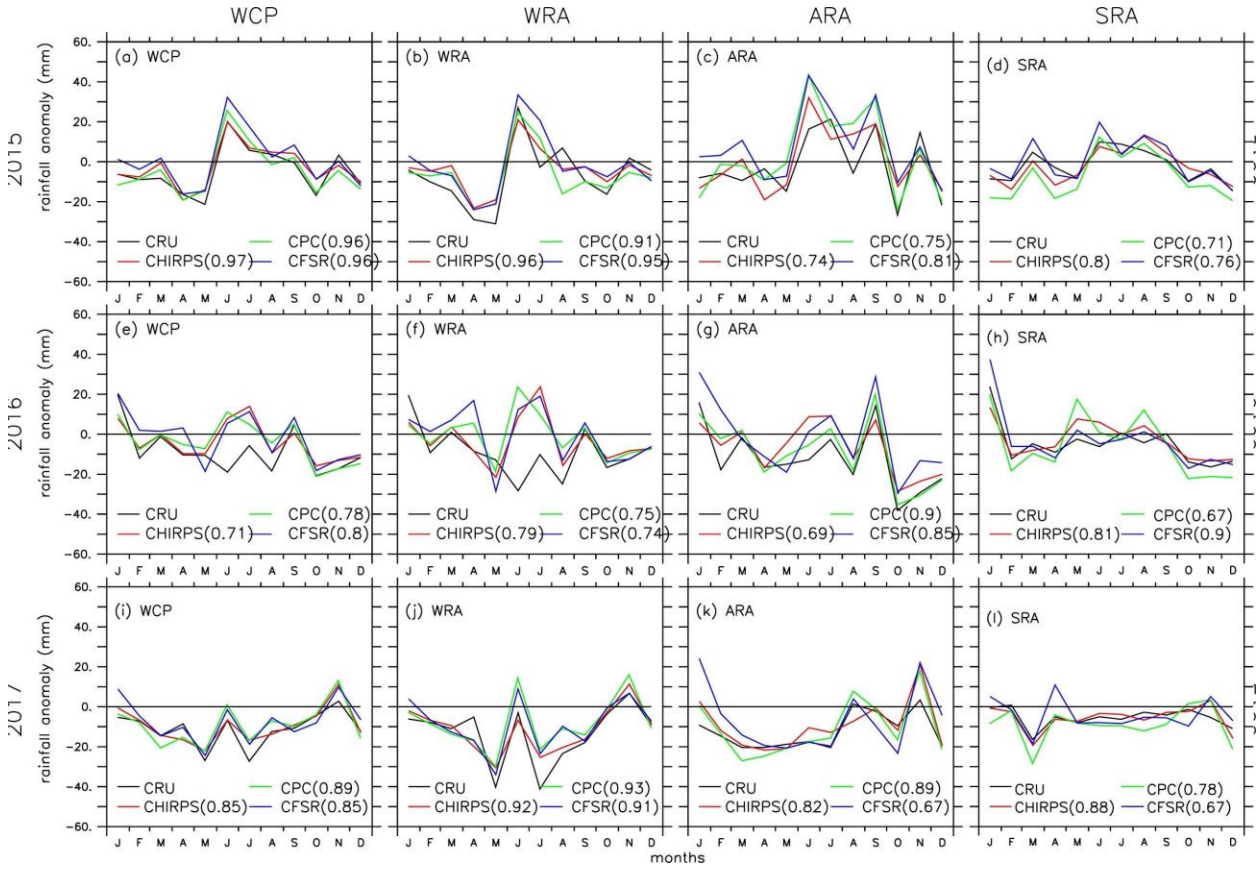

Figure 4.3 The intra-annual distribution of rainfall anomalies for the whole Western Cape Province (WCP; first column), the winter rainfall area (WRA; second column), the all-year rainfall area (ARA; third column) and the late-summer rainfall area (SRA; fourth column) during the three years of the drought (2015, 2016 and 2017), as depicted in the observation (i.e. CRU, CHIRPS and CPC) and reanalysis (CFSR) datasets. The correlation between each dataset and CRU is indicated in the brackets.

4.2 The Spatio-temporal Variation of COLs

Fig. 4.4b shows that there are peak occurrences of COL days over regions around the Western Cape, and that the province experiences more COLs than most areas of South Africa. Another preferential area is seen over the Drakensberg Mountains, but the frequencies are less than those over the Western Cape and surrounds. This indicates that COLs are more common to the west of the higher altitudes of the South African plateau. Several studies have also reported preferential areas in COLs west of mountainous regions (or continents). For example, Pinheiro et al. (2017) found a COL preferential area west of the Andes while Fuenzalida et al., 2005 showed a peak to the west of the Rockys (Fuenzalida et al., 2005). The peak in COL occurrence over the

Western Cape and surrounds can also be linked to the peak in Rossby wave breaking over the same area (Ndarana and Waugh, 2011), as COLs usually form from Rossby wave breaking (Favre et al., 2013). Singleton and Reason (2007b) along with Favre et al. (2013) also found the highest number of COLs over surrounding regions of the Western Cape, while Engelbrecht et al. (2013) also reported a peak in upper-level low pressure activity over this area. Therefore, there is good agreement about the COL preferential regions and while there are some differences between our results and previous studies these are mainly due to differences in smoothing and resolution.

Table 4.1 shows that the province experiences the highest number of COLs in JJA (which corresponds with the peak rainy season). This result contradicts the findings of Pinheiro et al. (2017) and Singleton and Reason (2007b), who reported the highest number of COLs in MAM. The discrepancy between these studies could be due to differences in the levels used for COL identification. Both of these studies used the 300 hPa level to identify the COLs, while our study used the 500 hPa level. COLs occur lower in the atmosphere in the winter than they do in the summer (Ndarana and Waugh, 2010). This is because jet streams inhibit wave breaking, which can reduce COL numbers. In winter, the sub-tropical jet is further north, and because it occurs further up in the atmosphere it is more likely to affect COLs at levels above 500 hPa. Which could explain why those previous studies did not find a winter maximum like in our study. Conversely, at 500 hPa, COLs are more influenced by the lower-lying polar front jet (PFJ), which lies further south during winter, which explains the winter maximum in 500 hPa COLs. To corroborate this, studies who identified COLs on the 500hPa level, also found that COLs occurred more frequently off the west coast of South Africa in winter (Fuenzalida et al., 2005; Ndarana and Waugh, 2010; Reboita et al., 2010; Favre et al., 2012). Fuenzalida et al. (2005) found this winter maximum to be unique to South Africa compared to other Southern Hemisphere COL regions although this result is not as clear in other studies.

The number of COLs and their associated precipitation amount over the Western Cape also varies from year to year (Fig. 4.4a). On average, the region experiences 10 COLs per year, but with a standard deviation of 5 COLs. The annual variation ranges between

-80% (in 1984) and 120% (in 1981) of the annual mean. Other COL studies, over different regions, have also reported significant inter-annual variability in COL numbers. For example, Pinheiro et al. (2017) reported a standard deviation of 6.7 COLs over Southern Africa. Fuenzalida et al. (2005) reported a 50% variability over South Africa and found that this region has the highest variability compared to the other southern hemispheric regions due to less frequent occurrences of COLs. Our results show that, in addition to the high variability of COL occurrence, a positive or negative anomaly in annual COL occurrence can persist for years. For example, a negative COL anomaly persisted up to five years in 2005-2009, and a negative COL anomaly persisted for six years in 1989-1994. However, there is no statistically significant trend in COL numbers over the Western Cape within the study period.

There is a strong correlation between annual COL frequency and COL precipitation (r = 0.81). For instance, the years with the highest COL numbers (e.g. 1981 and 1995) feature the highest COL precipitation, while the years with the lowest COL numbers show the lowest COL precipitation. However, there are years in which the anomalies in the COL numbers and the COL precipitation are opposite (e.g. 1996, 2013), thus implying that certain individual COLs can contribute more precipitation than others. The spatial distribution of COL precipitation (Fig.4.4c) is similar to that of the Western Cape precipitation pattern, showing low COL precipitation along the northern areas and high COL precipitation along the southern coastal areas, but with the maximum COL precipitation occurring over the eastern part of the ARA. The annual precipitation from COLs decreases from about 100 mm in the far eastern parts of the ARA, to 60 mm over the south coast, 45–60 mm along the Cape Fold Mountains and 15 mm ‘in the northern parts of the Western Cape’. However, the average annual COL precipitation over the whole province is about 34 mm $year^{-1}$, which is about 11% of the total annual precipitation (316 mm $year^{-1}$) over the province.

The sign of the changes in COL occurrence and COL precipitation over the Western Cape varied during the drought period (2015–2017; Fig. 4.4). In the first two years of the drought (2015 and 2016), the province experienced above normal COL days (about 10%) and

COL precipitation contribution (about 13–20%), but below normal (about -80% and -100%, respectively) in 2017 (Fig. 4.4a). In 2015, above average precipitation was seen across most of the WRA and ARA, and in 2016, while most parts of the province received below average COL precipitation, the dam areas actually received above average COL precipitation (Fig. 4.4c). In 2017, however, below average COL precipitation was experienced across the entire province (Fig. 4.4c). This suggests that the precipitation from COLs helped to minimise the intensity of the drought in 2015 and 2016, especially over the WRA and ARA. However, the drastic drop in COL precipitation in 2017 contributed to the severity of the drought in the third year.

The spatial distribution of COLs during the drought period (Fig. 4.4b) shows that, in 2015 and 2016, there was an increase in COL frequency over the west and south coasts. In 2017, however, there was a decrease in COL occurrences over most of the region of interest, and COLs were mainly seen further south of the Western Cape. Sousa et al. (2018) have shown that, during the drought, there was a southward extension of the South-Atlantic Anticyclone and a southward displacement of the jet stream, which led to more southward storm tracks. Along with this, the expansion of the sub-tropical high pressures strengthened the southward flow phase of the SALLJ (Sousa et al., 2018) leading to less moisture being transported from South America to Southern Africa. Atmospheric rivers were also shifted further south and thus two of the three major moisture sources for Western Cape winter rainfall, discussed in section 3, were decreased. On the other hand the shift in the PFJ explains why we see more COLs in 2015–2016; the PFJ is known to inhibit wave breaking at the 500 hPa level and hence, a southward shift of the jet allows for more wave breaking to occur over the region, in turn leading to enhanced COL formation (Ndarana and Waugh., 2010). Interestingly, despite these shifts in moisture during the period we see above average COL precipitation over the WRA and ARA during these years. This indicates that atmospheric rivers and moisture transported off South America is not the only important moisture source for COL systems over the Western Cape. This shall be explored further in the following sections. In 2017, however, we see fewer COLs, and below average COL precipitation across the

province, despite the poleward shift of the PFJ, suggesting that there may have been dynamically distinct processes at play in 2017 compared to 2015–2016.

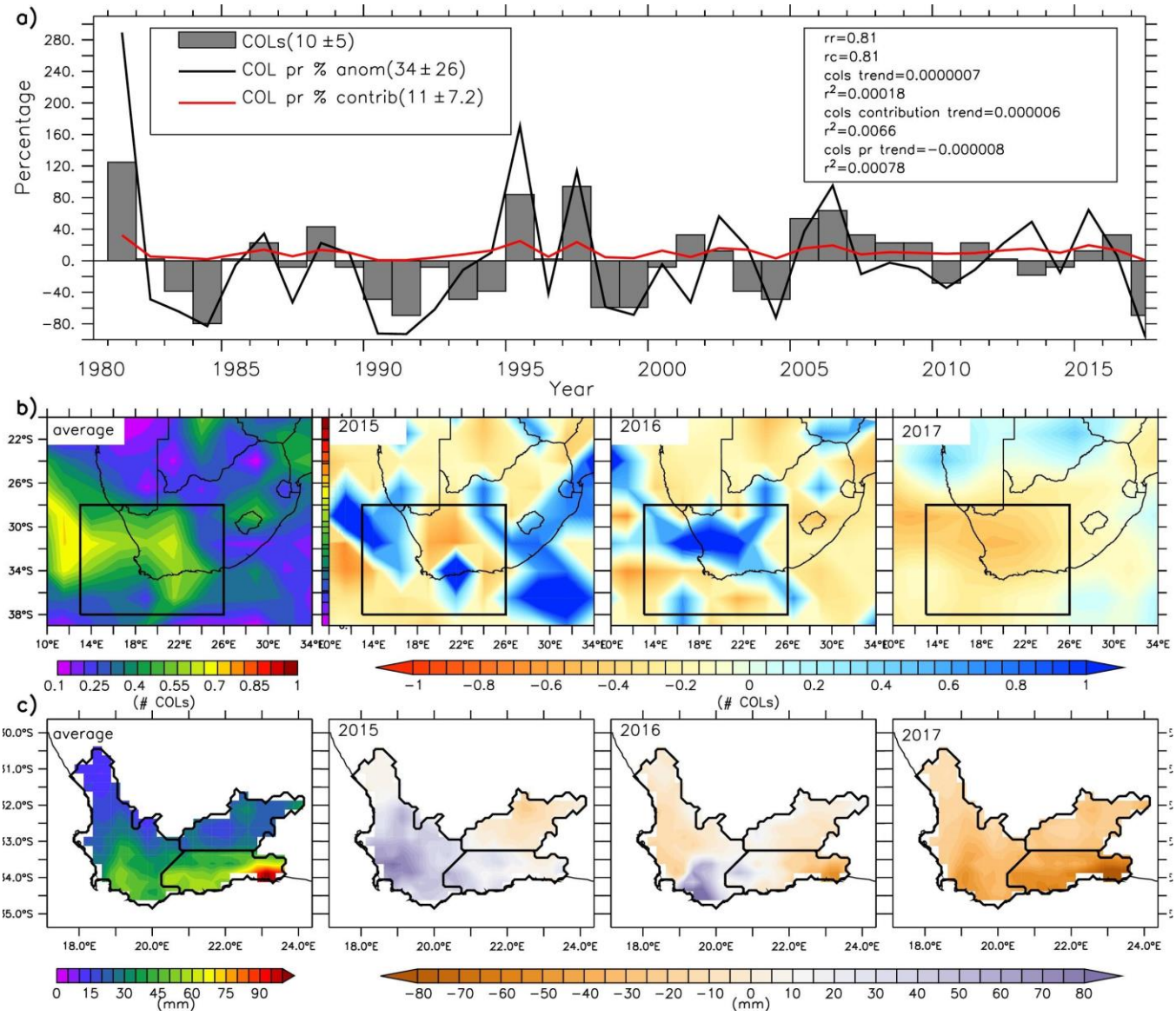

Figure 4.4: Panel (a): The plots show the yearly anomalies of COL numbers and COL precipitation calculated from the yearly mean for 1981-2017 over the Western Cape. The anomalies are represented in percentages. The plot also shows the yearly percentage contribution of COL precipitation to the overall annual precipitation of the Western Cape. The mean value for each variable is indicated in brackets in the key along with the standard deviation. rc shows the correlation between the COL numbers and precipitation contribution while rr indicates the correlation between COL numbers and COL precipitation. Panel (b): Climatology of the spatial pattern of COL days per year (1981-2017) summed over 2.5° X 2.5° grid boxes, along with the anomalies from this climatology for each of the drought years 2015, 2016 and 2017. The black square shows the region for which we identified Western Cape COLs. Panel (c): The spatial pattern of the climatology of COL precipitation per year (1981-2017), along with the anomalies from this climatology for each drought year 2015, 2016 and 2017.

Table 4.1: The average number of COL days occurring per year, per season and for each of the drought years.

	Annual	Summer	Autumn	Winter	Spring
Average no. of COLs.	9.8	1.5	2.8	3.1	2.4
2015	11.0	0.0	2.0	8.0	1.0
2016	13.0	3.0	5.0	5.0	0.0
2017	3.0	2.0	0.0	0.0	1.0

4.3 Patterns of COL Precipitation

The SOM analysis reveals that the spatial distribution of COL precipitation can be generally classified into four major patterns (Fig. 4.5), namely: NORP (no precipitation over the Western Cape); SERP (precipitation only over the south-east coast); WCRP (precipitation over only the west), and AORP (precipitation over most parts of the Western Cape). The first pattern (NORP; Node 9) features little or no precipitation over the entire Western Cape. This is the most dominant pattern, which accounts for 46% of COL occurrences over the region, this suggests that about 46% of COLs over the province produce little or no precipitation. This type of COL is quite deceptive, especially with forecasts from the South African Weather Service (SAWS) that often issue extreme precipitation warnings over the Western Cape whenever a COL is approaching the province. An example of such cases occurred in 2017, when in response to a SAWS forecast, the residents of the City of Cape Town prepared for an extreme precipitation event from a COL, with great expectations that it would provide relief from the severe drought. But it was a big disappointment, because the COL produced little precipitation (< 5 mm day^{-1}), even though it was characterised by strong winds and heavy clouds, as with any other COL. The atmospheric condition for NORP will be discussed in the next section. In contrast to NORP, the second pattern (AORP; Nodes 1, 2, 4 and 5) shows heavy precipitation (> 5 mm day^{-1}) over most parts of the province, with peak precipitation (up to 40 mm day^{-1}) occurring along the south coast. This pattern characterises about 22% of COLs over the province and shows the most widespread and intense precipitation of all the grouped patterns. Node 1 shows the highest peak in precipitation, suggesting that this COL precipitation pattern is responsible for heavy rain and floods in the region. The other two patterns (WCRP and SERP) characterise COLs that produce precipitation over only half of the province. While WRCP (Nodes 3 and 6; accounting for 15%) features precipitation over the western part of the province (with a precipitation peak over the WRA), SERP (Nodes 7 and 8; accounting for 17%) shows precipitation over the eastern part of the province (with a precipitation peak over the SRA). However, given the location of the Western Cape dams (Fig. 3.1), WRCP and AORP are the most important patterns for the Western Cape water supply, as these are the patterns that lead to precipitation over the dam areas.

The COL nodes (occurrence and precipitation; Figs. 4.6 and 4.7) have no preference for seasons, in that they can occur in any season. The only exception is Node 5, which does not occur in SON. Nevertheless, Node 1 mostly features and produces its maximum precipitation in MAM, Node 3 in JJA, and Node 6 in JJA (Figs. 4.6 and 4.7). In all seasons, Node 1 produces more precipitation than any other node, except in SON, when Node 4 gives the highest precipitation. With regard to the inter-annual variability of the COL nodes during the drought years, Fig. 4.6 reveals that some COL nodes occurred more frequently than normal in 2015 and 2016, suggesting that the COLs reduced the drought intensity in these two years. For instance, in 2015, Nodes 1, 3, 7 and 8 occurred more frequently than usual (Fig. 4.7) and produced more than their average seasonal precipitation. A comparison of our results with the SAWS synoptic maps[1] indicates that a Node 1 (an example of AORP) COL produced heavy precipitation over most parts of the Western Cape on 2 June 2015, and that a Node 3 (an example of WCRP) COL produced isolated showers over the western parts of the province on 3 and 10 June 2015. In 2016, Nodes 1, 5 and 7 also occurred more frequently than normal and released more than their average seasonal precipitation. A SAWS report[2] confirms that a Node 1 COL produced showers across the country on 26 July 2016. In contrast, in 2017, all COL nodes (except for Node 6) occurred less frequently and produced less than their average precipitation in all seasons. Node 6 (which is known for producing little or no precipitation) occurred more frequently in 2017, but only produced its normal seasonal precipitation. Hence, it can be deduced that the precipitation-bearing COLs helped to alleviate the drought in 2015 and 2016, but not in 2017.

[1] http://www.weathersa.co.za//media/data/publications//20150602.pdf
[2] http://www.weathersa.co.za//media/data/publications//20160727.pdf

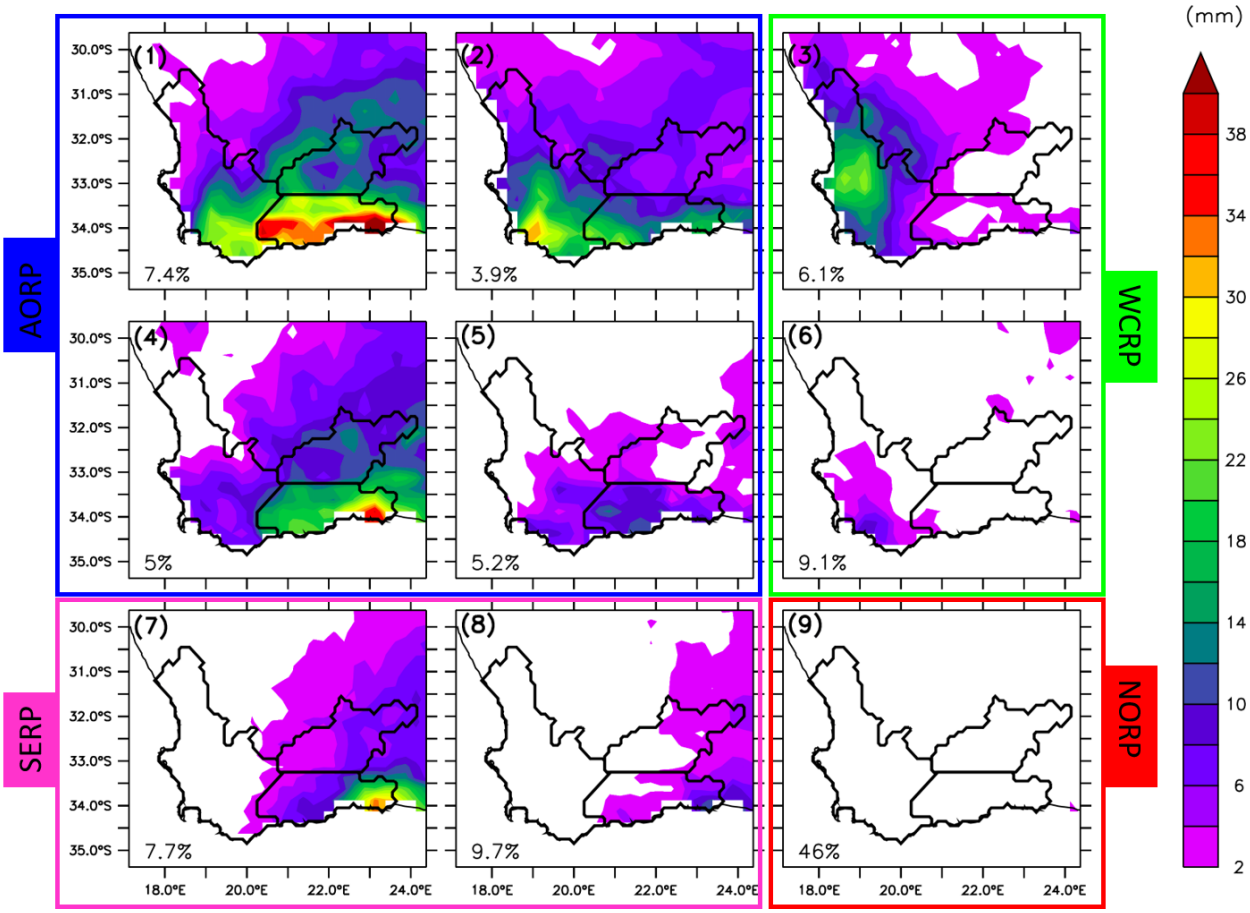

Figure 4.5: The SOM classification (3x3 nodes) of COL precipitation patterns over the Western Cape. The nodes are grouped into four main precipitation patterns: NORP (no precipitation over the Western Cape); SERP (precipitation only over the south-east coast); WCRP (precipitation over the only West Coast), and AORP (precipitation over most parts of the Western Cape). The percentage contribution of each node to the COL occurrence dataset is indicated in the node.

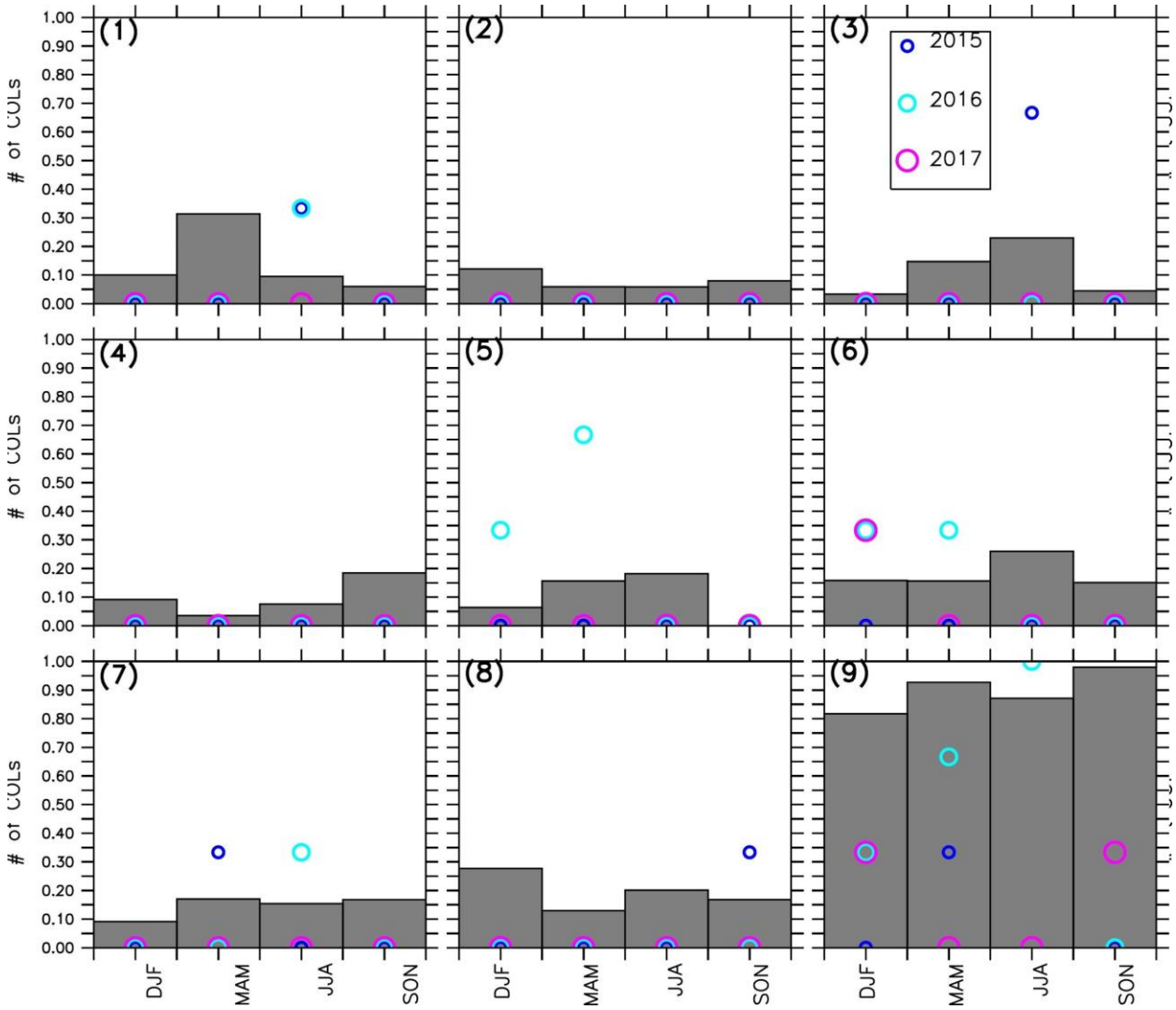

Figure 4.6: The seasonal variation of each COL node (events per season). The events per season for the drought years (2015, 2016 and 2017) are indicated with circles.

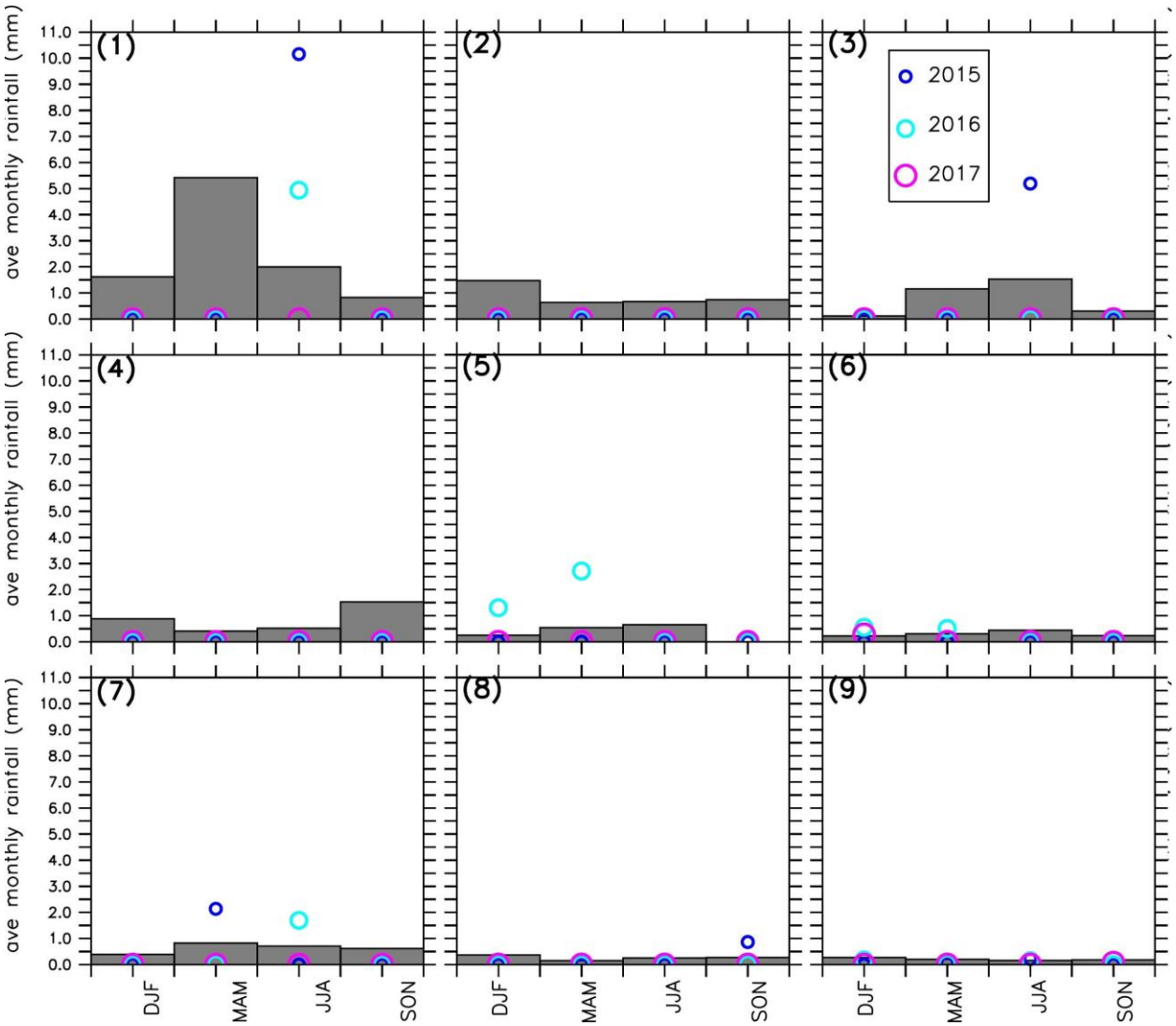

Figure 4.7: same as Fig. 4.6 but for COL precipitation.

4.4 The Composite of Atmospheric Conditions for the COL precipitation Patterns

There are some notable differences in the atmospheric conditions associated with the COLs in the various nodes (Figs. 4.8 and 4.9). For instance, in some nodes (i.e. Nodes 1, 4 and 7), COLs are associated with a strong pressure gradient, while other nodes (Nodes 3 and 9) have a weaker pressure gradient. Also, in some nodes, the COL is completely detached from the trough that produced it, while in others, it is still connected to the trough, with a northward orientation (in Nodes 1 and 7), or a north-east orientation (in Nodes 4, 5, 6 and 8), or a north-west orientation (in Nodes 2 and 3). Furthermore, although all the nodes feature precipitation east of the COL, the precipitation area is part of the COL's cyclonic flow in Nodes 1–8 but not in Node 9. Looking at the evolution of a node 1 and node 9 COL we can also see that the barotropic shear is weaker within a node 9 COL compared to a node 1 COL (Fig A14-A13).

The COL cyclonic flow in Node 9 is dry, and this dryness may be attributed to various factors. Firstly, the cyclonic flow is smaller and shallower than the other nodes. For example, the meridional width of the COL is less than 6 degrees wide in Node 9, but more than 10 degrees wide in Node 1. The low pressure center is about 5740 m in Node 9 and 5600 m in Node 1. This will influence the strength of the flow. Secondly, it seems that the COL in Node 9 is in its dissipating phase, as evidenced by its weak pressure gradient and its total detachment from the trough that generated it. Lastly, Node 9 lacks a well-organised transport of low-level moisture from the tropics towards the Western Cape, which is a prominent feature in all other nodes (Fig. 4.9). All the other nodes feature a strong moisture convergence zone, where the tropical easterly winds from the Indian Ocean meet the westerly flow from the Atlantic Ocean. This convergence belt acts as a conveyor through which moist air is transported from the tropics to the eastern part of the COL (i.e. over the Western Cape). In contrast, Node 9 features weak flows with weak convergence over most parts of the continent, as well as southerly flow (which deflects to the west) dominating over most parts of the Western Cape. As the southerly flow is usually dry, moisture flux divergence and little or no rain conditions dominate over the province.

Hence, the transport of moist air from the tropics to the Western Cape plays an important role in COL precipitation over the province. Higher precipitation values are seen when there is northerly moisture transport and strong convergence between this transport and the surface low. The position of the surface low furthermore determines the precipitation pattern. When the surface low circulation dominates the province, then more local precipitation occurs from the low, thus re-circulating moisture into the region; however, larger scale precipitation requires a northerly moisture input into the province.

The composite of the vertical structure of the wet and dry COLs (Nodes 1 and 9, respectively) indicates that there are notable differences between the systems (Fig. 4.10). Although both systems are cold-core lows, the dry COLs feature a weaker core than the wet COLs, because the dry COL is associated with weaker temperature and pressure gradients at all levels. For instance, at 500 hPa, while the core of the wet COLs is about 5°C colder and 100 m lower than its surroundings, the core of the dry COL is only about 2°C colder and 20 m lower than its surrounding. Hence, the dry COLs are weaker and less organised than their wet counterparts. In agreement with the thermal wind relationship, both wet and dry COLs strengthen with height, but the strengthening rate is much weaker in the dry COLs than in the wet COLs; consequently, the dry COLs reach a lower altitude than the wet COLs. The differences in the vertical structure of wet and dry COLs can be linked to the thermodynamics of the atmospheric conditions that initiate the COLs. Both systems form from a thermodynamic contrast between two air masses, viz. a warm air-mass (to the east) and a cold air-mass (to the west), but the contrast is higher for wet COLs than for dry COLs (Fig. 4.10). While the moist static energy of the cold air mass is almost the same in both wet and dry COLs, the moist static energy (MSE) of the warm air mass is lower in the dry COLs than in the wet COLs. For instance, within 20°E – 30°E, the MSE of the warm air mass is about 330 J kg^{-1} (i.e. below 400 J kg^{-1}) in the wet COL's atmosphere, but less than 322 J kg^{-1} in the dry COL's atmosphere. This is because the warm air mass is warmer and more humid than in the wet COL (i.e. 3°C and 8.0 g kg^{-1}) than in the dry COL. This is consistent with the presence of the southward transport of warm and moist air from the tropics in Node 1 and the lack of such transport in Node 9 (Fig. 4.10).

As discussed in section 3, the Western Cape gets some of its moisture from the South-East Atlantic and over South America which are transported via atmospheric rivers. The 2015-2017 drought decreased the transport of these moisture sources, however during the first two years of the drought COLs showed above average occurrence and precipitation. This indicates that these moisture sources may not be as important as they are for cold front systems. Ramos et al. (2019) also found an important moisture source for the Western Cape winter precipitation north of South Africa but were unsure whether this moisture source was from cloud bands which occur in the early or late winter months or from some other mechanism that occur throughout the winter months. Based on the results from this study it is clear that moisture flux from the tropics is important for COL precipitation and therefore COLs may be the mechanism behind this moisture source found by Ramos et al. (2019). However, looking at moisture flux and its convergence alone is not enough to conclude whether this is the case and therefore further study would have to be conducted.

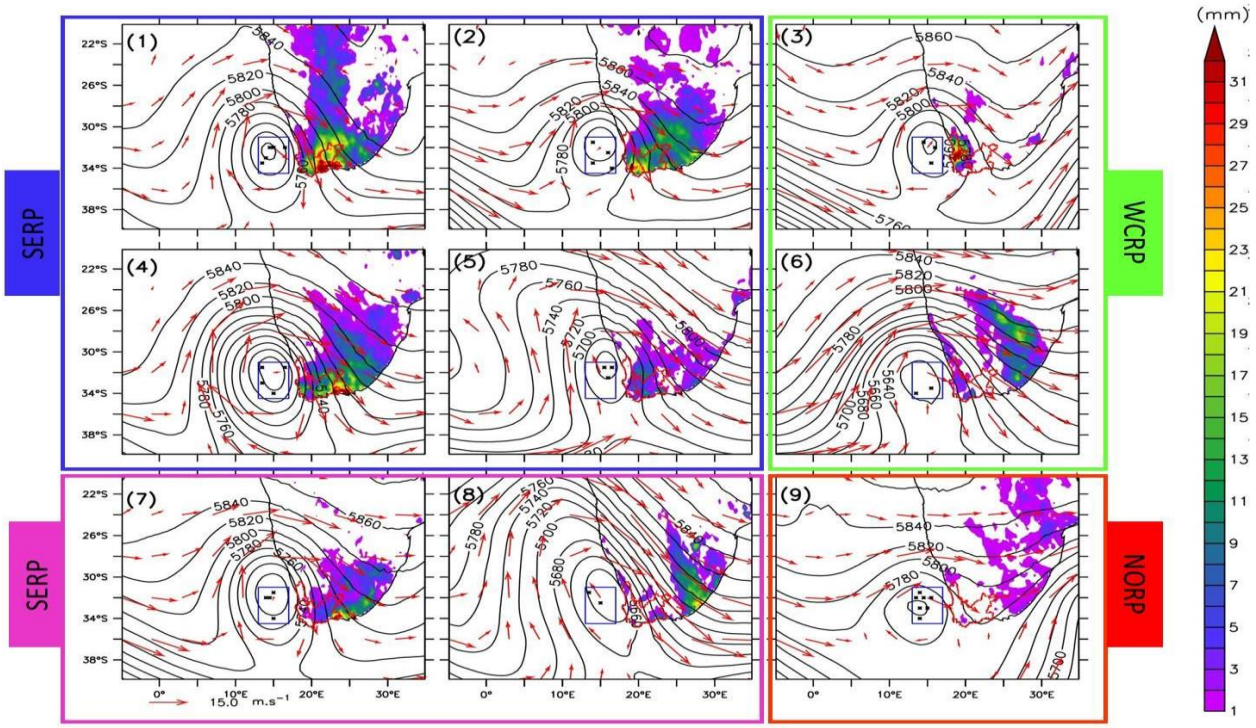

Figure 4.8: The composites of the 500 hPa geopotential height (m; contour) for the COL nodes shown in Fig. 4.5. The composites are only for COLs that are centered within the indicated blue box area; the black dots show the centers of the COLs. The associated precipitation patterns (mm; shaded) over South Africa are shown in the background.

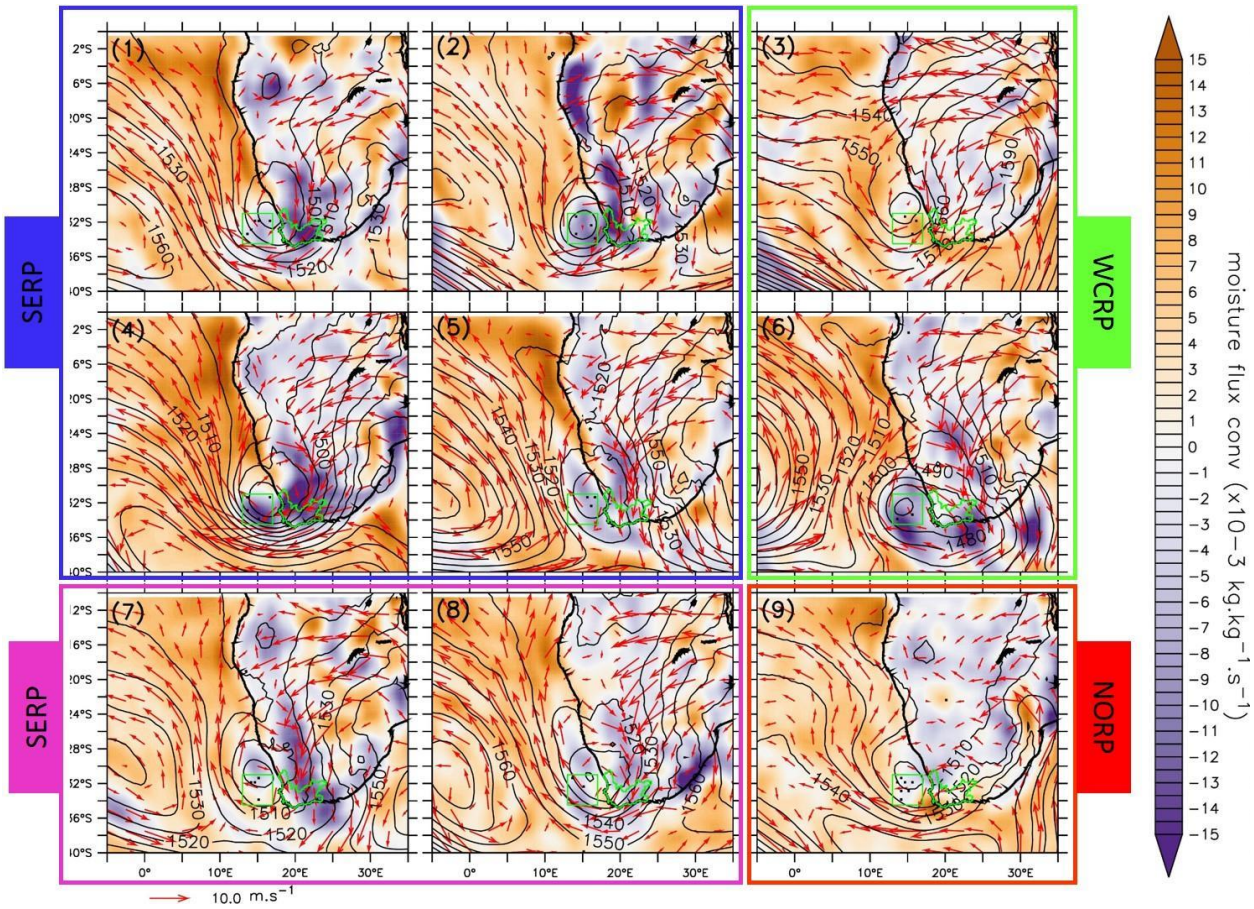

Figure 4.9: Same as Fig. 4.8 but for 850 hPa geopotential height (contour, m), 850 hPa winds (vectors), and integrated moisture flux convergence (shaded, x 10-3 kg.kg^{-1}.s^{-1}).

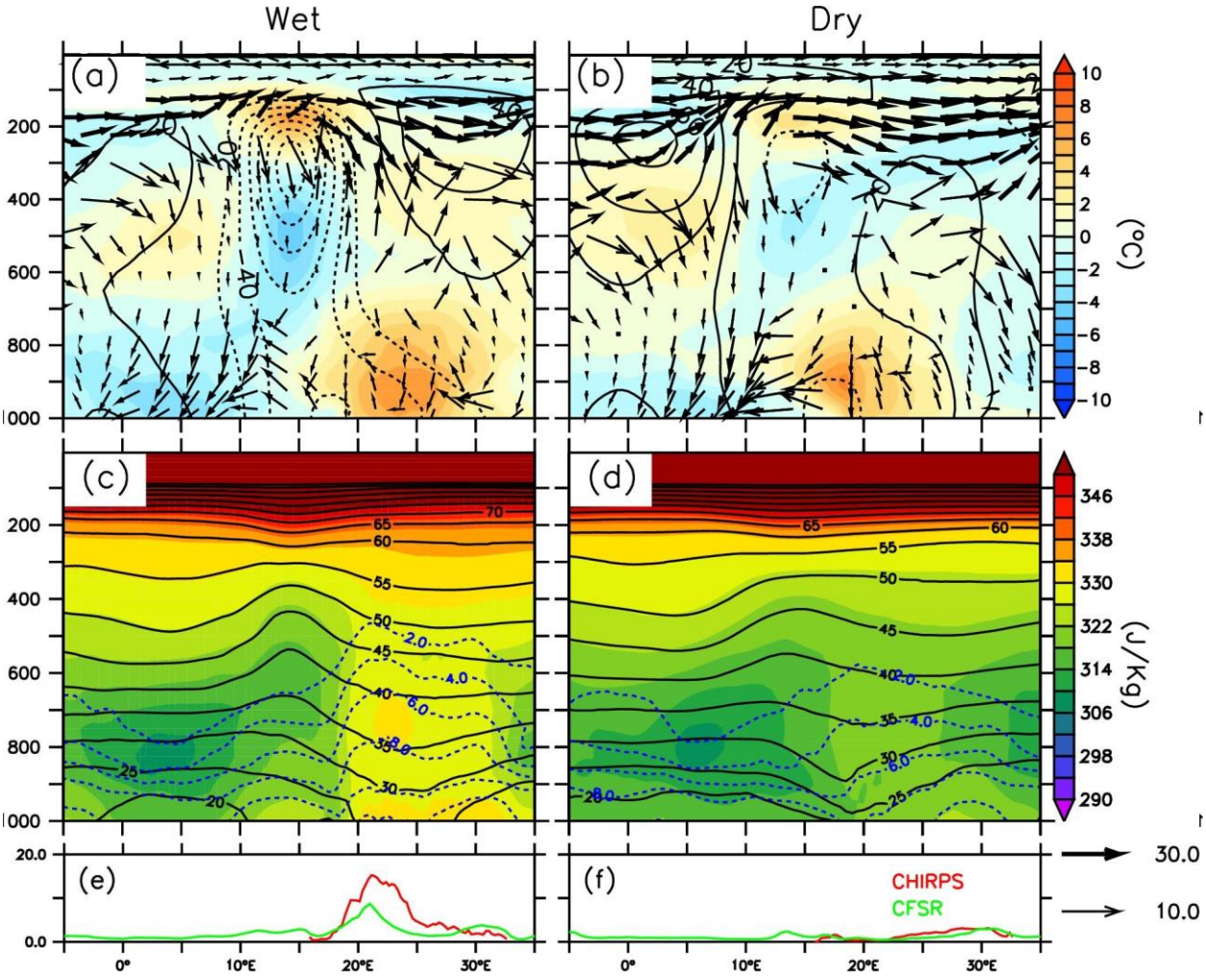

Figure 4.10: The vertical structure of Node 1 (wet) and 9 (dry) COLs and the associated atmospheric conditions. Panels (a) and (b) show the vertical cross section of zonal anomalies for temperature (shaded, ºC) and geopotential height (contour, m) with the associated zonal-vertical wind components (vectors). The thick vectors show wind vectors whose speeds are greater than 10 m.s^{-1}, and the thin vectors show wind speeds less than 10 m.s^{-1}. Panels (c) and (d) show the corresponding moist static energy (MSE; shaded, J.kg^{-1}), potential temperature (black contour, ºC) and specific humidity (blue dash, x 10-3 kg.kg^{-1}). Panels (e) and (f) show the associated zonal distribution of precipitation from CHIRPS (red line) and CFSR (green line). All the values are averaged between 31.5º - 34.5º S (The area chosen in Fig. 4.8 and 4.10).

Chapter 5 : Simulating Cut-off Low Precipitation over the Western Cape

This chapter evaluates the ability of the models in representing COLs over the Western Cape. First it examines whether the models were able to capture the general precipitation and synoptic feature over Southern Africa. We then discussed how well the models represent the spatial and temporal signal of COLs and COL precipitation over the Western Cape. The chapter then goes on to discuss whether the models were able to simulate the different COL precipitation patterns and dynamics over the Western Cape.

5.1 Simulating precipitation and Synoptic Features over Southern Africa

Figs. 5.1 and 5.2 show that both models (WRF and MPAS) correctly replicate the essential features in precipitation and circulation fields over Southern Africa at annual and seasonal scales. These features include the tropical precipitation peak within the intertropical convergence zone (ITCZ) and the west-east precipitation gradient south of 20^{o}S. The models furthermore agree with the observation and reanalysis datasets, viz. that most areas of the sub-continent (except the Western Cape) experience their highest precipitation in summer – December-January-February (DJF) – and the lowest in winter – June-July-August (JJA), and that the reverse is the case over the Western Cape. For both models, the pattern correlation (r) between the simulated data and the CHIRPS observations is more than 0.5 for both seasonal and annual results. The models also agree with the CFSR reanalysis on the positions of the high and low pressure systems over the region. As in CFSR, the models show the transport of moisture from the Indian Ocean (by the easterly flow) and the Atlantic Ocean (by the westerly flow) into the sub-continent. The convergence of these moisture fluxes results in a southward transport of tropical moist air over the region. In section 4.4 we discussed the importance of this

southward transport of moisture to the formation of COL precipitation over the Western Cape. Hence, it was found that both models realistically capture the synoptic drivers of COL and regional precipitation over Southern Africa.

Nevertheless, there are substantial biases in the simulated precipitation fields (Fig. 5.2). The magnitudes of the biases are generally larger in MPAS than in WRF. At the annual scale, MPAS overestimates precipitation along the tropical temperate troughs (TTT) band, i.e. precipitation and clouds that occur from tropical and extratropical synoptic interaction (Hart et al., 2013), with the maximum wet bias located in the tropics (about 8 $mm.day^{-1}$) and over the Drakensberg (about 6 $mm.day^{-1}$). In contrast, WRF underestimates the precipitation amount over the entire subcontinent, with the maximum dry bias (about -2 $mm.day^{-1}$) occurring in the northeastern parts of Southern Africa. Over the Drakensberg, the WRF simulation shows an added value by offsetting the dry bias in CFSR reanalysis, but MPAS overcorrects it with a wet bias. In the tropics, WRF corrects the wet bias in CFSR (about 1 $mm.day^{-1}$) with a dry bias of about -1 $mm.day^{-1}$, while MPAS amplifies the wet bias (by 4–6 $mm.day^{-1}$). However, the magnitudes and signs of these biases vary with the seasons. In MPAS, the magnitude of the tropical wet bias is more than 10 $mm.day^{-1}$ in the summer (DJF) but less than 2 $mm.day^{-1}$ in the winter, whereas the bias over the Drakensberg is up to 8 mm day^{-1} in the summer (DJF) but less than 2 $mm.day^{-1}$ in the winter (JJA). In the summer (DJF), WRF features a wet bias (about 4 $mm.day^{-1}$) over the Drakensberg and over the eastern parts of the tropical area, but a dry bias along the eastern coast. In other seasons, it shows a negative bias over the whole tropical area. Nevertheless, the bias of both models over the Western Cape is very small (<2 $mm.day^{-1}$ during all seasons).

The biases in the simulated precipitation over Southern Africa can be linked to biases in the simulated moisture flux over the region. The wet bias of the MPAS simulation in the tropics and over the Drakensberg occurs because the model overestimates the moisture transport from the north, leading to a stronger moisture convergence in the tropics and a stronger southwards moisture transport into the sub-tropics than is the case in the reanalysis. In contrast, the WRF simulation, which features a dry bias in the tropics, does

so because the westward transport of moisture from the Indian Ocean into the sub-continent deflects more northward in WRF than it does in CFSR, thus creating a dry bias over the eastern tropical region. Like MPAS, WRF also shows a stronger southward transport from the tropics than CFSR; however, this generally adds value, as it rectifies the dry bias seen in CFSR. This is true except in summer, when the greater southwards transport of moisture over the Drakensberg leads to a wet bias.

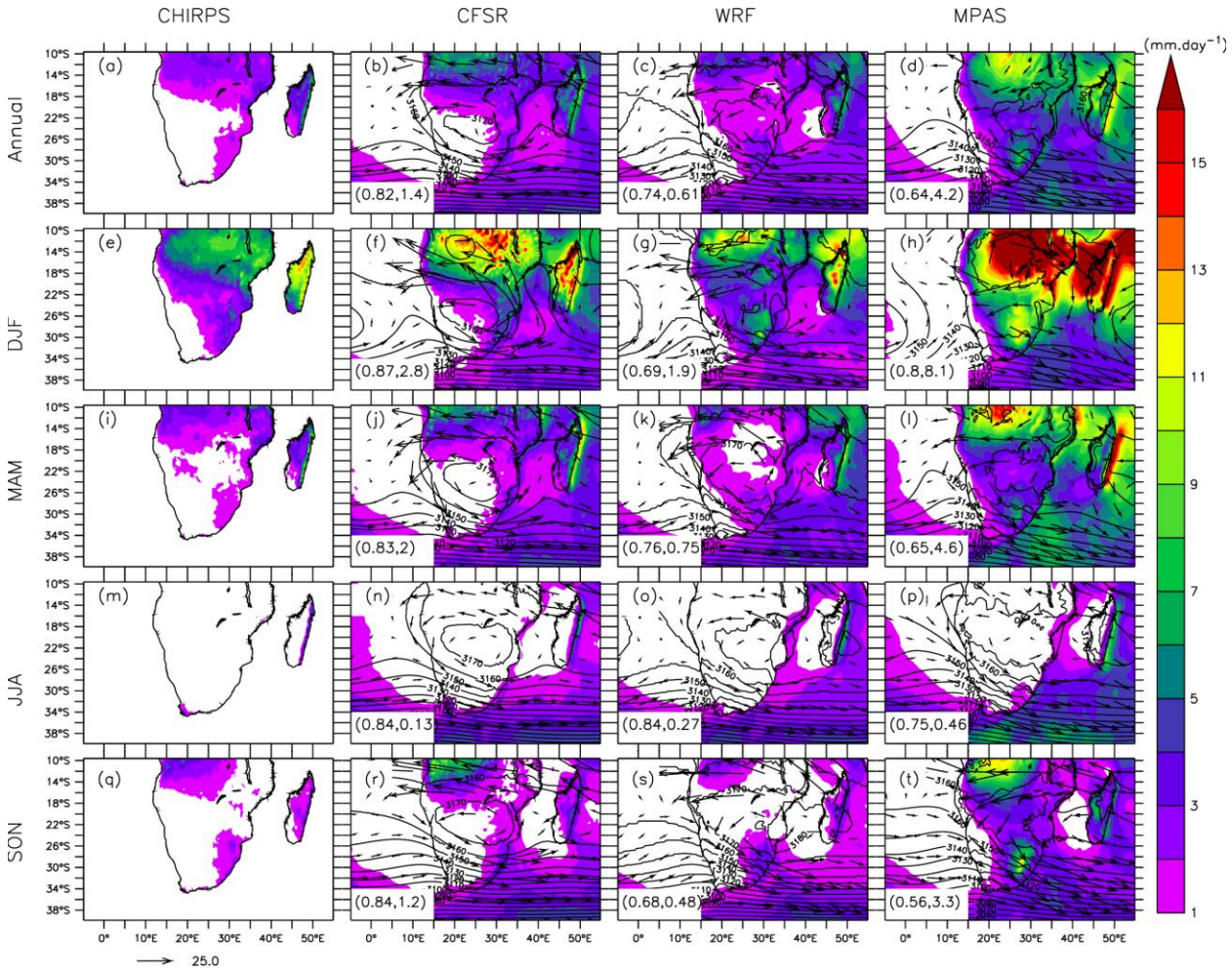

Figure 5.1: The spatial distribution of precipitation (shaded, mm.day^{-1}), 700 hPa geopotential height (contours, m) and 700 hPa moisture vectors (arrows) for the annual climatology (panels a – d), as well as the DJF (Summer; panels e – h), MAM (Autumn; panels i – l), JJA (Winter; panels m – p) and SON (Spring; panels q – t) climatology in 2007 – 2017, as observed by CHIRPS and depicted by CFSR, MPAS, and WRF datasets. The correlation and RMSE between each dataset and the CHIRPS observations is indicated in the brackets, respectively.

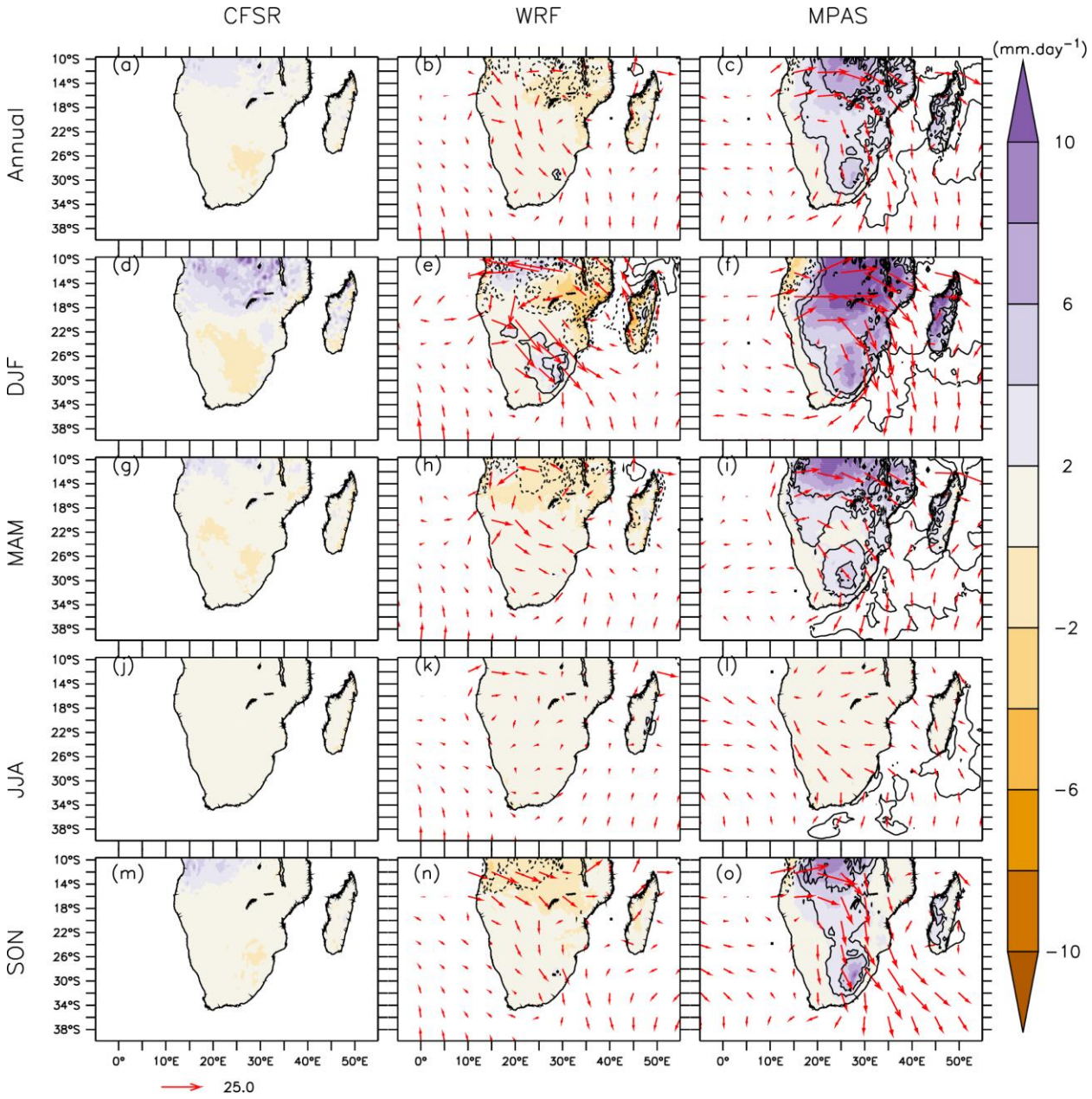

Figure 5.2: Biases in the spatial distribution of precipitation (shaded and contours of 2 mm.day^{-1}) and 700hPa moisture flux vectors (arrows, kg.m.s^{-1}) for annual climatology (panels a – c), as well as DJF (Summer; panels d – f), MAM (Autumn; panels g – i), JJA (Winter; panels j – l) and SON (Spring; panels m – o) climatology produced by the CFSR, MPAS, and WRF datasets. The CHIRPS observations are used as a reference for calculating the precipitation biases, while CFSR is used to calculate the geopotential and wind biases.

5.2 Spatio-temporal Variations in precipitation over the Western Cape

The two models (MPAS and WRF) give a credible representation of the spatio-temporal variation of precipitation over the Western Cape (Fig. 5.3). In agreement with CHIRPS, they show wetter conditions along the coasts (and over the Cape Mountain Belt) and drier conditions further north. The spatial correlation between the simulated and observed precipitation is more than 0.6 for MPAS and 0.86 for WRF. The RMSE is less than 250mm for MPAS and less than 75mm for WRF. Moreover, in general, they capture the annual cycle of precipitation over the province. However, the simulated precipitation does have some biases, the magnitudes of which are generally higher in MPAS than WRF. The most notable bias in the MPAS simulation occurs over the eastern parts of the province (in the summer rainfall area [SRA] and all year rainfall area [ARA]), where MPAS overestimates the annual precipitation (CHIRPS: <600 mm.year^{-1}r; MPAS: >900 mm.year^{-1}) by more than 300 mm.year^{-1} (Fig. 5.3). The overestimation, which occurs mainly in November to March (Fig. 5.3g and h), is an extension of the wet bias over the Drakensberg in MPAS (Fig. 5.2). The wet bias can be attributed to the stronger southward transport of tropical moisture toward South Africa in the model (Fig. 5.2). However, MPAS gives a better annual precipitation cycle than CFSR over the winter rainfall area (WRA), while WRF gives an annual precipitation cycle that is comparable to the observations (CHIRPS) over all the rainfall regimes (ARA, SRA and WRA). Over each of the rainfall regimes, the correlation of the WRF annual precipitation cycle with the observed data is strong ($r > 0.7$), the RMSEs are all less than 20 mm.month^{-1} and the bias is less than 20 mm.month^{-1}. In contrast, while the correlation between MPAS and the observed annual cycle is strong over the WRA and the SRA ($r > 0.7$), it is weak over the ARA ($r < 0.4$) (Fig. 5.3). The WRF simulation also performs better than MPAS at reproducing the inter-annual variability of precipitation over the Western Cape. While the correlation between the WRF and CHIRPS precipitation series is more than 0.6 (with a RMSE < 50 mm), the correlation between the MPAS and CHIRPS precipitation series is less than 0.1 (RMSE > 60mm). The worst discrepancy between MPAS and CHIRPS occurs in 2010 – 2012 and 2017. In 2010 and 2011, CHIRPS features a negative precipitation anomaly, but MPAS simulates

a positive anomaly. The reverse is the case in 2012. Moreover, while CHIRPS shows a negative precipitation anomaly for 2017, MPAS simulates a normal condition. In contrast, the WRF annual precipitation anomalies agree with the CHIRPS observations in most cases. The better performance of the WRF simulation in relation to MPAS may be attributed to many reasons. Firstly, it may be due to the lateral boundary condition in WRF (an RCM) and not in MPAS (a GCM). The forcing of the WRF simulation at the lateral boundary with CFSR data could force the simulation towards the reanalysis values. Secondly, the convective parameterisation scheme in WRF may be more realistic or better tuned than that of MPAS.

The two models have different perspectives of the 2015 – 2017 drought over the Western Cape (Figs. 5.4 and 5.5); overall, WRF performs better than MPAS in simulating the drought characteristics. For example, in agreement with CHIRPS observations, WRF shows that the drought persists for three years, with the largest water deficit in 2017, whereas MPAS indicates that the drought only persists for the first two years (2015 – 2016) with normal precipitation in 2017 (Fig. 5.4i). However, in the spatial distribution of the precipitation anomalies, both models feature their best agreement with CHIRPS in 2016 ($r = 0.27$, RMSE = 62 mm for MPAS and $r = 0.57$, RMSE = 53 mm for WRF) and their worst disagreement in 2015 ($r = -0.25$ for MPAS, RMSE = 63 mm and $r = 0.13$, RMSE = 54mm for WRF). In 2015, CHIRPS shows dry conditions over the WRA and wet conditions over the ARA. This agrees with previous studies (UMLINDI, 2015; Mahlalela et al., 2018), which showed wetter conditions over the ARA. WRF agrees with CHIRPS observations over the WRA, but disagrees with it over the ARA; meanwhile, MPAS gives an opposite pattern to CHIRPS. In 2016, all the datasets agree on dry conditions over the ARA and over part of the WRA. In 2017, the datasets (except MPAS) agree that the precipitation deficit covers most parts of the province and that the highest precipitation deficit (>100% below normal) occurs over the WRA; in contrast, MPAS, the outlier, simulates a precipitation surplus over most parts of the province, except over the western part of the WRA, where it indicates a weak precipitation deficit. MPAS also struggles to reproduce the monthly distribution of the anomalies as observed over each province

during the drought (for MPAS, -0.38 ≤ r ≤ 0.71 and 19 ≤ RMSE ≤ 47, while for WRF, 0.25 ≤ r ≤ 0.93 and 5 ≤ RMSE ≤ 28) (Fig. 5.5).

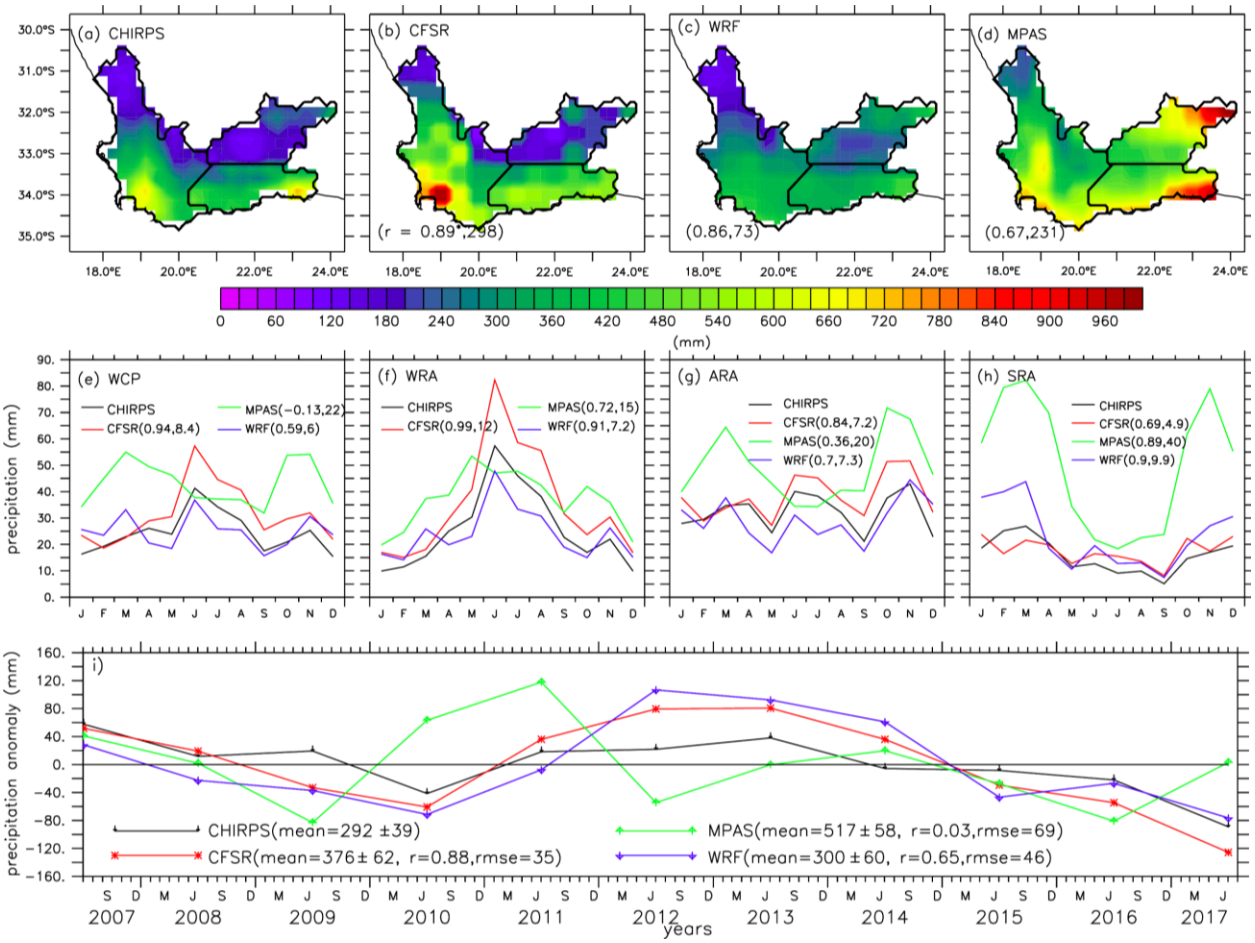

Figure 5.3: The spatial-temporal variation of precipitation over Western Cape as observed by the CHIRPS observations and depicted by the CFSR, MPAS and WRF datasets. Panels (a – d) show the annual precipitation amount (mm. year^{-1}), the middle panels (e – h) present the annual cycle of precipitation (mm.month^{-1}) for the whole Western Cape Province (WCP), the winter rainfall area (WRA), the all year rainfall area (ARA) and the late summer rainfall area (SRA), while the bottom panel (i) shows the inter-annual variability of the annual precipitation anomalies from the 2007-2017 climatology. The correlation and RMSE between each dataset and CHIRPS is indicated in brackets, respectively.

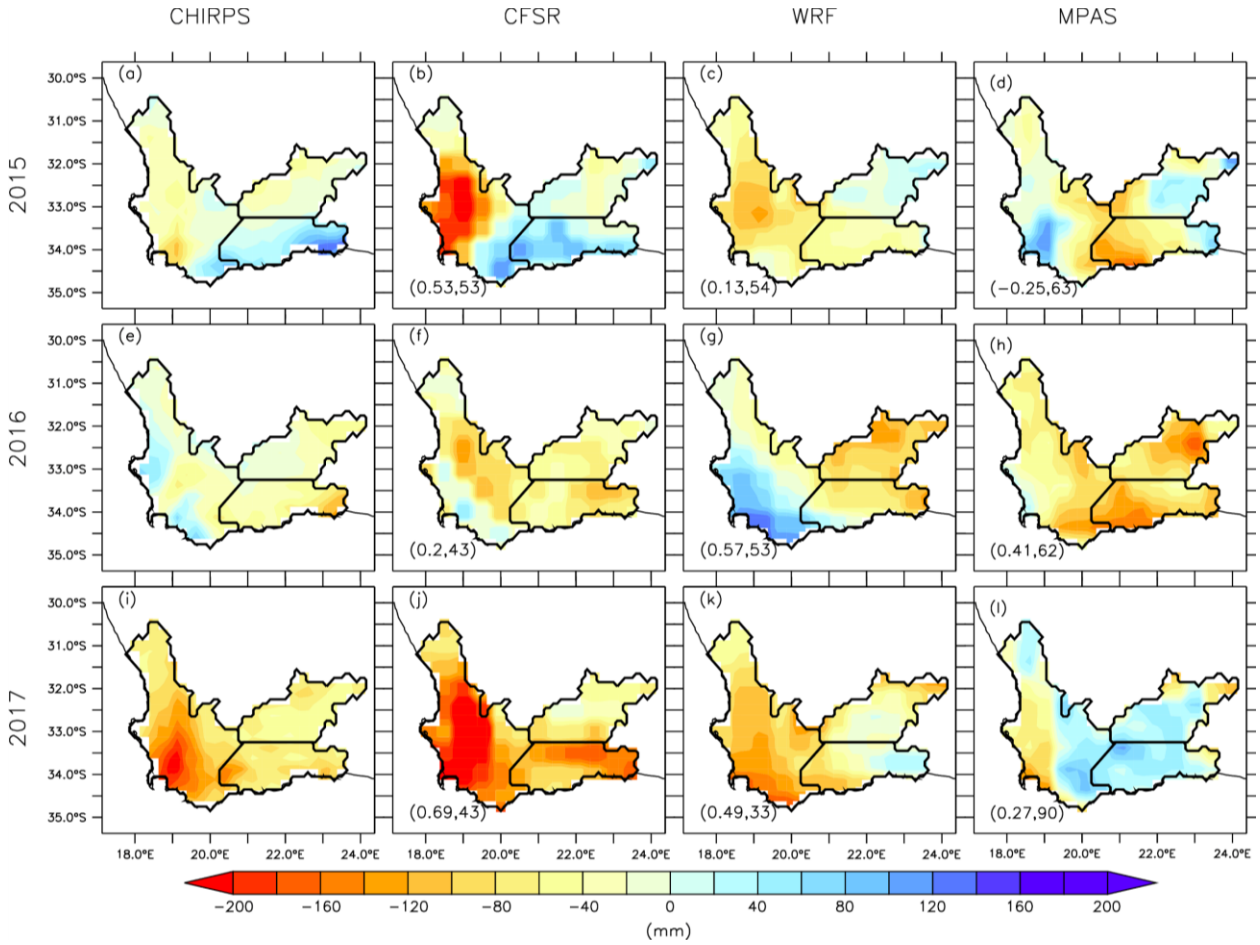

Figure 5.4: The spatial distribution of precipitation anomalies during the three years of drought (2015 – 2017), as observed by CHIRPS, and indicated by the CFSR, MPAS and WRF datasets. The correlation and RMSE between each dataset and CHIRPS is indicated in brackets, respectively.

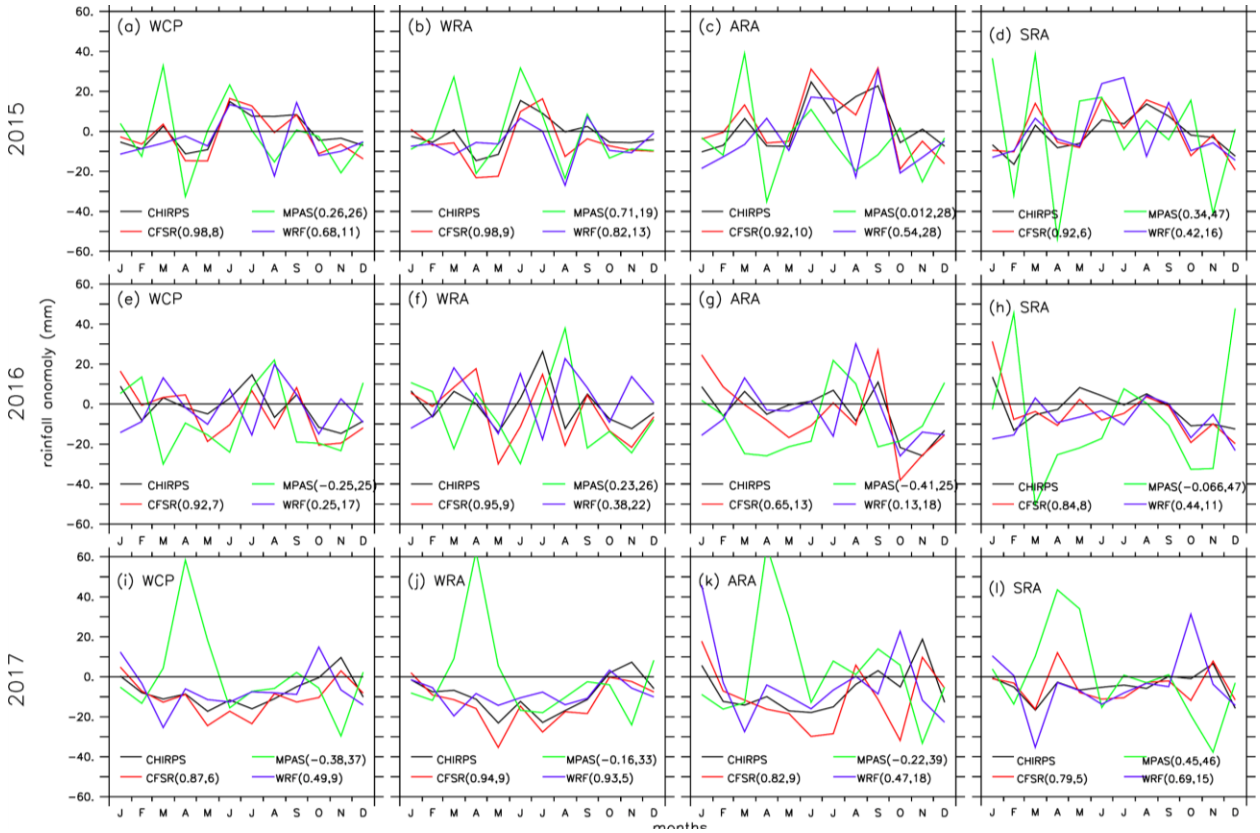

Figure 5.5: The intra-annual distribution of precipitation anomalies during the three-year drought (2015 – 2017) over the whole Western Cape Province (WCP), the winter rainfall area (WRA), the all year rainfall area (ARA) and the late summer rainfall area (SRA), as observed by CHIRPS and indicated by CFSR, MPAS and WRF. The correlation and RMSE between each dataset and CHIRPS is indicated in brackets, respectively.

5.3 Spatio-temporal Variations of COLs and Associated precipitation over the Western Cape

The two models (MPAS and WRF) agree with the CFSR reanalysis on the spatial distribution of the COL frequency over South Africa ($r > 0.5$). In the climatological fields (Fig. 5.6), the three datasets concur that the Western Cape is a hotspot for COL occurrences, although the frequency of the COLs over the Western Cape and surrounds is more pronounced in the simulations than in the reanalysis. This agrees with previous studies (e.g., Singleton and Reason, 2007b; Ndarana and Waugh, 2010; Engelbrecht et al., 2013; Favre et al., 2013). Given that COLs usually form from Rossby wave breaking, the hotspot in COLs over the Western Cape agrees well with the peak in Rossby wave breaking around the Western Cape (Ndarana and Waugh, 2010). The good agreement between the simulated and reanalysis distribution of the COLs shows that the models are correctly able to capture the dynamics behind COL formation over this area.

However, there are some discrepancies among the datasets on the inter-annual variability of the COL frequency over the Western Cape, especially during the 2015 – 2017 droughts (Fig. 5.6). For instance, in 2015, CFSR and MPAS feature positive anomalies (20% and 60% respectively), while WRF indicates a negative anomaly (-60% respectively); however, there is better agreement between WRF and CFSR ($r=0.37$) on the spatial distribution of the anomalies than between MPAS and CFSR (0.11). In 2016, WRF and MPAS simulate negative anomalies (60% each), while CFSR indicates a positive anomaly (40%); meanwhile, there is still a better agreement between WRF and CFSR ($r = 0.30$) on the spatial distribution of anomalies than between MPAS and CFSR ($r = 0.02$). In 2017, while MPAS simulates a normal COL frequency, WRF and CFSR feature negative anomalies, with a better agreement with the spatial distribution of the anomalies. In general, with reference to CFSR, WRF gives a better representation of spatio-temporal COLs over the Western Cape than MPAS does, possibly because the WRF simulation is forced at the lateral boundaries with CFSR, while MPAS is not. Heinzeller et al. (2016) compared the ability of MPAS and WRF to simulate the West African Monsoon. They found that MPAS captured the timing of the onset better than WRF, but that MPAS

overestimated the precipitation over the region. Similarly, Sakaguchi et al. (2016) found that MPAS simulated excess precipitation within the region of grid refinement, especially convective precipitation. This explains why MPAS overestimates precipitation over most of tropical Southern Africa. Sakaguchi et al. (2016) found that the increased resolution in MPAS influences the westerly jet and generally leads to a poleward shift in its position within the grid refined region. The position of the grid refinement also has varying remote effects on the westerly jet outside of the refined region. This may further indicate why our WRF simulation outperforms MPAS in terms of COL frequency, as the westerly jet is sensitive to the grid refined region.

With reference to the CHIRPS observations, both models (WRF and MPAS) give a realistic climatology of COL precipitation over the Western Cape, but the WRF simulations outperform those of MPAS (Figs. 5.6 and 5.7). The spatial correlation between the WRF and CHIRPS climatology is about 0.85 (Fig. 5.7c), while the one between MPAS and CHIRPS is less than 0.5 (Fig. 5.7d). The major shortcoming in the MPAS results is the location of the maximum COL precipitation over the SRA instead of over the ARA. This shortcoming is an extension of the MPAS wet bias over the Drakensberg (as discussed in Section 3.2). However, both models struggle to reproduce the temporal variability in COL precipitation, especially during the 2015 – 2017 drought period (Fig. 5.6b). The correlation between the time series of the simulated and observed COL precipitation is less than 0.25 for both models ($r = 0.22$ for WRF; $r = -0.20$ for MPAS). While WRF agrees with the CHIRPS observations on the negative COL precipitation anomaly in 2017, it disagrees with the observations on the positive anomalies in 2015 and 2016. Conversely, MPAS agrees with CHIRPS on the positive COL precipitation anomaly in 2015 and disagrees with the positive anomaly in 2016 and the negative anomaly in 2017. Therefore, while the CHIRPS observations show that the positive anomalies in COL precipitation reduce the drought intensity in the first two years (2015 and 2016), and while the negative anomaly intensifies the drought intensity in 2017, WRF indicates that the negative COL precipitation anomaly contributes to the drought over the three years, while MPAS simulates that the negative COL anomaly only contributes to the drought in 2016. The disagreement between the simulated and observed COL precipitation also features in the

spatial distribution of the COL precipitation anomalies during the droughts ($r < 0.47$ and RMSE > 18 mm). For instance, while CHIRPS shows that negative COL precipitation anomalies cover the entire province in 2017, WRF and MPAS indicate that they only cover parts of the province in 2017.

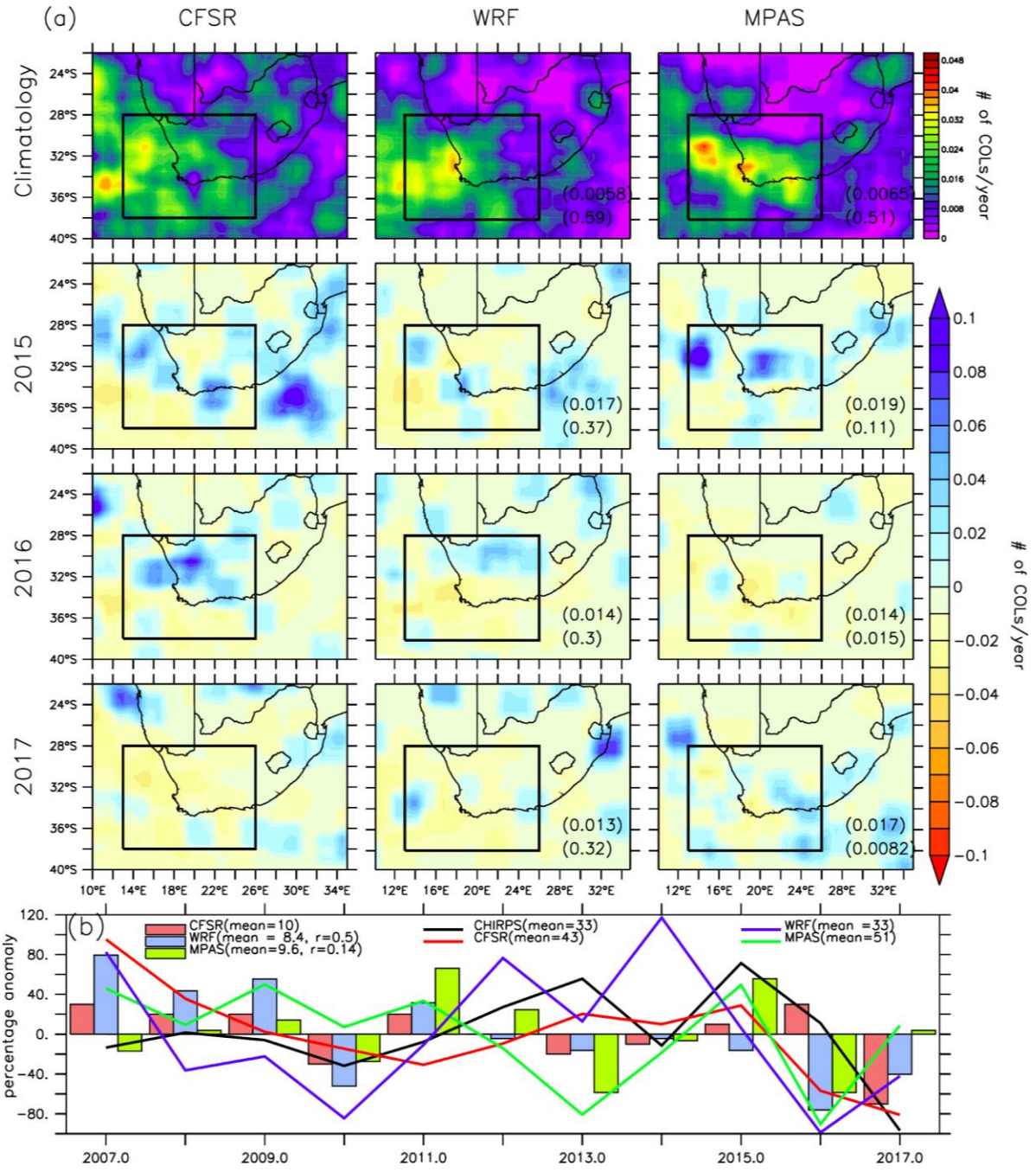

Figure 5.6: Panel (a) shows the average spatial pattern of numbers of yearly COL days (1981 – 2017), along with the COL anomalies of the number of COL days for each of the drought years (2015 – 2017). All the COL day-related spatial patterns have been smoothed using 6-grid boxcar smoothing. The black square shows the region for which we identified Western Cape COLs. The correlation and RMSE between the model results and that of CFSR are indicated in the brackets. Panel (b) shows the percentage anomaly of COL numbers and COL precipitation, along with the percentage of contribution of COL precipitation to the annual precipitation of the Western Cape for CFSR COLs and CHIRPS precipitation, CFSR, MPAS and WRF. The correlation between the COL numbers in the model data and CFSR is indicated by r.

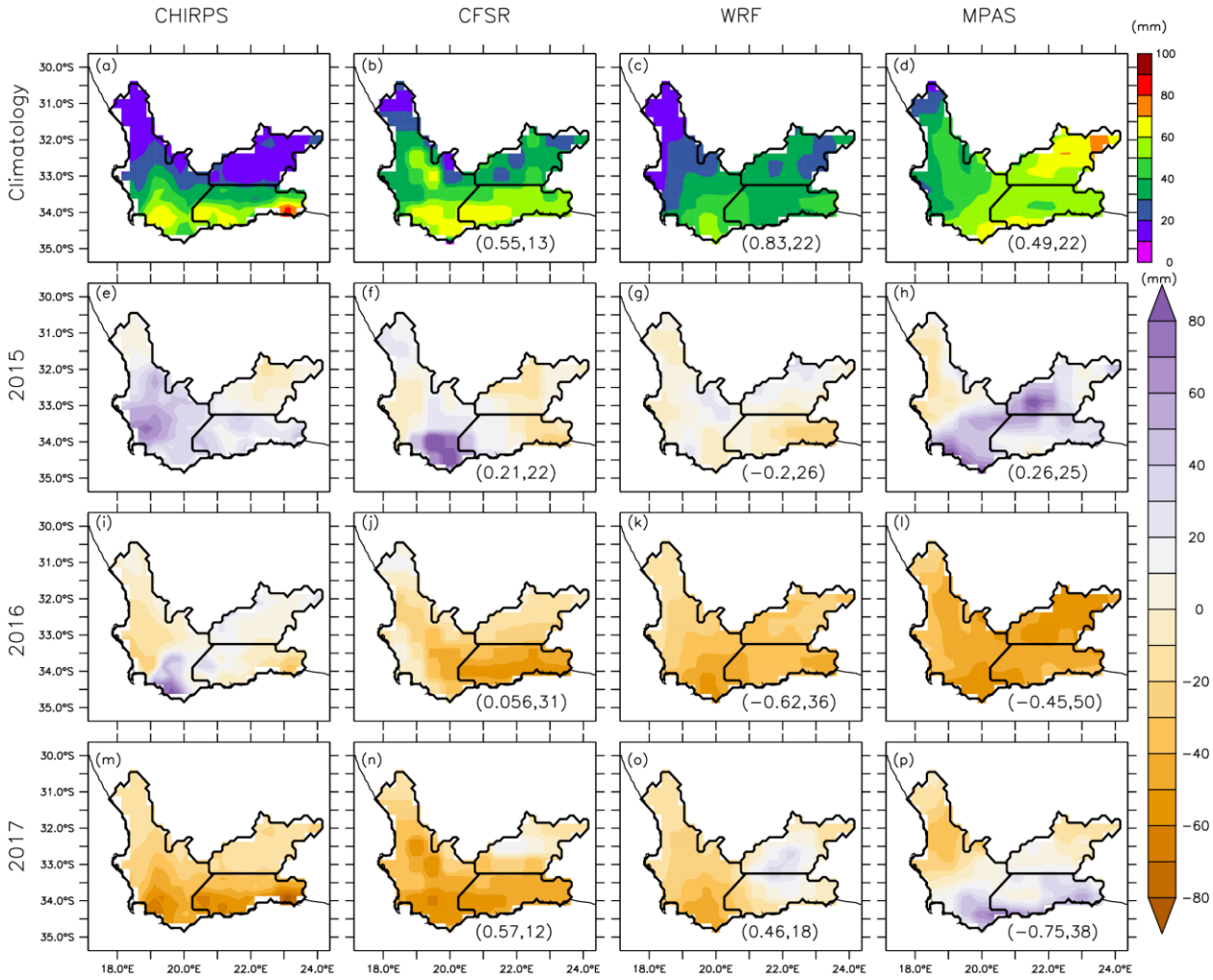

Figure 5.7: The climatology of annual COL precipitation (panels a – d; in 2007 – 2017) and the anomalies from this climatology during the three drought years (i.e., 2015 – 2017), as observed by CHIRPS and depicted by CFSR, MPAS and WRF. The correlation and RMSE between each dataset and CHIRPS is indicated in the brackets, respectively.

5.4 Simulating the Major Patterns of COL precipitation over the Western Cape

The SOM analysis shows that the COL precipitation distribution over the Western Cape can be classified into four main patterns (Fig. 5.8). The first pattern (hereafter, AORP) features precipitation over the entire province, but with a peak precipitation over the south coast (Nodes 1, 2, 4 and 5); this pattern constitutes 25.3% of the dataset. The second pattern (hereafter, WCRP – Nodes 3 and 6) shows the peak precipitation over the western part of the province and accounts for 17.7% of the dataset. The third pattern (hereafter, SERP – Nodes 7 and 8) features the peak precipitation over the eastern part of the province and makes up 19.4% of the dataset. The fourth pattern (hereafter, NORP) shows little or no precipitation over the whole province (i.e., Node 9) and accounts for 38% of the dataset. These SOM patterns are similar to those obtained by in section 4.3 using only CHIRPs data, which suggests that the addition of the simulated COL precipitation distribution does not alter the grouping of the SOM results. In section 4.4 we discussed the different synoptic circulations associated with each group pattern and showed that the wet COL patterns (e.g. AORP) are associated with a stronger horizontal pressure gradient and a more organised southward transport of tropical moisture toward the Western Cape than the dry COL pattern (i.e., NORP).

Both models give good and comparable contributions of COL precipitation patterns (Fig. 5.8). Their percentage contributions to the SOM nodes compare well with the observations in AORP (Nodes 1, 2, 3 and 4) and WCRP (Nodes 3 and 6). Nevertheless, the models underestimate the frequency of NORP: each model only contributes 18% of the pattern, while CHIRPS accounts for more than 38%. This suggests that their convective schemes may be too sensitive in triggering convection from the weak convergence provided by dry COL dynamics. It could also be that the simulated moisture convergence is stronger than the observed. Unfortunately, it is difficult to diagnose this further, because the CFSR reanalysis that could serve as a reference for the link between the precipitation and moisture flux convergence also underestimates the frequency of NORP by accounting for less than 26% of the pattern. In contrast, the models

overestimate the frequency of node 8 in SERP where WRF contributes > 35% and MPAS > 30% but CFSR accounts for < 25% and CHIRPS < 10%. MPAS also overestimates node 7 in SERP (MPAS > 45%, CHIRPS < 25% and CFSR < 15%). The largest contribution of the MPAS model to this pattern can be attributed to the extension of the wet bias to the Western Cape (Fig. 5.2). Nevertheless, there is good agreement between the models and the observations on the seasonal distribution of all the COL precipitation patterns. For instance, they concur with the observations that, while each pattern can occur in all the seasons, AORP is most frequent in September-October-November (SON), WCRP is most frequent in JJA and NORP occurs more during March-April-May (MAM).

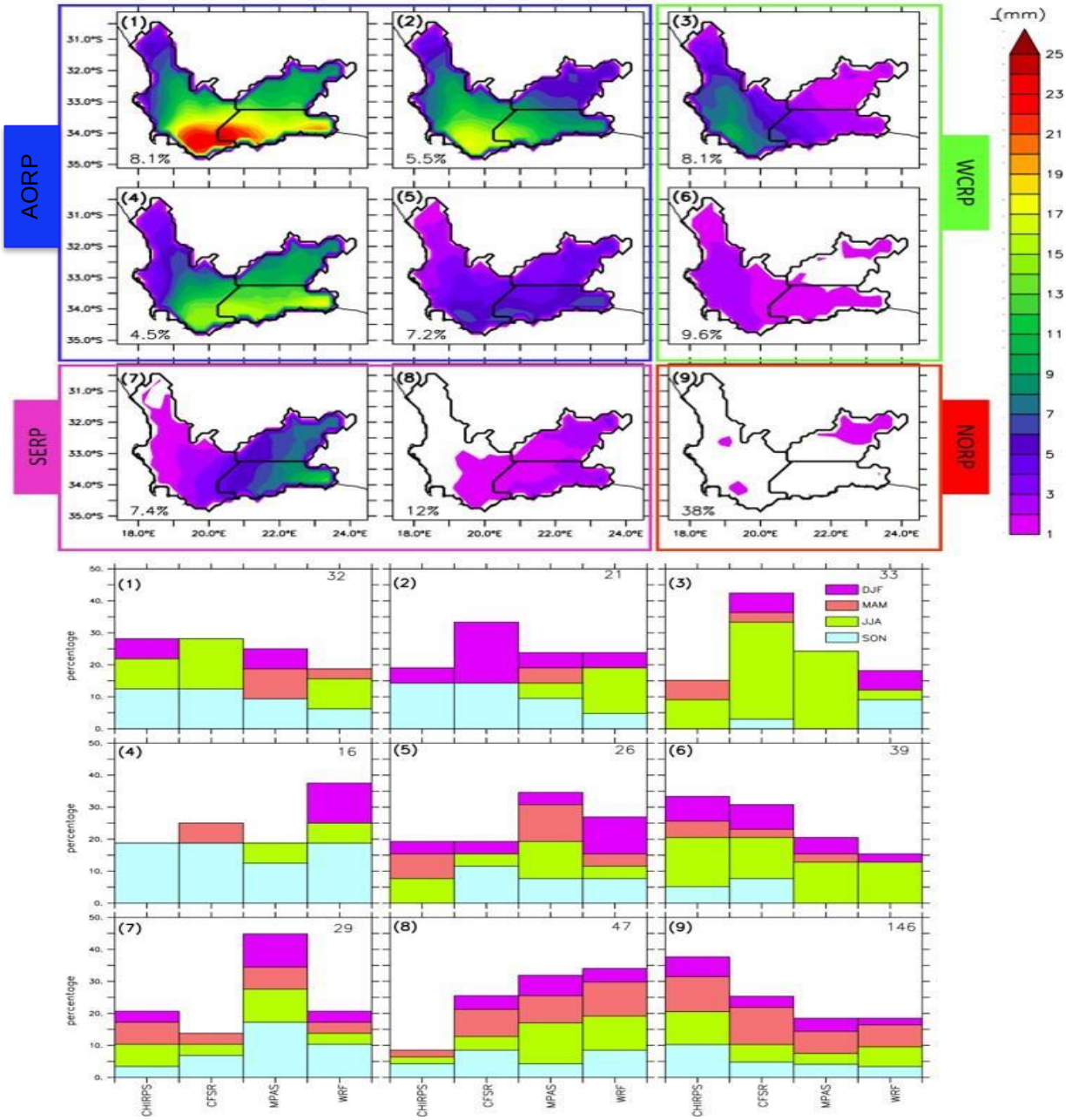

Figure 5.8: The top panel shows the SOM classification (3x3 nodes) of COL precipitation patterns over the Western Cape. The nodes are grouped into five main precipitation patterns: NORP (no precipitation over the Western Cape; node 9); SERP (precipitation only over the south-east coast; nodes7 and 8); WCRP (precipitation only over the West Coast; nodes 3 and 6), and AORP (precipitation over most parts of the Western Cape; nodes 1, 2, 4 and 5). The percentage contribution of each node to the COL occurrence dataset is indicated in the node. The bottom panel shows the percentage of the total number of nodes in each SOM node and season for the period 2007 –2017.

5.5 Simulating the Structure of Wet and Dry COLs

To examine how well the models (MPAS and WRF) capture the structure of COLs, we present the horizontal and vertical structures of three wet COLs (one from each dataset: CFSR, MPAS and WRF) in Fig. 5.9 and three dry COLs in Fig. 5.10. To ensure a fair comparison, all the selected wet COLs are from Node 1, while all the selected dry COLs are from Node 9. In addition, the centers of all the selected COLs fall within a 2^o x 2^o boxed area (i.e., 32^o – 36^o S and 14^o – 16^o E). However, within this boxed area, it was difficult to obtain wet (or dry) COLs with the same dates in the three datasets. As a result, the selected three wet (or dry) COLs all have different dates in the datasets.

The simulated wet COLs (WRF and MPAS) have a similar structure (horizontal and vertical) as in the reanalysis (CFSR) (Fig. 5.9). In the horizontal structure (Figs. 5.9a – f), the three datasets feature a synoptic-scale low pressure system (5660, 5650, 5690 m at 500 hPa for CFSR, WRF and MPAS, respectively), detached from the mid-latitude westerly flow located south of the low. Associated with the low-pressure is a low-level north-westerly flow, transporting moisture from the tropical Atlantic Ocean to most parts of Southern Africa, specifically towards the Western Cape. Although there is another transport of low-level moisture (by the north-easterly wind) from the Indian Ocean into the continent, the moisture is directed towards the eastern part of South Africa and not towards the Western Cape. However, the models and CFSR results agree that the southward transport of tropical moisture (mainly from the tropical Atlantic Ocean) fuels COL precipitation over the Western Cape. In the vertical structure (Fig. 5.9g – i), the three datasets indicate that the low pressure is a cold-core system that tilts westward with height. The coldest core (i.e., the largest zonal temperature anomaly: -10^oC, -8^oC and -2^oC in CFSR, WRF and MPAS, respectively) occurs at 500 hPa, while the deepest low (i.e., the largest geopotential anomaly: -100m, -240m, -100m in CFSR, WRF and MPAS) is at 250 hPa. All the datasets feature a warm moist air mass east of the cold core. This warm air mass, which extends from the surface to the upper levels of the atmosphere, is the moisture-laden tropical air from the tropical Atlantic Ocean towards the Western Cape. The moist static energy (MSE) of the warm air mass is higher than that of the cold-core air (especially below 500 hPa), meaning that the warm air mass is more buoyant than the

cold air mass. Hence, at the interface, the warm air mass rises, while the cold-core air mass sinks. This is evidenced by the upward wind vectors in the warm air mass and the downward wind vectors in the cold air mass. All the datasets show that the rising of the warm air mass at the interface is responsible for the COL precipitation east and south of the low pressure center.

The models also agree with CFSR that, while the structures of the wet and dry COLs have some features in common, there are notable differences between them (Figs. 5.9 and 5.10). For instance, in all three datasets, the dry COLs still feature the low pressure system that is detached from the mid-latitude westerlies, and the associated north-westerly flow still transports moist air from the tropical Atlantic Ocean towards the Western Cape. However, the MSE of the tropical moist warm is lower in the dry COLs (< 3 $J.kg^{-1}$ at 700 hPa, for all the datasets) than in the wet COLs (> 4 $J.kg^{-1}$ at 700 hPa, for all the datasets). This is because the air mass is less warm and less moist in the dry COLs than in the wet COLs. This implies that the tropical warm and moist air that fuels COL precipitation over the Western Cape is less buoyant in dry COLs. This is evidenced by the weaker horizontal temperature gradient between the warm and cold air masses (a -2^{o}C temperature anomaly in the cold air mass for all the models) and the shallower low pressure center (-10m, -120m, -30m for CFSR, WRF and MPAS) in dry COLs. Hence, the three datasets indicate that the dry COLs are weaker than the wet COLs, and that they produce little or no precipitation over the Western Cape, because the tropical air mass that fuels the COLs is colder and drier in the dry COL than in the wet COL. These results align with our findings from section 4.4 and previous studies. In section 4.4 we discussed the importance of the warm, moist air mass in the formation of COLs. Molekwa et al. (2014), who classified COLs as low, medium or high precipitation inducing COLs over the Eastern Cape of Southern Africa, found that the most important factors in this classification are the surface conditions and the positions of the surface lows. This is consistent with our results because the surface conditions over the sub-continent influence the temperature and moisture of the warm moist tropical air mass, as it moves towards the Western Cape. Porcù et al. (2007) similarly studied the vertical structure of COLs over the Mediterranean and found that precipitation is determined by the surface

low and the depth of the COLs, with deeper COLs producing more precipitation. This is also evident in our model simulations, as the dry COLs all show a shallower low pressure center.

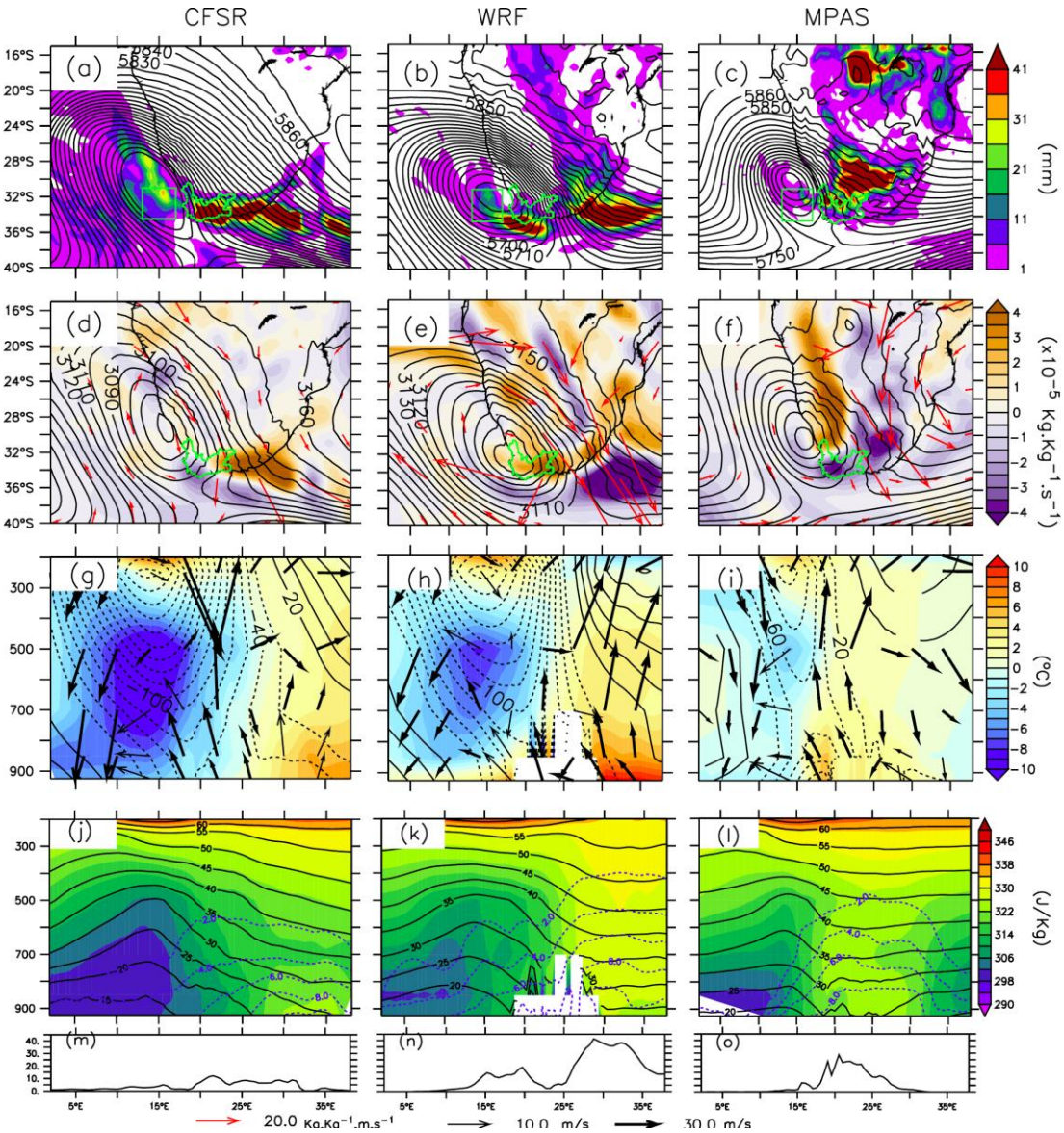

Figure 5.9: The horizontal and vertical structure of a wet COL as depicted by CFSR, WRF and MPAS. Panels (a – c) show the horizontal distribution of the precipitation (shaded, mm.day^{-1}) and 500 hPa geopotential height (contours, m), while Panels (d – f) show the corresponding vertically integrated moisture flux (arrows), vertically integrated moisture flux convergence (shaded) and 700 hPa geopotential height (contours). Panels (g – i) present the vertical cross-section of zonal anomalies for temperature (shaded, ^{o}C) and geopotential height (contour, m) with the associated zonal-vertical wind components (vectors). The thick vectors show wind vectors whose speeds are greater than 10 m.s^{-1}, whereas the thin vectors show wind speeds less than 10 m.s^{-1}. Panels (j – l) show the corresponding moist static energy (MSE) (shaded, J.kg^{-1}), potential temperature (black contour, ^{o}C) and specific humidity (blue dash, x10^{-3} kg.kg^{-1}). Panels (m – o) show the associated zonal distribution of precipitation. All the values are averaged between 30.4^{o} and 34.8^{o} S. All the COLs are taken from Node 1 (in Fig. 5.8) and their centers fall within the area demarcated with the box indicated in panels (a – c).

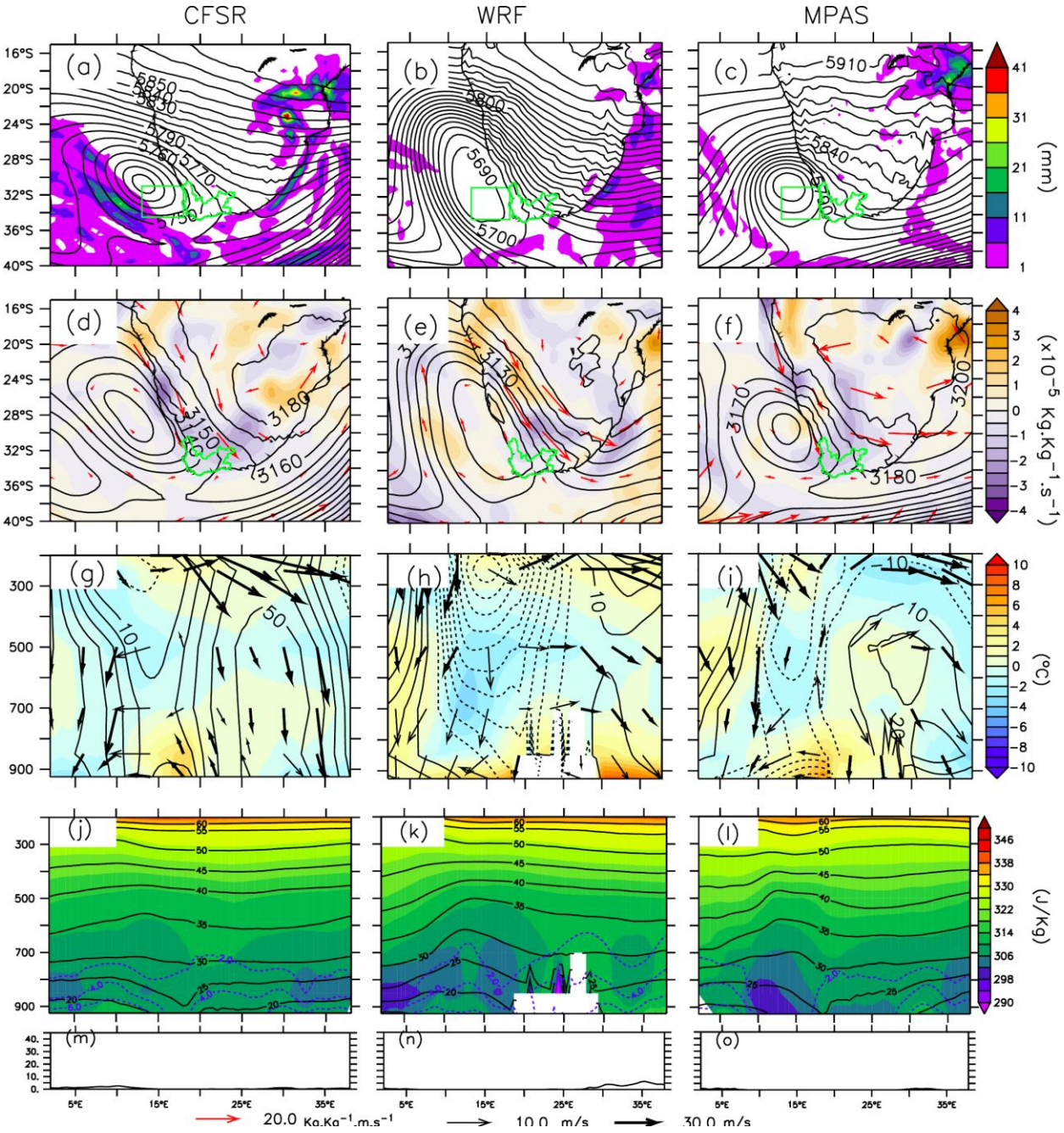

Figure 5.10: Same as Fig. 5.9, but for dry COLs taken from Node 9 (in Fig. 5.8).

Chapter 6 : The Influence of Topography on Cut-off Lows over Southern Africa

This chapter explores the influence of topography on COLs over Southern Africa. The chapter looks at the formation, track and precipitation of three different COLs in multi-ensemble simulations and discusses how the topography sensitivity experiments influence these characteristics. The vertical structure of a COL and the influence of topography on this structure is also analysed.

6.1 Characteristics of COLs in the Control Experiment

There are some similarities in the characteristics of the three COLs identified in June 2015. The COLs feature a similar pattern in their tracks (Fig. 6.1). They all first travel in a northerly direction, and then move in a south-easterly direction, before following an easterly direction. This pattern could be due to the influence of the westerlies (i.e. the waves and flow direction). This is in agreement with Favre et al. (2013), who show that COLs move in an easterly direction over South Africa due to the background flow. Fig. 6.1 also shows that the three COLs have a similar response to the perturbation in the initial conditions. For the three COLs, all the simulation ensemble members follow the same general track pattern. This is also true for the precipitation (Fig. 6.2). While the ensemble mean shows lower values of precipitation, the timing and peaks and dips in precipitation amongst the ensemble members are generally similar (Fig. 6.2). This indicates that the general track pattern and precipitation signal are robust, meaning that it is not sensitive to the initial condition perturbation.

Despite the above similarities among the COLs, there are notable differences among them regarding the location of their genesis, tracks and precipitation amounts. Firstly, all three COLs have different genesis points (Fig. 6.1). While COL1 and COL2 originate over the ocean, the formation of COL1 (i.e. at 15.64°E, 32.07067°S) occurs more than 518 km

north-east of COL2 (i.e. at 10.14°E, -31.97°S). And, in contrast to these two COLs, COL3 forms over the continent. Secondly, the uncertainty in the genesis position (due to initial condition perturbations) is higher for COL3 than for the other two COLs. This may be because COL3 forms over the continent, while the other two (COL1 and COL2) form over the Atlantic Ocean. The continental boundary layers are usually more unstable (and may be more sensitive to initial condition perturbation) than the marine boundary layers. Thirdly, the COLs differ in the extent of their meridional movement over the continent. While the movement of COL1 and COL3 is mostly south-easterly over the continent, the movement of COL2 is mostly easterly. COL1 shows the largest amounts of precipitation compared to the other two COLs (Fig. 6.3), and its precipitation seems to peak towards the end of its lifespan (Fig. 6.2). This is not surprising, as greater releases of latent heat tend to dissipate COLs, which may be why the COL lifespan ends shortly after the peak in precipitation (Pinheiro et al., 2017). COL3 produces less precipitation than COL1 but its peak precipitation also occurs towards the end of its lifespan (Fig. 6.2). COL2, in contrast, shows the lowest amount of precipitation, and its peak in precipitation occurs towards the beginning of its track (Fig. 6.2). In terms of the ensemble spread, COL1, like its track, shows less spread than the other two COLs, thus indicating a system whose precipitation is less sensitive to initial conditions (Fig. 6.2). Therefore, while the COLs do show general similarities in their tracks, the differences in the regions of genesis, the tracks, the precipitation signal and the influence of the initial conditions mean that it is necessary to analyse each of the COL events in detail.

The COL characteristics in WRF compare well with those in the driving dataset (FNL) (Figs. 6.1 - 6.4). In both WRF and FNL datasets, the directions of COL movement with the associated spatial distribution of synoptic temperature and precipitation are similar. However, there are notable differences between the two datasets. In FNL the tracks of COL2 and COL3 are located west of those simulated in WRF and the COLs do not travel as far east as in the WRF simulations. This discrepancy may be related to the differences in horizontal resolution or physics parameterization of the FNL and WRF models. However, the discrepancy influences the spatial distribution of the COL precipitation in

the datasets such that, in FNL, the peak of COL precipitation occurs west of that in the WRF simulation (for both COL2 and COL3).

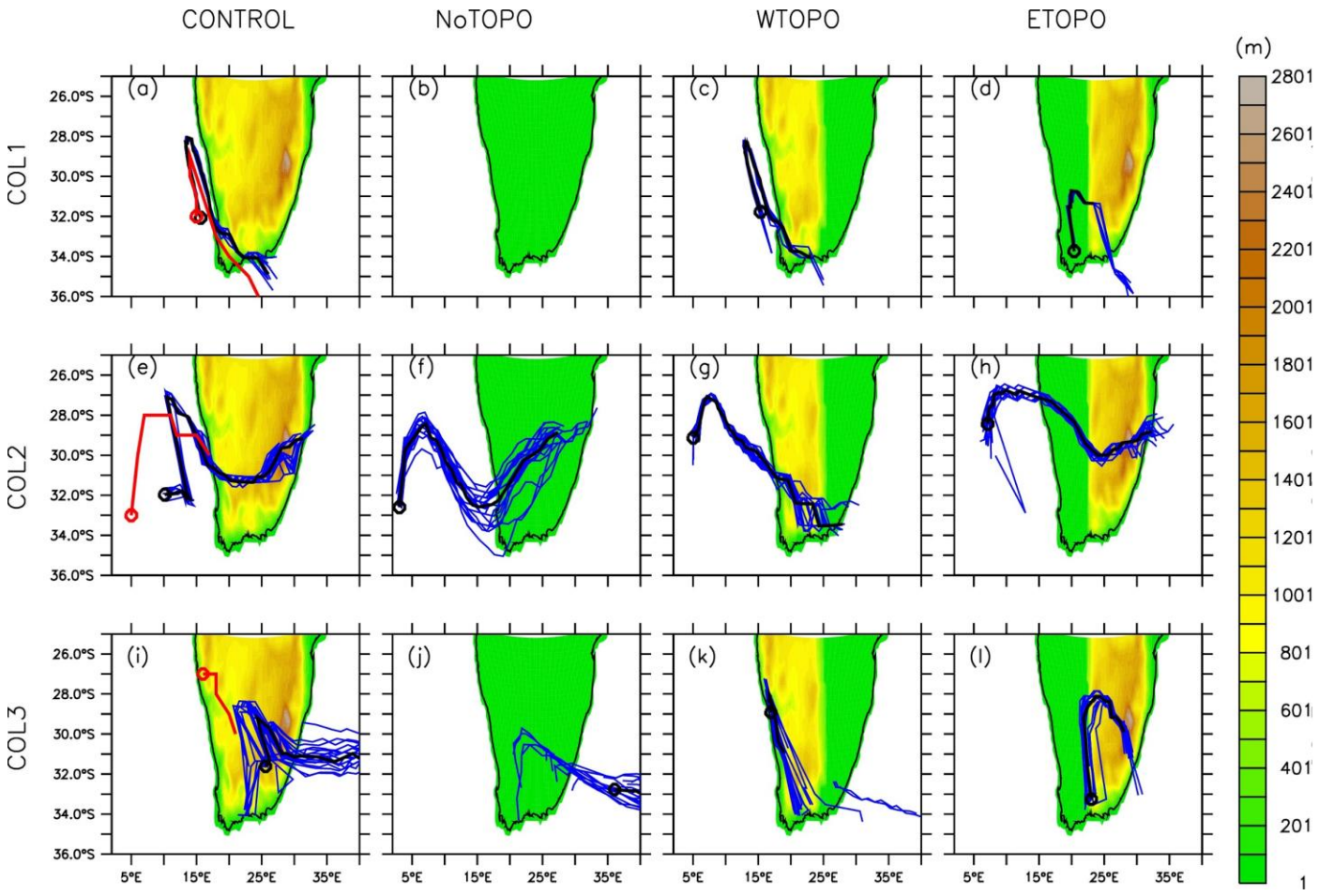

Figure 6.1: The topography (shaded; m) and COL tracks (line) in each experiment: the control experiment (CONTROL; default topography); No topography experiment (NoTOPO), West topography experiment (WTOPO), and East topography experiment (ETOPO). The blue line shows the COL track for the individual simulations, while the black line shows the COL track of the ensemble mean and the red line shows the track in the FNL data.

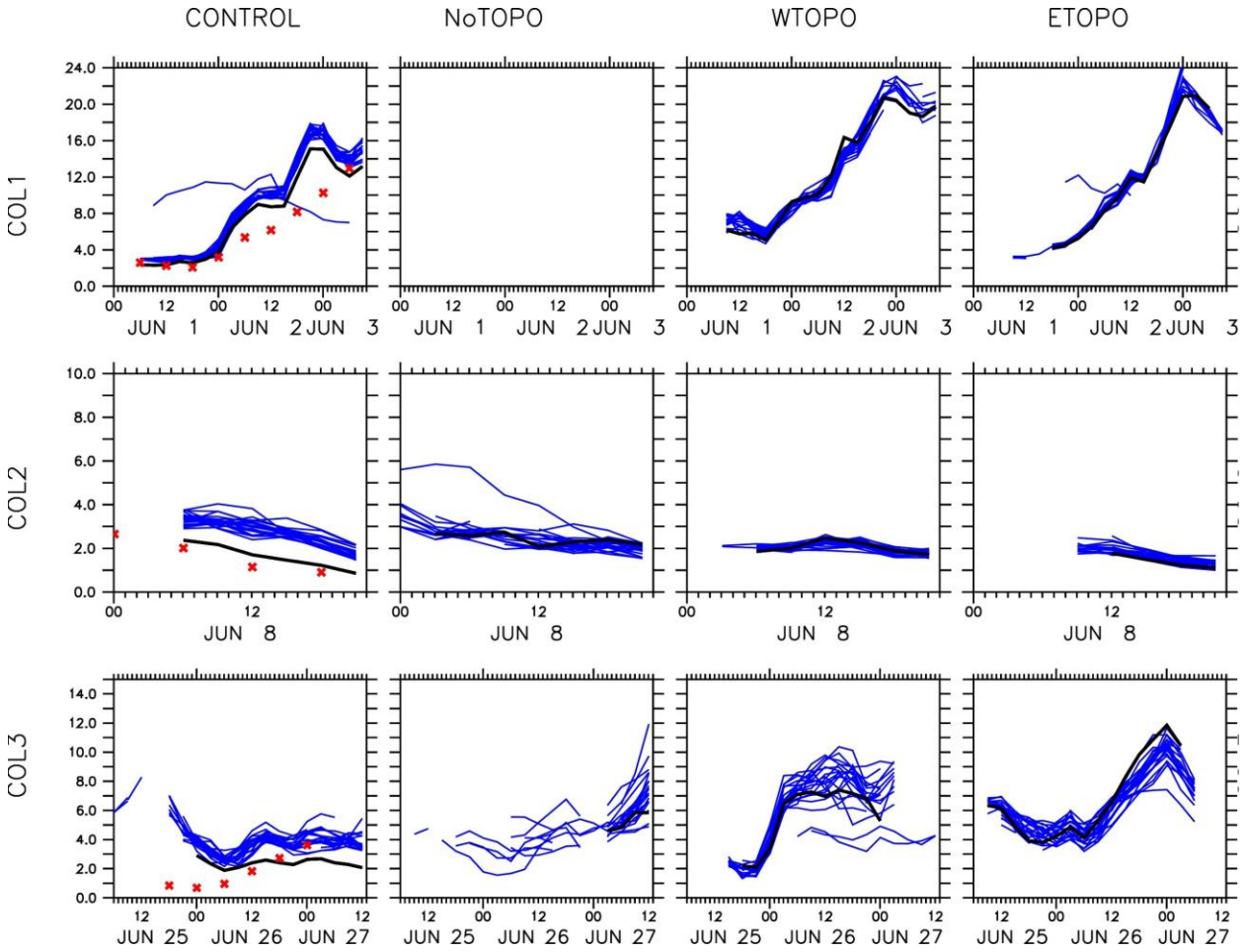

Figure 6.2: The temporal evolution of the precipitation (mm.day^{-1}) from the COLs (i.e. COL1, COL2, and COL3) in the four experiment (CONTROL, NoTOPO, WTOPO and ETOPO). The values are obtained by averaging the precipitation (>0.1 mm.day^{-1}) over the grid points within a 20°° x 20° box around the COL center. The box has the same center with the COL and moves with the COL. The blue line shows the precipitation for the individual simulations, while the black line shows the ensemble mean and the red symbols shows the precipitation in the FNL data.

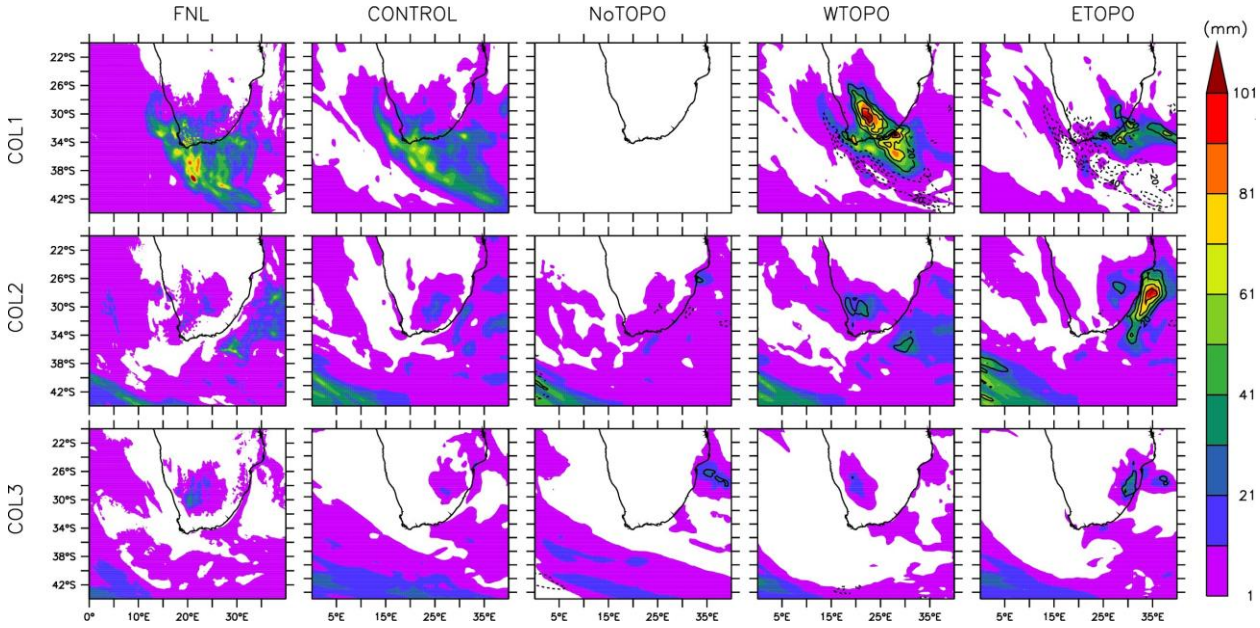

Figure 6.3: The cumulative precipitation (shaded; mm) for each COL (i.e. COL1, COL2 and COL3), for the FNL data and the ensemble mean of each experiment (i.e. CONTROL, NoTOPO, WTOPO, and ETOPO). The contours show the difference between the CONTROL and other experiments (i.e. Experiment - CONTROL).

6.2 Influence of Topography on the COLs

6.2.1 COL Origin

The changes in topography influence the origin of the simulated COLs, but the magnitude of such influence differs (Fig. 6.1). For COL1 (Fig. 6.1a - d), the COL origin over the Atlantic Ocean (around 15.6°E 32°S) remains unchanged in the CONTROL and WTOPO experiment, but it shifts inland in the ETOPO experiment (around 15.6°E 32°S) and the COL does not form at all in the NoTOPO experiment. This suggests that the topography helps in the formation of COL1. In the case of COL2 (Fig. 6.1e - h), the influence of the topography is weaker. While the origin of the COL changes with the modification in topography, the magnitude of the change is smaller than that of COL1. In addition, COL2 still forms in the NoTOPO experiment. This indicates that changes in topography play little or no role in the origin of COL2. In the case of COL3, the origin is over land in the four experiments but in different locations. While the origin of COL3 appears to be at a similar location in the CONTROL and NoTOPO experiments for more than half of the simulations (52%), some ensemble members (48%), including the ensemble mean,

indicate formation further east over the ocean in the NoTOPO experiments. In the WTOPO experiment, a few (<30%) of the simulation ensemble members show the origin of COL3 closer to the origin in the CONTROL experiment; however, most shift the origin to the west coast, possibly because of the absence of the eastern topography in the WTOPO experiment. In the ETOPO experiments, all the simulation ensemble members initiate the COL3 at the sharp slope of the eastern topography. This suggests that the presence of the eastern topography is essential for the formation of COL3 over the continent. Hence, the influence of the topography on COL genesis is more pronounced in the case of a COL that forms over or near the sub-continent (i.e. COL1 and COL3) than for a COL that forms far away from the sub-continent (i.e. COL2). The dynamics behind the initiation of the COLs near the mountain is explored further in Section 3.3.4.

Fig. 6.4 shows that the synoptic conditions could also determine the magnitude of the topographic influence on the COL. For instance, in the CONTROL experiment, the synoptic patterns associated with the COL formation are similar for COL1 and COL3 but differ for COL2. The synoptic scale temperature and geopotential height gradient are weaker in COL2 than in COL1 (and COL3); hence the synoptic wind is weaker in COL2, but the size of the COL is bigger. Garreaud and Fuenzalida (2007) performed a topography sensitivity experiment in a COL case study over South America, and found that removing topography did not influence the formation of the COL. Instead, they found that the elongated trough had stronger winds on the eastward side of the trough and weaker winds on the westward side, with the ridge leading to winds that flow almost perpendicularly to the trough. Garreaud and Fuenzalida (2007) argued that this asymmetry in wind direction led to the cutting off of the trough. This may be why COL1 and COL3 did not form as easily, as the strong winds in the trough may not allow for as much asymmetry, and therefore the topography is required to provide these conditions. This suggests that the stronger wind makes the formation of COLs more difficult (especially over the ocean), but that, as the system approaches the steep topography over land, this provides additional forcing, which enhances the formation of the COLs.

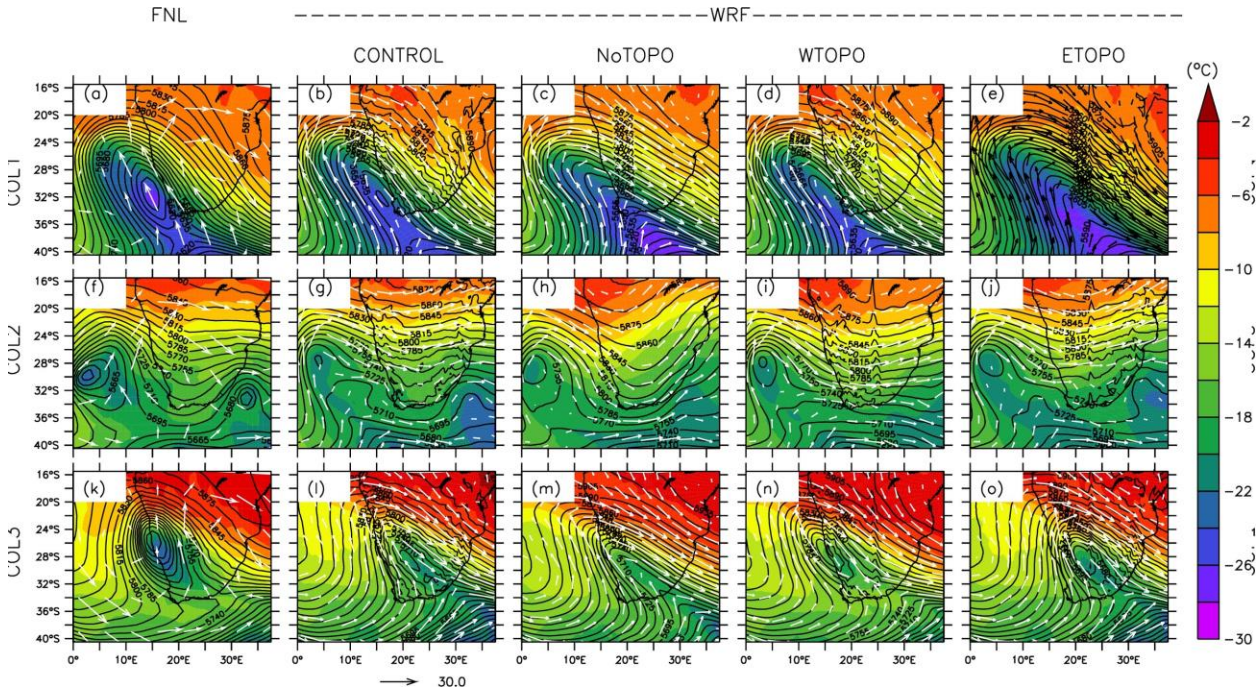

Figure 6.4: The 500hPa temperature (shaded), geopotential height (contour; m) and winds (arrow; m.s^{-1}) on the starting dates of COL1 (1 June 2015 06:00), COL2 (8 June 2015 06:00) and COL3 (26 June 2015 00:00) in the control experiment (CONTROL). The corresponding plots for other experiments (NoTOPO, WTOPO and ETOPO) are also for these dates, and the FNL data is included for comparison.

6.2.2 COL Track

The influence of topography on COL tracks also differs among the COLs (Fig. 6.1). Nevertheless, in most cases, the COLs appear to deflect southward as they approach steep topography. For example, in the CONTROL and WTOPO experiments, COL1 forms over the ocean and moves northward, but shifts southward as it approaches the west mountain range. In the ETOPO, it forms over land (near the eastern escarpment) and shifts southwest as it moves over the eastern escarpment. This is also true for COL2 that forms over the ocean in the four experiments. It moves southward as it approaches the western topography (in the CONTROL and WTOPO experiments) or eastern topography (in ETOPO experiment) but moves northward as it approaches the flat continent (in NoTOPO experiment). Although the result is a bit complex with COL3, which forms over the continent in all the experiments, the COL still exhibits a southward shift upstream of the western topography (in the CONTROL and WTOPO experiments) and eastern topography.

COL tracks are known for their erratic behaviour, however the sensitivity experiments show that topography can influence these tracks. In a southern hemispheric COL climatology study Fuenzalida et al. (2005) concluded that COLs in the South-American region are perturbed by the Andes Mountains. They stated that upwind from the mountains the COLs tracked North-eastward and on the lee side they tracked south-eastward/eastward. However, these studies looked at the differences in direction from the beginning of the track to the mid-point and the end of the track to the mid-point and not necessarily the entire movement of the track. In which case our results generally agree with those findings. In a fluid tank study, Boyer and Chen (1988) found that their COLs blowing over a model of the Rocky Mountains tracked equatorward first and then as the COL approached topography tracked polewards and then over the mountains tracked more equatorward/easterly. This is what we see in most of our tracks. This suggests that as COLs cut-off they may move northward, perhaps to do with some kind of inertia effect, then as COLs encounter mountains, they can act as barriers steering the COLs towards the poles and once this barrier is overcome, they generally flow eastward with the background flow. While more in-depth studies are needed to fully conclude these

effects, one can see that there are some general similarities in the influence of topography on COL tracks.

6.2.3 COL Precipitation

The change in topography produces inconsistent changes in the temporal variation of the precipitation from the COLs, but it produces consistent changes in the spatial distribution of the accumulated precipitation over the sub-continent during the COL periods (Figs. 6.2 and 6.3). In the case of COL1 and COL3, the evolution of the precipitation follows a similar pattern in all the experiments, although the magnitude of the COL peak precipitation is higher in the ETOPO and WTOPO experiments (about 20 $mm.day^{-1}$) than in the CONTROL experiment (about 16 $mm.day^{-1}$). In the case of COL2, the precipitation rate remains the same over the COL duration in the four experiments. Nevertheless, Fig. 6.2 shows that, for all the COLs, the eastern and western topography have opposite influences on the spatial distribution of precipitation over the sub-continent. The removal of the western topography (i.e. in the ETOPO experiment) reduces the accumulated COL precipitation over the western part of the sub-continent, while the removal of the eastern topography (i.e. in the WTOPO experiment) increases the accumulated COL precipitation over the western part of the sub-continent. This suggests that the presence of the western topography promotes COL precipitation over the western areas of the sub-continent, while the presence of the east topography hinders precipitation over the region. This is consistent with the findings of Koseki and Demissie (2018), who found that the Drakensberg mountain range inhibits the transport of tropical moisture into the western regions of South Africa. Section 4.4 and section 5.5 showed that the transport of tropical moisture is important for wet COLs over the Western Cape in both the reanalysis and model data.

6.2.4 COL Dynamics

To explore the influence of topography in the formation of COLs, Fig. 6.5 shows the vertical structure of the atmospheric variables before the center of COL1 reaches the

mountain range (1 June 2015) and when it is over the mountain range (3 June 2015) in the CONTROL experiment, in comparison with the same dates in the NoTOPO experiment. In general, the vertical structure of the atmospheric conditions for 1 June 2015 is similar in the CONTROL and NoTOPO experiments. For instance, both experiments feature a relatively dry, cold polar air mass (south-easterlies) forming a wedge under a relatively moist, warm tropical air mass (i.e. north-westerlies) (Fig. 6.5a and b). While the warm air mass rises, the cold air mass sinks. Above 700 mb, the polar air mass is associated with a relatively low pressure, while the tropical air mass is associated with a relatively high pressure. The resulting pressure gradient leads to a strong north-westerly jet (i.e. thermal wind, around 250 mb), located between the two air masses. However, although this is a good atmospheric condition for COL formation, COL1 only develops in the CONTROL experiment but not in the NoTOPO experiment, because the westerly wave is not deep enough to produce a closed low in NoTOPO (Fig. 6.4). This suggests that the presence of the topography contributes to the deepening of the westerly wave to form COL1 in the CONTROL experiment, by producing low-level convergence and strong upward motion near the mountains (Fig. 6.5d). This upward motion can lift the moist warm air to the level of free convection to initiate deep convection, which may weaken the westerly component of the jet and enhance the meridional component. This will enhance the influence of blocking in deepening the waves and provide additional forcing in initiating the formation of COL1 in the CONTROL.

Furthermore, Fig. 6.5 shows that the topography delays the westward propagation of the westerly waves over the mountains. For 3 June 2015, the atmospheric condition in the CONTROL experiment shows that the system has moved eastward by about 5° but the structure is still similar to that of 1 June 2015, except that the contrast between the warm and cold air masses is weaker. But in the NoTOPO experiment, the system has moved away from the study region, and the vertical structure of the atmospheric condition is different from that of 1 June 2015. The potential vorticity also illustrates this. For 1 June 2015, both CONTROL and NoTOPO both show strong negative vorticity values extending downwards, thus indicating stratospheric intrusion, which often occurs during strong trough or COL conditions. But for 3 June 2015, while the presence of the stratospheric

intrusion is still evident in the CONTROL experiment, it is absent in the NoTOPO experiment, because the intrusion has moved much further east. The moist static energy (MSE) shows that the region in the CONTROL experiment is still influenced by the structure of the COL, as indicated by higher MSE values in the warm air mass. However, in the NoTOPO experiment, the MSE and potential temperature show greater stability, which also leads to less vertical ascent in the NoTOPO experiment compared to the CONTROL. Therefore, the topography contributes to the initiation and propagation of COL1 through blocking. This blocking role that topography plays has been documented in other studies too (Boyer and Chen, 1988; Miky Funatsu et al., 2004).

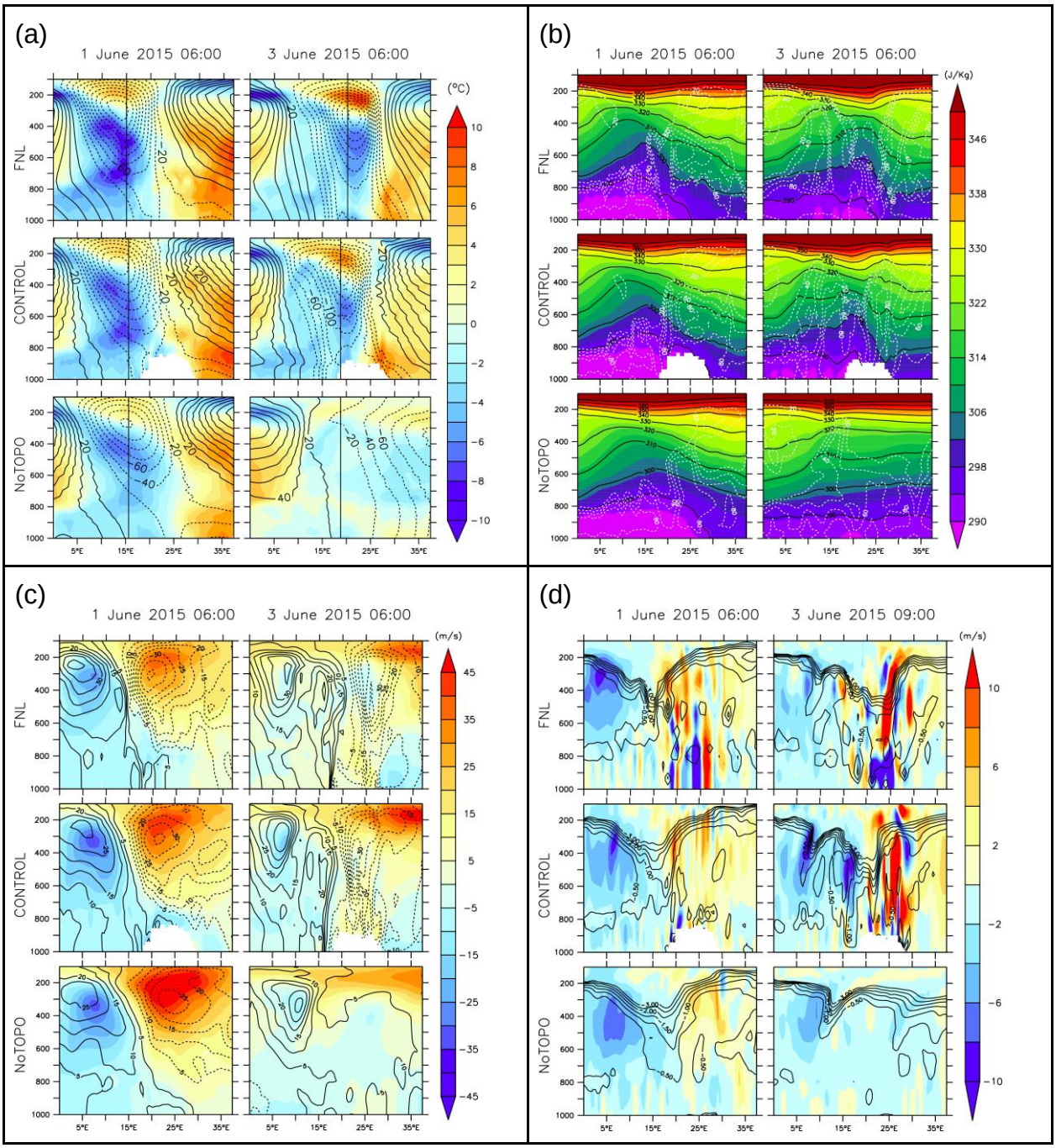

Figure 6.5: The vertical structure of the atmospheric variables before the center of COL1 reaches the mountain range (1 June 2015) and when it is over the mountain range (1 June 2015) in the CONTROL experiment, with the corresponding plots of the FNL DATA and NoTOPO experiment (same dates). The variables are: (a) zonal anomalies of temperature (shaded, °C) and geopotential height (contours, m); (b) Moist static energy (shaded, J.kg^{-1}), potential temperature (black contour; K) and relative humidity (white contour, %); (c) zonal wind (shaded, m.s^{-1}) and meridional wind (contour, m.s^{-1}); and (d) vertical velocity (shaded, m.s^{-1}) and potential vorticity (contour, PVU).

Chapter 7 : Conclusion

7.1 Summary

As part of an effort to improve understanding of COL characteristics over the Western Cape and to enhance prediction, this study has investigated some of the COLs characteristics over the province, focusing on the 2015-2017 drought, and examined the capability of two climate models (WRF and MPAS) in simulating COLs over the area. This study has also explored how the Southern African terrain influences the COL characteristics. Daily precipitation data from three observation datasets (CRU, CHIRPS and CPC) and one reanalysis (CFSR) dataset were analysed to study the precipitation variability in the Western Cape, while CFSR and CHIRPS were used to examine the characteristics of COLs and their associated precipitation patterns. A SOM was applied to classify the COL precipitation patterns into 9 patterns (or nodes), which were grouped into four major patterns. The study evaluated the capability of two climate models (WRF and MPAS) in simulating COLs over the area. The model simulations were compared with observation (CHIRPS) and reanalysis (CFSR) datasets. The evaluation focused on how well the models reproduced the spatial and temporal variation of precipitation, COL frequency and COL precipitation patterns over the Western Cape, with special emphasis on the 2015 – 2017 drought. The SOM was used to check how well the models captured the seasonal frequency of the major COL precipitation patterns over the region. We analysed how well the models reproduced the horizontal and vertical structures of COLs and the differences in the atmospheric conditions for wet and dry COLs. The study also used the WRF model to simulate three different COLs (COL1, COL2 and COL3) in four experiments (CONTROL, NoTOPO, WTOPO and ETOPO). While CONTROL used the real Southern African topography, NoTOPO used no topography (flat terrain), WTOPO used only western topography and ETOPO used only eastern topography. The COL

formation, track, precipitation and vertical structure were analysed to understand how different parts of the Southern African terrain influence COLs.

The results of the study can be summarised as follows:

- In general, the observed and reanalysis precipitation datasets agree on the spatio-temporal distribution of precipitation over the Western Cape, but there are some notable discrepancies among them. However, among the satellite and reanalysis precipitation products, CHIRPS gives the most comparable results to CRU observations, especially during the three drought years (2015–2017).

- Climatologically, the Western Cape area receives 10 COLs per year, but with a standard deviation of 5 COLs. Moreover, while a positive anomaly in COL occurrence can last for 5 years, a negative anomaly can also last for a similar period.

- On average over the studied period, 1981-2017, COLs contribute 11% of the annual precipitation over the Western Cape and generally more COLs leads to greater annual precipitation. However, a positive anomaly of annual COL frequency does not always translate to an increase in COL annual precipitation contribution (and vice versa), because individual COLs can give different precipitation amounts.

- The COL precipitation contribution differs over the three drought years (2015–2017). In 2015 and 2016, the COL annual precipitation was above average, meaning that the COL precipitation helped to alleviate the severity of the drought in those two years. But in 2017, the COL annual precipitation was below normal, as the COLs mainly occurred further south of the country.

- The spatial distribution of COL precipitation over the Western Cape can be grouped into four major patterns. The first pattern (AORP, 22%) shows

precipitation over most of the Western Cape; the second (WCRP, 15%) shows precipitation only over the west and south-west coast; the third (SCRP, 17%) shows precipitation only over the south-east coast; and the fourth (NORP, 46%) shows little precipitation over the Western Cape. Hence, more than 45% of COLs over the province produce little or no precipitation.

- Unlike the wet COLs (i.e. AORP, WCRP, SCRP), the dry COLs (NORP) lack a strong southward transport of warm and moist air from the tropics towards the Western Cape. Hence, in comparison with the wet COLs, the dry COLs are associated with a colder and drier warm air mass, as well as with a weaker temperature and moisture contrast between warm and cold air masses, a shallower low pressure core, and a weaker pressure gradient

- Both WRF and MPAS capture the general characteristics and drivers of Southern African precipitation, but there are some notable differences in relation to the moisture flux transport over the sub-continent.

- Although both models reproduce the spatial distribution of precipitation over the Western Cape well ($r \geq 0.6$), WRF outperforms MPAS in simulating the annual precipitation cycle and inter-annual precipitation of the area.

- Both models show different signs of precipitation anomalies during the 2015 – 2017 drought, but the WRF simulation gives a better representation of the drought characteristics than the MPAS simulation.

- The models agree with CFSR in that the Western Cape is a hotspot for COL activity, although they struggle to capture the inter-annual variability of the COL frequency. The inter-annual variability is better reproduced in WRF than in MPAS.

- Both models give a credible representation of the seasonal frequency of COL precipitation patterns as observed, except that they under-estimate the frequency of dry COLs through the seasons.

- In agreement with the reanalysis, the models show that the transport of warm, moist air from the tropical Atlantic Ocean fuels COL precipitation over the Western Cape and that the moist static energy in the warm moist air is lower in the dry COLs than in the wet COLs.

- Topography influences the origin and formation of COLs, but the influence is greater for the COLs (i.e. COL1 and COL3) that formed in the vicinity of the sub-continent than the COL (i.e. COL2) that formed far from the subcontinent. COL1 does not form in the NoTOPO experiments.

- The COL tracks are also sensitive to the topography. Although the influence differs for each COL, there is a similarity in that as the COLs approach topography their tracks become more southerly. COL1 and COL2 shift southward as they approach the western topography in the CONTROL and WTOPO experiment and shift southward as they approach the eastern topography in the ETOPO experiment. The track of COL3 is complicated due to its formation over land, but it does show southward movement upstream of topography.

- Topography does not seem to influence the timing of peaks in precipitation during the COL lifecycle, but it does influence the spatial distribution of precipitation. The western topography enhances precipitation over the western part of Southern Africa while the eastern topography reduces precipitation to the region.

- The vertical structure of COL1 indicates that topography plays a role in providing the force needed for the system to become cut-off. The topography promotes uplift of warm moist air to initiate deep convection, which may weaken the zonal strength of the jet and allow for the formation of the COL.

- Topography also decelerates westerly wave systems. The system moves faster in the NoTOPO experiment than in the CONTROL experiment.

Table 7.1: A summary of the hypotheses and their results

Hypothesis	Comment: True or False
Hypothesis 1: Changes in characteristics of COLs (i.e. tracks frequency and the associated precipitation) over the Western Cape contributes to the 2015-2017 drought in the province.	The hypothesis is **false** in 2015 - 2016, when an increase in COL frequency and the associated precipitation reduced the severity of the drought. But, the hypothesis is **true** in 2017, when a decrease in COL frequency and the associated precipitation enhanced the severity of the drought
Hypothesis 2: The characteristics of COLs over the Western Cape can be reproduced by the Weather Research and Forecasting (WRF) and the Model Prediction Across Scales (MPAS) models.	This hypothesis is **true** for WRF model, but **false** for MPAS model.
Hypothesis 3: The characteristic of COLs over South Africa is influenced by the complex topography of southern Africa.	This hypothesis is **true.**

7.2 Concluding Remark

These above results complement findings of previous studies on the roles of different atmospheric process in the 2015-2017 droughts over the Western Cape. Sousa et al. (2018) linked the drought with a shift in the sub-tropical jet southwards and a southward expansion of the sub-tropical anticyclones. This weakened the remote moisture sources and atmospheric rivers and led to the southward shift in moisture transport and storm tracks, leading to a persistent decrease in moisture transport over the ocean to the west

of the Western Cape throughout the drought period (Sousa et al., 2018). Mahlalela et al. (2018) also linked the consistently dry conditions over most of the province (in the early winter months, April-May in 2015-2017) to the southward shift of the jets, showing anomalous higher pressures over high latitudes and the southward shift in storm tracks. Results of our study have shown how COLs contributed to the drought. In the first two years of the drought (2015-2016), the COLs occurred more frequently (than normal) and produced precipitation. Although the addition of COL precipitation did not offset the dry conditions from the southward shift of the storm tracks, it alleviated the drought. This also suggests that the COLs were not affected (i.e. by the southward expansion of the anticyclones) the same way other precipitation systems were affected. Nevertheless, in the last year of the drought (2017), COL occurrence and precipitation fell below average, adding to the already dry conditions. This suggests a distinction between the dynamics of the 2015-2016 and 2017 drought years. It also emphasizes the importance of understanding the relative contribution of different systems to the Western Cape annual precipitation and knowing what influences these contributions.

7.3 Suggestions for Further Study

Further investigations are suggested to improve the understanding and prediction of COLs over the Western Cape and Southern Africa: The statistics may be sensitive to the algorithm used to identify the COLs. Future studies could apply several algorithms (developed according to the different characteristics of COLs) to identify the COLs. The results of such studies would help to quantify the uncertainties in the COL statistics and provide a more robust information on the characteristics of COLs during the drought period. The resolution of the reanalysis (0.5° x 0.5°) used in the present study may be too low to adequately capture the local effects of topography on COLs. Using multi-reanalysis datasets with higher resolution is another way of enhancing the robustness of the results. Lagrangian studies of moisture sources during Western Cape COL days could provide more robust conclusions on COL moisture transport and sources.

In the present study, only one long simulation was performed with each model due to computational constraints. The results of the study could be improved in future studies.

For example, the models were run using one set of parameterisation schemes; moreover, for MPAS, the out-of-the-box conditions were used because it is a fairly new model. In future studies, therefore, different parameterisation schemes could be used to test the sensitivity to COLs and COL-related precipitation. Using a regional climate model for the topography sensitivity experiments raises some issues with the topography signal being present within the boundary conditions, while this would be more related to changes in the westerly wave structures and less to the influence on COL characteristics, it would still be useful for future studies to understand the influence of boundary conditions on simulated COLs characteristics. The three COLs used in the sensitivity experiments were chosen during the same month and year; hence, they may not be a good representation of all COL events over Southern Africa. Therefore, more COL case studies are required to understand the influence of topography on COLs occurring in different seasons.

References

1. Abatzoglou, J.T., 2016. Contribution of cutoff lows to precipitation across the United States. *Journal of Applied Meteorology and Climatology*, *55*(4), pp.893-899.
2. Abiodun, B.J., Abba Omar, S., Lennard, C. and Jack, C., 2016. Using regional climate models to simulate extreme rainfall events in the Western Cape, South Africa. *International Journal of Climatology*, *36*(2), pp.689–705.
3. Abiodun, B.J., Makhanya, N., Petja, B., Abatan, A.A. and Oguntunde, P.G., 2018. Future projection of droughts over major river basins in Southern Africa at specific global warming levels. *Theoretical and Applied Climatology*, pp.1-15.
4. Awan, N.K. and Formayer, H., 2017. Cutoff low systems and their relevance to large-scale extreme precipitation in the European Alps. *Theoretical and Applied Climatology*, *129*(1-2), pp.149-158.
5. Betts, A.K. and Miller, M.J., 1986. A new convective adjustment scheme. Part II: Single column tests using GATE wave, BOMEX, ATEX and arctic air-mass data sets. *Quarterly Journal of the Royal Meteorological Society*, *112*(473), pp.693–709.
6. Blamey, R. and Reason, C.J.C., 2007. Relationships between Antarctic sea-ice and South African winter rainfall. *Climate Research*, *33*(2), pp.183-193.
7. Blamey, R.C., Ramos, A.M., Trigo, R.M., Tomé, R. and Reason, C.J.C., 2018. The influence of atmospheric rivers over the South Atlantic on winter rainfall in South Africa. *Journal of Hydrometeorology*, *19*(1), pp.127-142.
8. Botai, C., Botai, J., de Wit, J., Ncongwane, K. and Adeola, A., 2017. Drought characteristics over the western cape province, South Africa. *Water*, *9*(11), p.876.
9. Boyer, D.L. and Chen, R.R., 1988. The interaction of a mechanically driven three-wave zonal background flow with model mountains in the Northern Hemisphere. *Meteorology and Atmospheric Physics*, *39*(1), pp.1-13.
10. Brown, J.N., McIntosh, P.C., Pook, M.J. and Risbey, J.S., 2009. An investigation of the links between ENSO flavors and rainfall processes in southeastern Australia. *Monthly Weather Review*, *137*(11), pp.3786–3795.
11. Campetella, C.M. and Possia, N.E., 2007. Upper-level cut-off lows in southern South America. *Meteorology and Atmospheric Physics*, *96*(1-2), pp.181-191.

12. Crétat, J., Pohl, B., Richard, Y. and Drobinski, P., 2012. Uncertainties in simulating regional climate of Southern Africa: sensitivity to physical parameterizations using WRF. *Climate dynamics*, *38*(3-4), pp.613-634.
13. Dieppois, B., Pohl, B., Rouault, M., New, M., Lawler, D. and Keenlyside, N., 2016. Interannual to interdecadal variability of winter and summer southern African rainfall, and their teleconnections. *Journal of Geophysical Research: Atmospheres*, *121*(11), pp.6215-6239.
14. Dowdy, A.J., Mills, G.A. and Timbal, B. 2011. Large-scale indicators of Australian East Coast Lows and associated extreme weather events, CAWCR Technical Report 37 [Available online at http://www.cawcr.gov.au/publications/]
15. Dudhia, J., 1989. Numerical study of convection observed during the winter monsoon experiment using a mesoscale two-dimensional model. *Journal of the atmospheric sciences*, *46*(20), pp.3077–3107.
16. Du Plessis, J.A. and Schloms, B., 2017. An investigation into the evidence of seasonal rainfall pattern shifts in the Western Cape, South Africa. *Journal of the South African Institution of Civil Engineering*, *59*(4), pp.47-55.
17. Dyson, L.L., 2015. A heavy rainfall sounding climatology over Gauteng, South Africa, using self-organising maps. *Climate dynamics*, *45*(11-12), pp.3051-3065.
18. Engelbrecht, C.J., Engelbrecht, F.A. and Dyson, L.L., 2013. High-resolution model-projected changes in mid-tropospheric closed-lows and extreme rainfall events over southern Africa. *International Journal of Climatology*, *33*(1), pp.173–187.
19. Engelbrecht, C.J., Landman, W.A., Engelbrecht, F.A. and Malherbe, J., 2015. A synoptic decomposition of rainfall over the Cape south coast of South Africa. *Climate Dynamics*, *44*(9-10), pp.2589-2607.
20. Engelbrecht, C.J. and Landman, W.A., 2016. Interannual variability of seasonal rainfall over the Cape south coast of South Africa and synoptic type association. *Climate dynamics*, *47*(1-2), pp.295-313.
21. Engelbrecht, F.A., McGregor, J.L. and Engelbrecht, C.J., 2009. Dynamics of the Conformal-Cubic Atmospheric Model projected climate-change signal over southern Africa. *International Journal of Climatology: A Journal of the Royal Meteorological Society*, *29*(7), pp.1013-1033.

22. Estie, K.E., 1981. The Laingsburg flood disaster of 25 January 1981. *South African Weather Bureau Newsletter*, *383*, pp.19-32.
23. Favre, A., Hewitson, B., Lennard, C., Cerezo-Mota, R. and Tadross, M., 2013. Cut-off lows in the South Africa region and their contribution to precipitation. *Climate dynamics*, *41*(9-10), pp.2331-2351.
24. Favre, A., Hewitson, B., Tadross, M., Lennard, C. and Cerezo-Mota, R., 2012. Relationships between cut-off lows and the semiannual and southern oscillations. *Climate dynamics*, *38*(7-8), pp.1473-1487.
25. Fragoso, M., Trigo, R.M., Zêzere, J.L. and Valente, M.A., 2010. The exceptional rainfall event in Lisbon on 18 February 2008. *Weather*, *65*(2), pp.31-35.
26. Francis, J.A. and Vavrus, S.J., 2012. Evidence linking Arctic amplification to extreme weather in mid-latitudes. *Geophysical Research Letters*, *39*(6).
27. Fuenzalida, H.A., Sánchez, R. and Garreaud, R.D., 2005. A climatology of cutoff lows in the Southern Hemisphere. *Journal of Geophysical Research: Atmospheres*, *110*(D18), pp.1596-1613.
28. Funk, C.C., Peterson, P.J., Landsfeld, M.F., Pedreros, D.H., Verdin, J.P., Rowland, J.D., Romero, B.E., Husak, G.J., Michaelsen, J.C. and Verdin, A.P., 2014. A quasi-global precipitation time series for drought monitoring. *US Geological Survey Data Series*, *832*(4), pp.1-12.
29. Garreaud, R. and Fuenzalida, H.A., 2007. The influence of the Andes on cutoff lows: A modeling study. *Monthly Weather Review*, *135*(4), pp.1596-1613.
30. Gimeno, L., Trigo, R.M., Ribera, P. and Garcia, J.A., 2007. Special issue on cut-off low systems (COL). *Meteorology and Atmospheric Physics*, *96*(1), pp.1-2.
31. Godoy, A.A., Possia, N.E., Campetella, C.M. and García Skabar, Y., 2011. A cut-off low in southern South America: Dynamic and thermodynamic processes. *Revista Brasileira de Meteorologia*, *26*(4), pp.503-514.
32. Goliger, A.M. and Retief, J.V., 2002. Identification of zones of strong wind events in South Africa. *Journal of Wind Engineering and Industrial Aerodynamics*, *90*(11), pp.1227-1235.
33. Harris, I.C. and Jones, P.D. (2019): CRU TS4.02: Climatic Research Unit (CRU) Time-Series (TS) version 4.02 of high-resolution gridded data of month-by-month variation

in climate (Jan. 1901- Dec. 2017). Centre for Environmental Data Analysis, Accessed 19 November 2018

34. Hart, N.C., Reason, C.J. and Fauchereau, N., 2013. Cloud bands over southern Africa: seasonality, contribution to rainfall variability and modulation by the MJO. *Climate dynamics*, *41*(5-6), pp.1199-1212.
35. Heinzeller, D., Duda, M.G. and Kunstmann, H., 2016. Towards convection-resolving, global atmospheric simulations with the Model for Prediction Across Scales (MPAS) v3.1: An extreme scaling experiment. *Geoscientific Model Development*, *9*(1), p.77.
36. Hirota, N., Takayabu, Y.N., Kato, M. and Arakane, S., 2016. Roles of an atmospheric river and a cutoff low in the extreme precipitation event in Hiroshima on 19 August 2014. *Monthly Weather Review*, *144*(3), pp.1145-1160.
37. Holloway, A.J., Fortune, G., Chasi, V., Beckman, T., Pharoah, R., Poolman, E., Punt, C. and Zweig, P., 2010. *RADAR Western Cape 2010: Risk and development annual review*. Disaster Mitigation for Sustainable Livelihoods Programme (DiMP).
38. Hong, S.Y., Dudhia, J. and Chen, S.H., 2004. A revised approach to ice microphysical processes for the bulk parameterization of clouds and precipitation. *Monthly Weather Review*, *132*(1), pp.103-120.
39. Hong, S.Y., Noh, Y. and Dudhia, J., 2006. A new vertical diffusion package with an explicit treatment of entrainment processes. *Monthly weather review*, *134*(9), pp.2318-2341.
40. Hu, K., Lu, R. and Wang, D., 2010. Seasonal climatology of cut-off lows and associated precipitation patterns over Northeast China. *Meteorology and atmospheric physics*, *106*(1–2), pp.37–48.
41. Janjić, Z.I., 1994. The step-mountain eta coordinate model: Further developments of the convection, viscous sublayer, and turbulence closure schemes. *Monthly weather review*, *122*(5), pp.927-945.
42. Knippertz, P.E.T.E.R. and Martin, J.E., 2007. The role of dynamic and diabatic processes in the generation of cut-off lows over Northwest Africa. *Meteorology and Atmospheric Physics*, *96*(1-2), pp.3-19.
43. Kohonen, T., 1990. The self-organizing map. *Proceedings of the IEEE*, 78(9), pp.1464–1480.

44. Koppen, W., 1886. Die Bewegung der barometrischen Minima in den Tagen vom 20 bis 24 Januar 1886 üuber Europa. *Met Zeitschr*, *3*, p.505.
45. Koseki, S. and Demissie, T., 2018. Does the Drakensberg dehydrate southwestern Africa?. *Journal of arid environments*, *158*, pp.35-42.
46. Kramer, M., Heinzeller, D., Hartmann, H., van den Berg, W. and Steeneveld, G.J., 2018. Assessment of MPAS variable resolution simulations in the grey-zone of convection against WRF model results and observations. *Climate Dynamics*, pp.1-24.
47. Lavender, S.L. and Abbs, D.J., 2013. Trends in Australian rainfall: Contribution of tropical cyclones and closed lows. *Climate dynamics*, *40*(1–2), pp.317–326.
48. Lennard, C. and Hegerl, G., 2015. Relating changes in synoptic circulation to the surface rainfall response using self-organising maps. *Climate dynamics*, *44*(3–4), pp.861–879.
49. Lennard, C.J., Coop, L., Morison, D. and Grandin, R., 2013. *Extreme events: Past and future changes in the attributes of extreme rainfall and the dynamics of their driving processes*. Climate Systems Analysis Group, University of Cape Town.
50. Liu, Y., Weisberg, R.H. and Mooers, C.N., 2006. Performance evaluation of the self-organizing map for feature extraction. *Journal of Geophysical Research: Oceans*, *111*(C5).
51. Llasat, M.C., Martín, F. and Barrera, A., 2007. From the concept of “Kaltlufttropfen”(cold air pool) to the cut-off low. The case of September 1971 in Spain as an example of their role in heavy rainfalls. *Meteorology and Atmospheric physics*, *96*(1-2), pp.43-60.
52. Llasat, M.C. and Puigcerver, M., 1990. Cold air pools over Europe. *Meteorology and atmospheric physics*, *42*(3-4), pp.171-177.
53. Mahlalela, P.T., Blamey, R.C. and Reason, C.J.C., 2018. Mechanisms behind early winter rainfall variability in the southwestern Cape, South Africa. *Climate* d*ynamics*, pp.1–19.
54. Maoyi, M.L., Abiodun, B.J., Prusa, J.M. and Veitch, J.J., 2018. Simulating the characteristics of tropical cyclones over the South West Indian Ocean using a Stretched-Grid Global Climate Model. *Climate dynamics*, *50*(5–6), pp.1581–1596.

55. McInnes, K.L. and Hubbert, G.D., 2001. The impact of eastern Australian cut-off lows on coastal sea levels. *Meteorological Applications*, *8*(2), pp.229-244.
56. Miky Funatsu, B., Gan, M.A. and Caetano, E., 2004. A case study of orographic cyclogenesis over South America. *Atmósfera*, *17*(2), pp.91-113.
57. Mlawer, E.J., Taubman, S.J., Brown, P.D., Iacono, M.J. and Clough, S.A., 1997. Radiative transfer for inhomogeneous atmospheres: RRTM, a validated correlated-k model for the longwave. *Journal of Geophysical Research: Atmospheres*, *102*(D14), pp.16663–16682.
58. Molekwa, S., Engelbrecht, C.J. and deW Rautenbach, C.J., 2014. Attributes of cut-off low induced rainfall over the Eastern Cape Province of South Africa. *Theoretical and applied climatology*, *118*(1–2), pp.307–318.
59. Muller, M., 2018. Cape Town's drought: don't blame climate change. *Nature* 559, pp. 74-176 (2018)
60. *Naik, M. and Abiodun, B.J., Projected changes in drought characteristics over Western Cape, South Africa. Meteorological Applications.*
61. *Nath, P.K. and Behera, B., 2011. A critical review of impact of and adaptation to climate change in developed and developing economies. Environment, development and sustainability, 13(1), pp.141-162.*
62. Ndarana, T., Bopape, M.J., Waugh, D. and Dyson, L., 2018. The Influence of the Lower Stratosphere on Ridging Atlantic Ocean Anticyclones over South Africa. *Journal of Climate*, *31*(15), pp.6175-6187.
63. Ndarana, T. and Waugh, D.W., 2010. The link between cut-off lows and Rossby wave breaking in the Southern Hemisphere. *Quarterly Journal of the Royal Meteorological Society*, 136(649), pp.869–885.
64. Ndarana, T. and Waugh, D.W., 2011. A climatology of Rossby wave breaking on the Southern Hemisphere tropopause. *Journal of the Atmospheric Sciences*, *68*(4), pp.798-811.
65. Nieto, R., Gimeno, L., de La Torre, L., Ribera, P., Gallego, D., García-Herrera, R., García, J.A., Nuñez, M., Redaño, A. and Lorente, J., 2005. Climatological features of cutoff low systems in the Northern Hemisphere. *Journal of climate*, *18*(16), pp.3085-3103.

66. Nieto, R., Gimeno, L., De la Torre, L., Ribera, P., Barriopedro, D., García-Herrera, R., Serrano, A., Gordillo, A., Redano, A. and Lorente, J., 2007. Interannual variability of cut-off low systems over the European sector: The role of blocking and the Northern Hemisphere circulation modes. *Meteorology and Atmospheric Physics*, *96*(1-2), pp.85-101.
67. Nieto, R., Sprenger, M., Wernli, H., Trigo, R.M. and Gimeno, L., 2008. Identification and Climatology of Cut-off Lows near the Tropopause. *Annals of the New York Academy of Sciences*, *1146*(1), pp.256-290.
68. Otto, F.E., Wolski, P., Lehner, F., Tebaldi, C., Van Oldenborgh, G.J., Hogesteeger, S., Singh, R., Holden, P., Fučkar, N.S., Odoulami, R.C. and New, M., 2018. Anthropogenic influence on the drivers of the Western Cape drought 2015 – 2017. *Environmental Research Letters*, *13*(12), p.124010.
69. Palmén, E., 1949. Origin and Structure of High-Level Cyclones South of the: Maximum Westerlies. *Tellus*, *1*(1), pp.22-31.
70. Park, S.H., Klemp, J.B. and Kim, J.H., 2019. Hybrid mass coordinate in WRF-ARW and its impact on upper-level turbulence forecasting. *Monthly Weather Review*.
71. Pharoah, R., Holloway, A., Fortune, G., Chapman, A., Schaber, E. and Zweig, P., 2016. *OFF the RADAR*: *Summary Report. High Impact Weather Event in the Western Cape, South Africa*. For the Provincial Disaster Management Centre, Western Cape by Research Alliance for Disaster and Risk Reduction, Department of Geography and Environmental Studies, Stellenbosch University.
72. Pienaar, L. and Boonzaaier, J., 2018. Drought policy brief Western Cape Agriculture. *Western Cape Department of Agriculture (WCDoA) and the Bureau for Food and Agricultural Policy (BFAP), Elsenburg*.
73. Pinheiro, H.R., Hodges, K.I., Gan, M.A. and Ferreira, N.J., 2017. A new perspective of the climatological features of upper-level cut-off lows in the Southern Hemisphere. *Climate Dynamics*, *48*(1-2), pp.541-559.
74. Pohl, B., Dieppois, B., Crétat, J., Lawler, D. and Rouault, M., 2018. From synoptic to interdecadal variability in Southern African rainfall: toward a unified view across time scales. *Journal of Climate*, *31*(15), pp.5845-5872.

75. Pohl, B., Rouault, M. and Roy, S.S., 2014. Simulation of the annual and diurnal cycles of rainfall over South Africa by a regional climate model. *Climate dynamics*, *43*(7-8), pp.2207-2226.
76. Porcù, F., Carrassi, A., Medaglia, C.M., Prodi, F. and Mugnai, A., 2007. A study on cut-off low vertical structure and precipitation in the Mediterranean region. *Meteorology and Atmospheric Physics*, *96*(1-2), pp.121-140.
77. Portmann, R., Crezee, B., Quinting, J. and Wernli, H., 2018. The complex life cycles of two long-lived potential vorticity cut-offs over Europe. *Quarterly Journal of the Royal Meteorological Society*, *144*(712), pp.701-719.
78. Price, J.D. and Vaughan, G., 1993. The potential for stratosphere-troposphere exchange in cut-off-low systems. *Quarterly Journal of the Royal Meteorological Society*, *119*(510), pp.343-365.
79. Ramos, A.M., Blamey, R.C., Algarra, I., Nieto, R., Gimeno, L., Tomé, R., Reason, C.J. and Trigo, R.M., 2019. From Amazonia to southern Africa: Atmospheric moisture transport through low-level jets and atmospheric rivers. *Annals of the New York Academy of Sciences*, *1436*(1), pp.217–230.
80. Ratna, S.B., Ratnam, J.V., Behera, S.K., Rautenbach, C.D., Ndarana, T., Takahashi, K. and Yamagata, T., 2014. Performance assessment of three convective parameterization schemes in WRF for downscaling summer rainfall over South Africa. *Climate dynamics*, *42*(11-12), pp.2931-2953.
81. Ratnam, J.V., Behera, S.K., Doi, T., Ratna, S.B. and Landman, W.A., 2016. Improvements to the WRF seasonal hindcasts over South Africa by bias correcting the driving SINTEX-F2v CGCM fields. *Journal of Climate*, *29*(8), pp.2815–2829.
82. Ratnam, J.V., Behera, S.K., Masumoto, Y., Takahashi, K. and Yamagata, T., 2012. A simple regional coupled model experiment for summer-time climate simulation over southern Africa. *Climate dynamics*, *39*(9-10), pp.2207-2217.
83. Reason, C.J.C., Rouault, M., Melice, J.L. and Jagadheesha, D., 2002. Interannual winter rainfall variability in SW South Africa and large scale ocean–atmosphere interactions. *Meteorology and Atmospheric Physics*, *80*(1-4), pp.19-29.
84. Reason, C.J.C. and Rouault, M., 2005. Links between the Antarctic Oscillation and winter rainfall over western South Africa. *Geophysical research letters*, *32*(7).

85. Reboita, M.S., Nieto, R., Gimeno, L., Da Rocha, R.P., Ambrizzi, T., Garreaud, R. and Krüger, L.F., 2010. Climatological features of cutoff low systems in the Southern Hemisphere. *Journal of Geophysical Research: Atmospheres*, *115*(D17).
86. Risbey, J.S., Pook, M.J., McIntosh, P.C., Ummenhofer, C.C. and Meyers, G., 2009. Characteristics and variability of synoptic features associated with cool season rainfall in southeastern Australia. *International Journal of Climatology*, *29*(11), pp.1595–1613.
87. Roffe, S.J., Fitchett, J.M. and Curtis, C.J., 2019. Classifying and mapping rainfall seasonality in South Africa: a review. *South African Geographical Journal*, *101*(2), pp.158-174.
88. Saha, S., Moorthi, S., Pan, H.L., Wu, X., Wang, J., Nadiga, S., Tripp, P., Kistler, R., Woollen, J., Behringer, D. and Liu, H., 2010. The NCEP climate forecast system reanalysis. *Bulletin of the American Meteorological Society*, *91*(8), pp.1015-1058.
89. Sakaguchi, K., Lu, J., Leung, L.R., Zhao, C., Li, Y. and Hagos, S., 2016. Sources and pathways of the upscale effects on the Southern Hemisphere jet in MPAS-CAM4 variable-resolution simulations. *Journal of Advances in Modeling Earth Systems*, *8*(4), pp.1786–1805.
90. Singleton, A.T. and Reason, C.J.C., 2006. Numerical simulations of a severe rainfall event over the Eastern Cape coast of South Africa: sensitivity to sea surface temperature and topography. *Tellus A: Dynamic Meteorology and Oceanography*, *58*(3), pp.335-367.
91. Singleton, A.T. and Reason, C.J.C., 2007a. A numerical model study of an intense cutoff low pressure system over South Africa. *Monthly weather review*, *135*(3), pp.1128–1150.
92. Singleton, A.T. and Reason, C.J.C., 2007b. Variability in the characteristics of cut-off low pressure systems over subtropical southern Africa. *International Journal of Climatology: A Journal of the Royal Meteorological Society*, *27*(3), pp.295-310.
93. Skamarock, W.C., Klemp, J.B., Duda, M.G., Fowler, L.D., Park, S.H. and Ringler, T.D., 2012. A multiscale nonhydrostatic atmospheric model using centroidal Voronoi tessellations and C-grid staggering. *Monthly Weather Review*, *140*(9), pp.3090-3105.
94. Skamarock, W.C., Klemp, J.B., Dudhia, J., Gill, D.O., Barker, D.M., Duda, M.G., Huang, X.Y., Wang, W. and Powers, J.G., 2008. A description of the advanced

research WRF version 3, NCAR Technical Note. *National Center for Atmospheric Research: Boulder, CO, USA*.

95. Sousa, P.M., Blamey, R.C., Reason, C.J., Ramos, A.M. and Trigo, R.M., 2018. The 'Day Zero' Cape Town drought and the poleward migration of moisture corridors. *Environmental Research Letters*, *13*(12), p.124025.
96. StatsSA (Statistics South Africa) (2011) Statistics by place, population, Census 2011, Western Cape. http://www.statssa.gov.za/?page_id=964. Accessed 18 March 2019
97. Stucki, P., Rickli, R., Brönnimann, S., Martius, O., Wanner, H., Grebner, D. and Luterbacher, J., 2012. Weather patterns and hydro-climatological precursors of extreme floods in Switzerland since 1868. *Meteorologische Zeitschrift*, *21*(6), pp.531–550.
98. Taljaard, J.J., 1985. *Cut-off lows in the South African region* (No. 14). Weather Bureau, Department of Transport.
99. Tennant, J., 1994. The influence of orography and local sea-surface temperature anomalies on the development of the 1987 Natal floods: a general circulation model study. *South African Journal of Science*, *90*(1), pp.45-49.
100. Tyson, P.D. and Preston-Whyte, R.A., 2000. *Weather and climate of southern Africa*. Oxford University Press.
101. UMLINDI, Issue 12, December 14, 2015. Available: http://www.arc.agric.za/arc-iscw/Newsletter%20Library/UMLINDI%20Issue%202015-12,%2014%20December%202015.pdf [12 April 2019]
102. USGS (2010). *GMTED 2010, Global Multi-resolution Terrain Elevation Data 2010 (GMTED2010)*. U.S. Geological Survey.
103. Visser, W.P., 2018. A perfect storm: The ramifications of Cape Town's drought crisis. *TD: The Journal for Transdisciplinary Research in Southern Africa*, *14*(1), pp.1-10.
104. Weber, T., Haensler, A. and Jacob, D., 2018. Sensitivity of the atmospheric water cycle to corrections of the sea surface temperature bias over southern Africa in a regional climate model. *Climate dynamics*, *51*(7-8), pp.2841-2855.

105. Weldon, D. and Reason, C.J.C., 2014. Variability of rainfall characteristics over the South Coast region of South Africa. *Theoretical and applied climatology*, *115*(1-2), pp.177-185.

106. Wernli, H. and Sprenger, M., 2007. Identification and ERA-15 climatology of potential vorticity streamers and cutoffs near the extratropical tropopause. *Journal of the atmospheric sciences*, *64*(5), pp.1569-1586.

107. Wolski, P., Jack, C., Tadross, M., van Aardenne, L. and Lennard, C., 2018. Interannual rainfall variability and SOM-based circulation classification. *Climate dynamics*, *50*(1–2), pp.479–492.

108. Xie, P., 2009: CPC Unified Gauge-Based Analysis of Global Daily Precipitation. NOAA Climate Prediction Center,http://ftp.cpc.ncep.noaa.gov/precip/CPC UNI777PRCP, Accessed 19 November 2018

109. Zhang, Q., Körnich, H. and Holmgren, K., 2013. How well do reanalyses represent the southern African precipitation?. *Climate dynamics*, *40*(3-4), pp.951-962.

110. Zwart, S.J., Mishra, B. and Dembélé, M., 2018, May. Satellite rainfall for food security on the African continent: performance and accuracy of seven rainfall products between 2001 and 2016. In *Remote Sensing and Hydrology Symposium: Earth Observation for Integrated Water and Basin Management: New possibilities and challenges for adaptation to a changing environment*.

Appendix

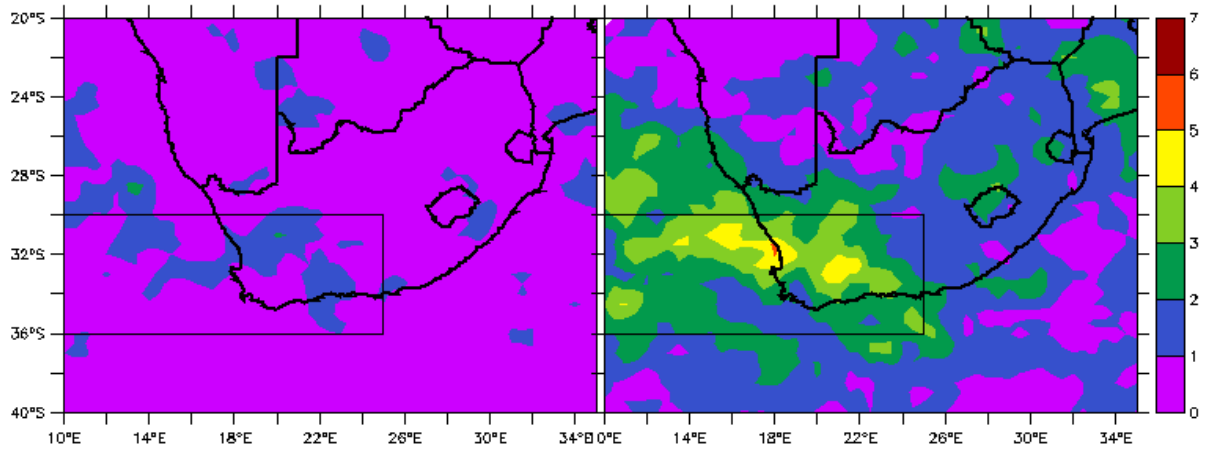

Figure A1: The COL numbers are shown for 300hPa (left panel) and 500hPa (right panel) with the black box indicating the area chosen for Western Cape COLs (area 1).

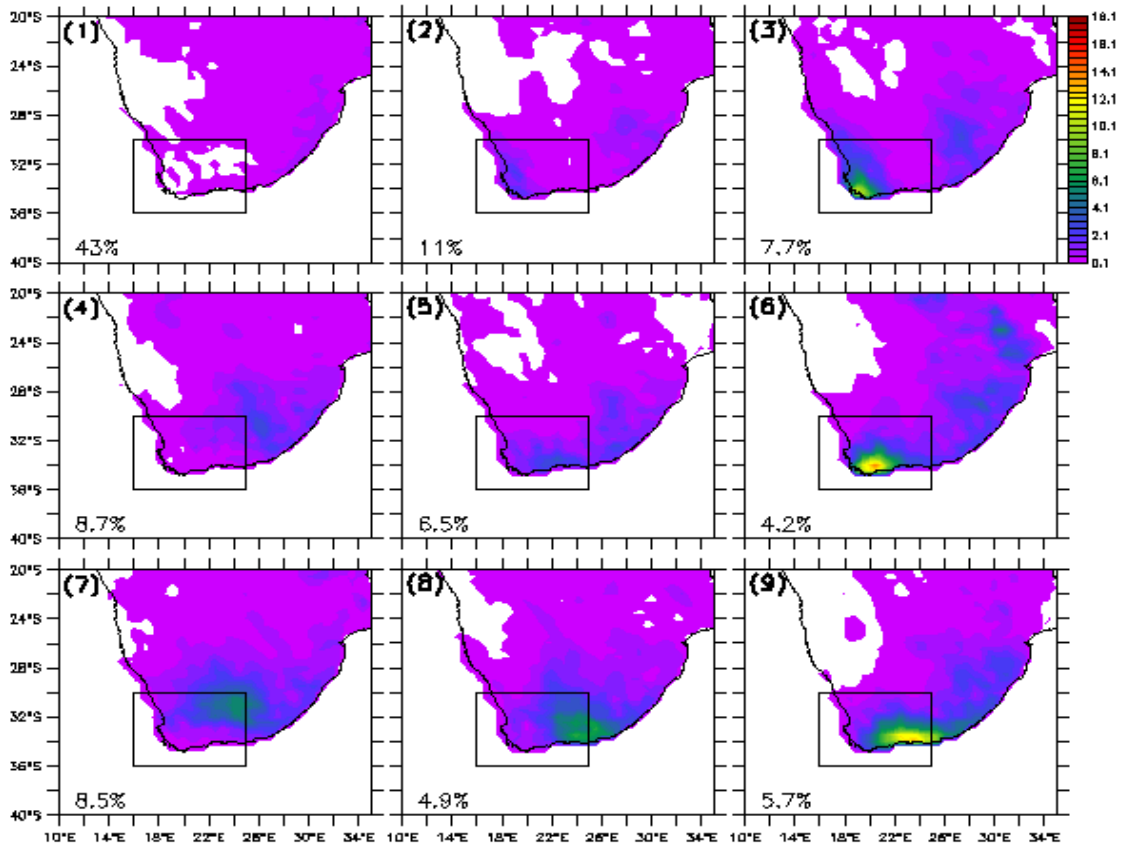

Figure A2: The SOMs analysis with the area chosen in Fig. A1.

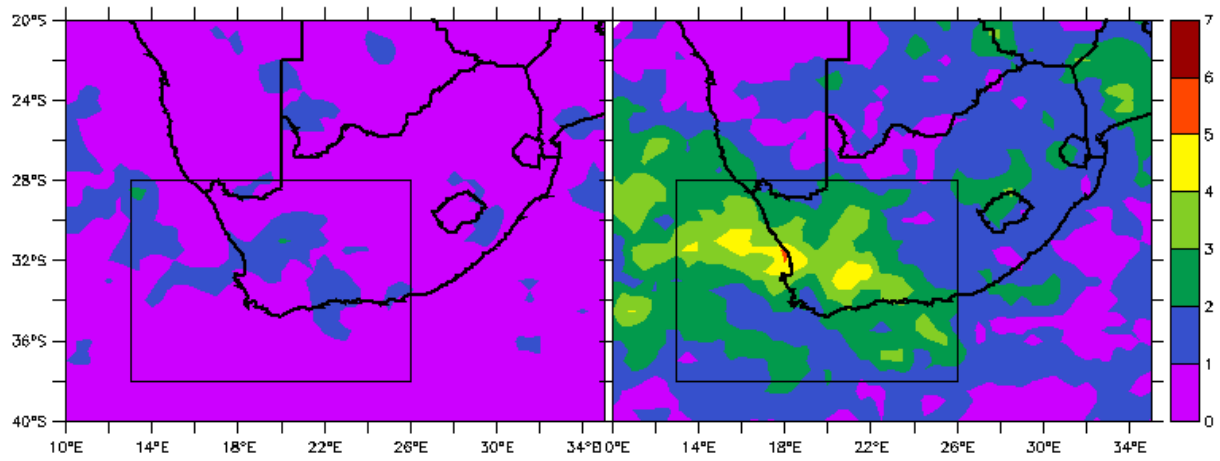

Figure A3: The same as Fig. A1 but for area 2 (the area we decided to choose for the rest of the studies analysis).

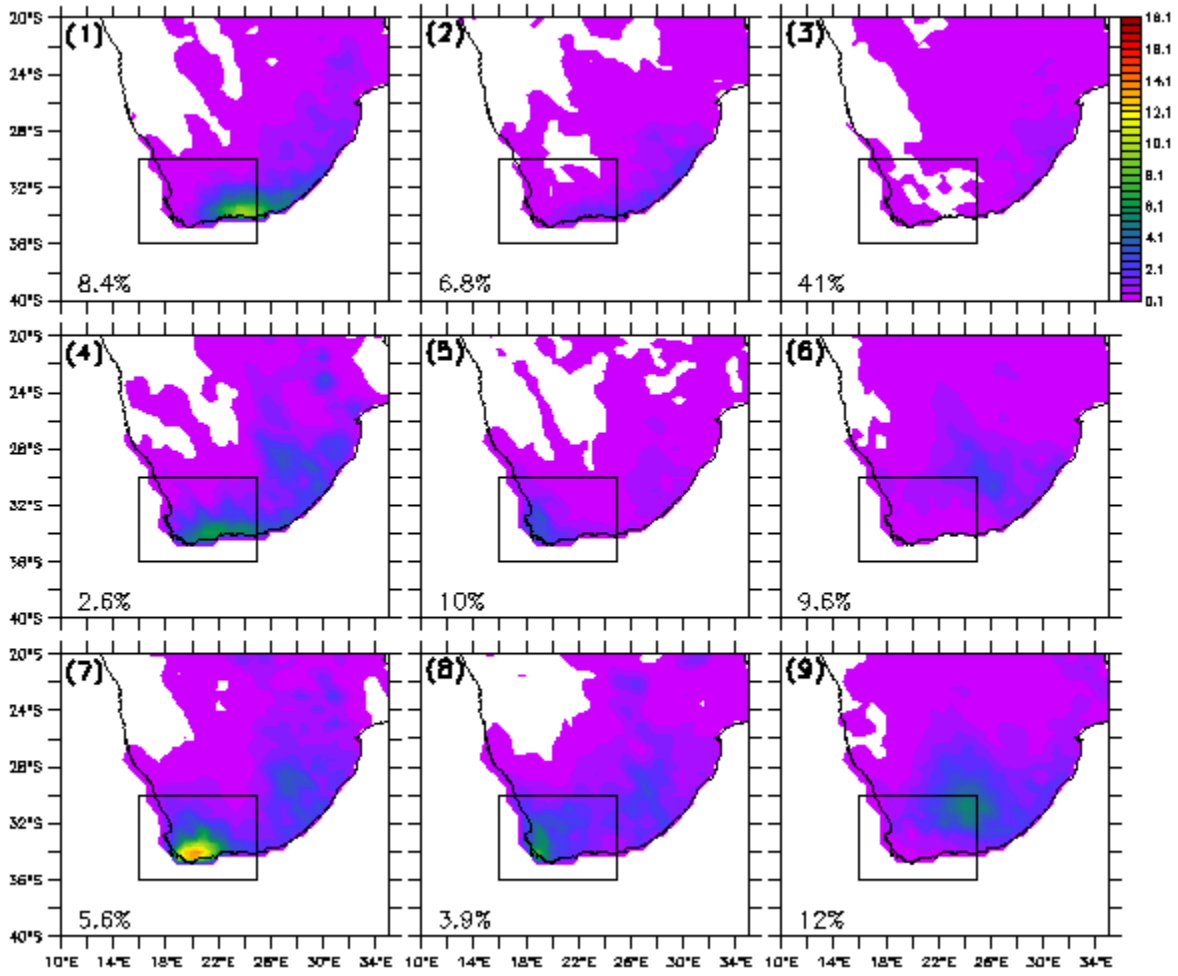

Figure A4: The same as Fig. A2 but for area 2

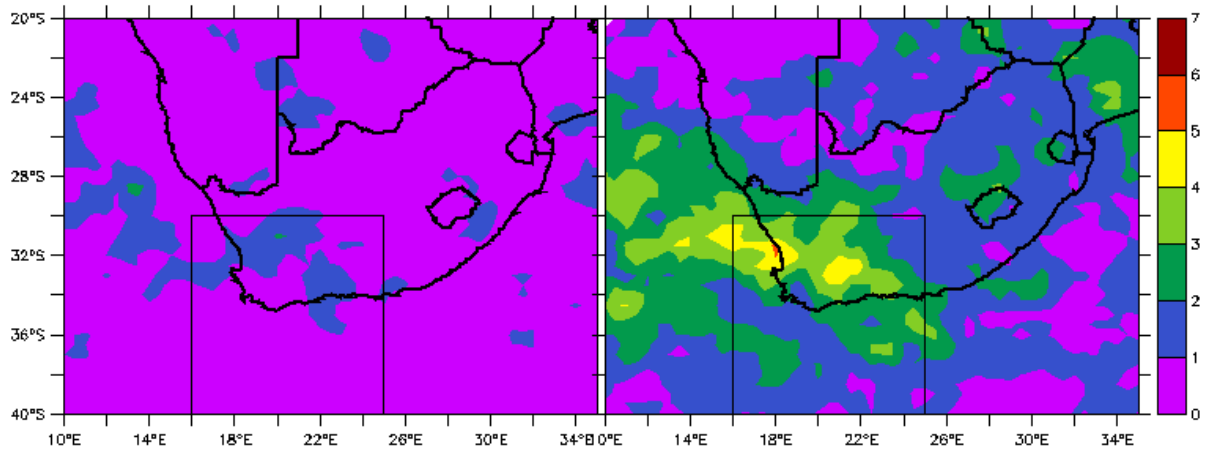

Figure A5: The same as Fig. A1 but for area 3

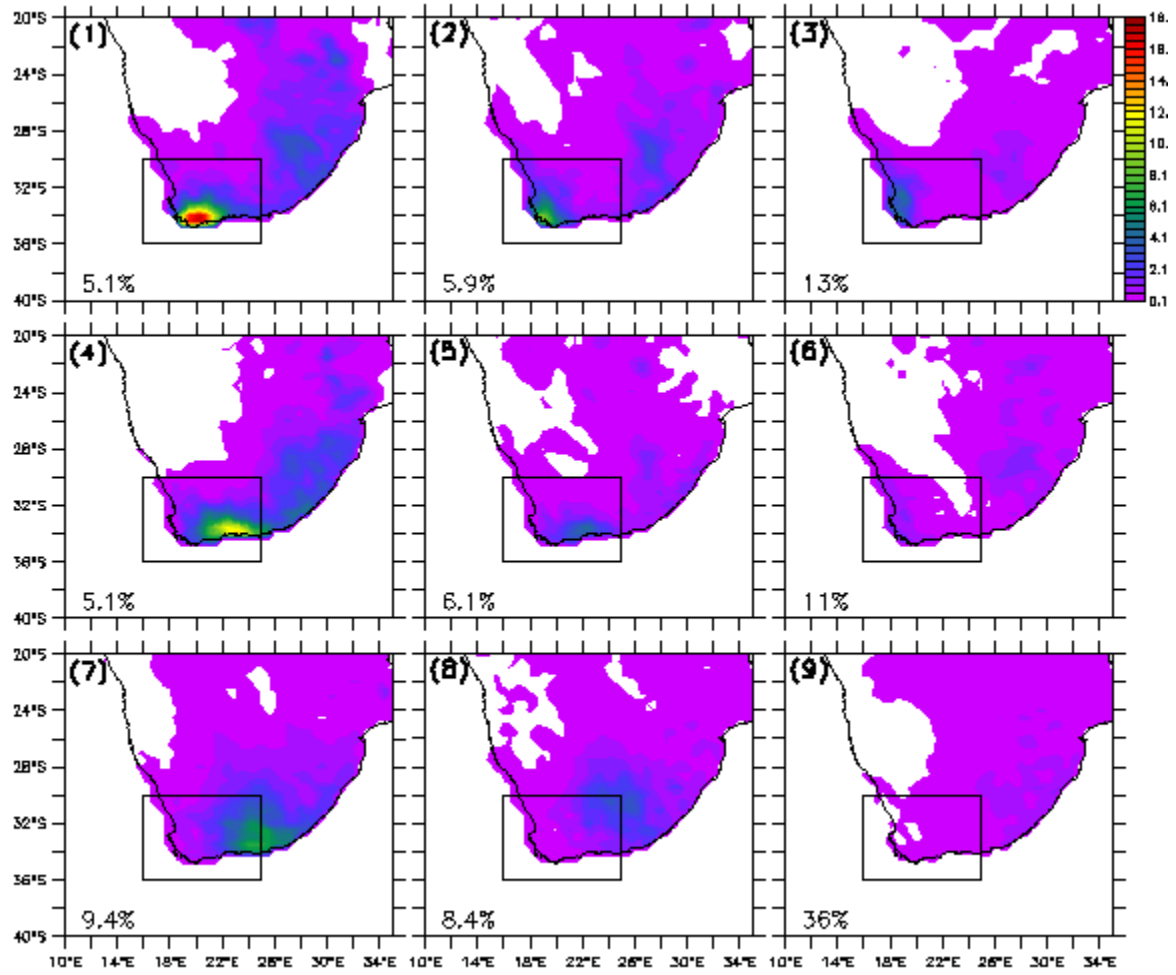

Figure A6: The same as Fig. A2 but for area 3

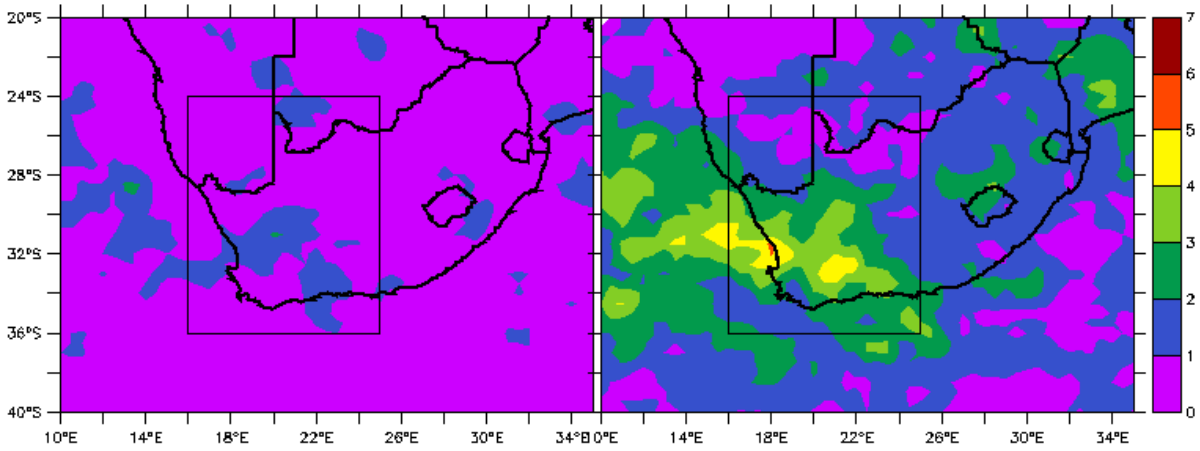

Figure A7: The same as Fig. A1 but for area 4

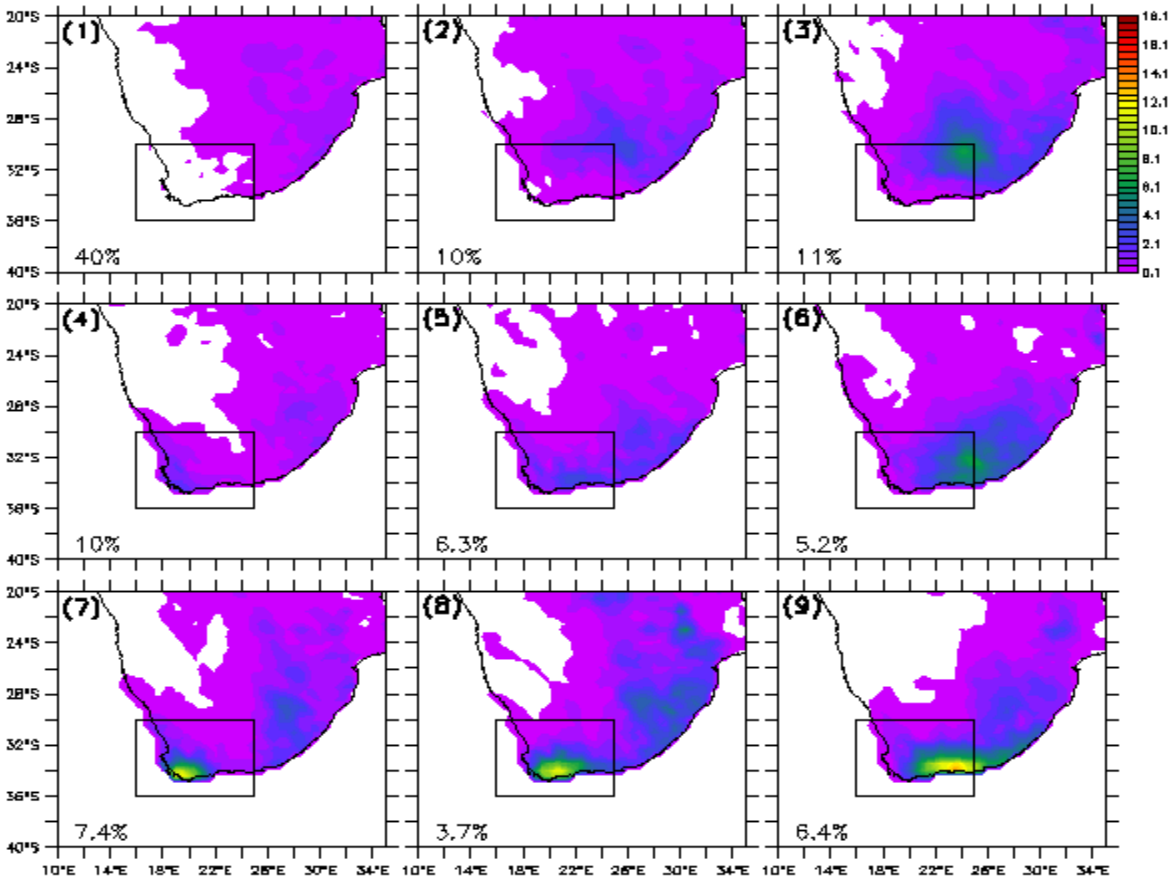

Figure A8: The same as Fig. A2 but for area 4

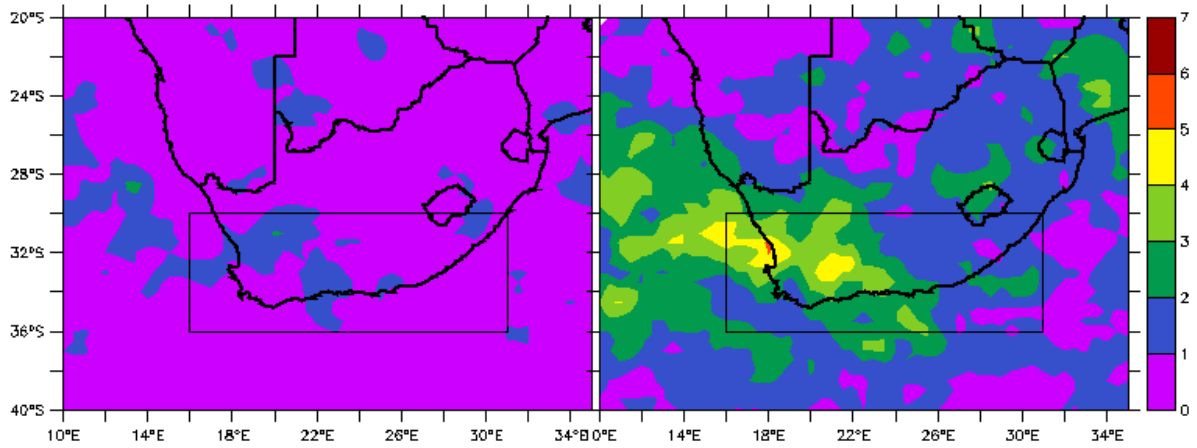

Figure A9: The same as Fig. A1 but for area 5

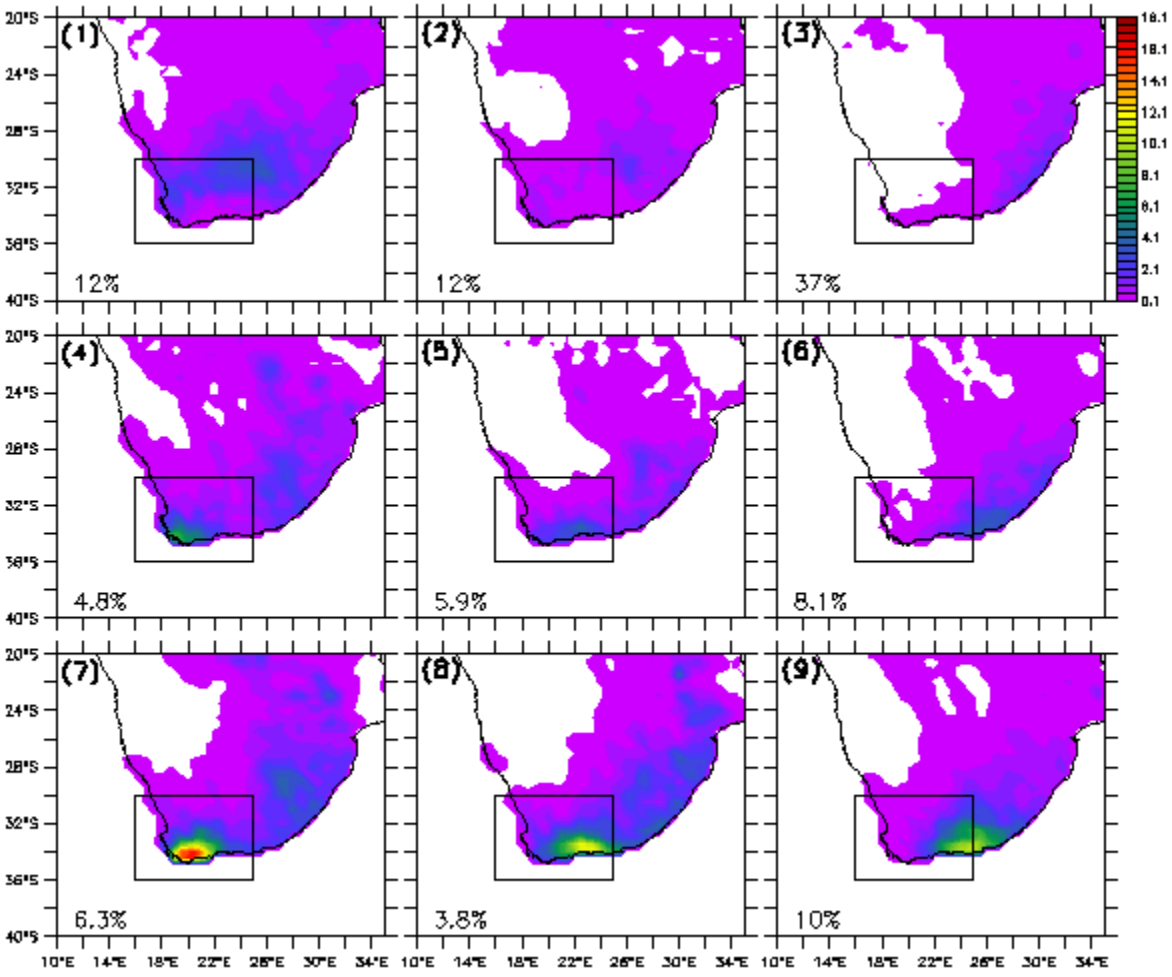

Figure A10: The same as Fig. A2 but for area 5

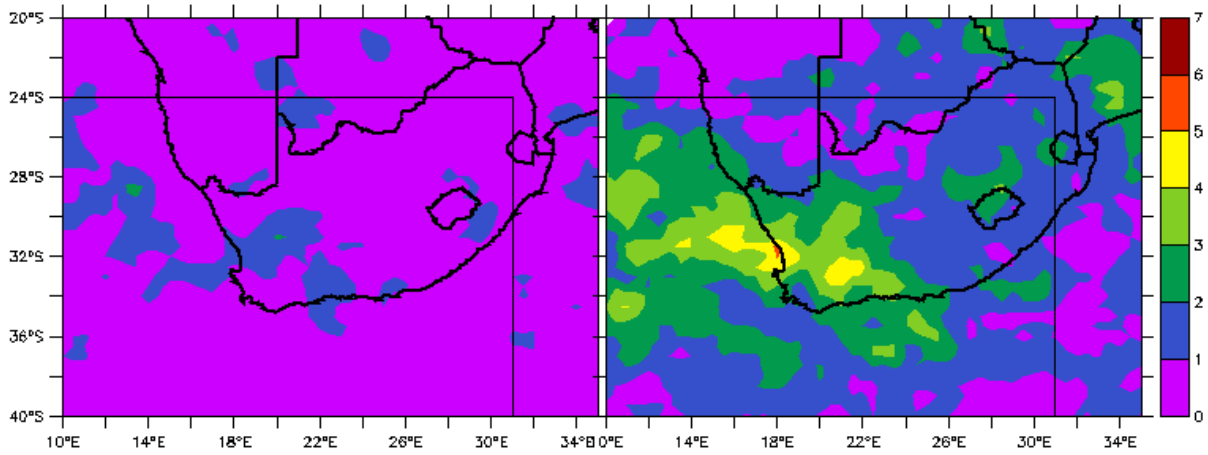

Figure A11: The same as Fig. A1 but for area 6

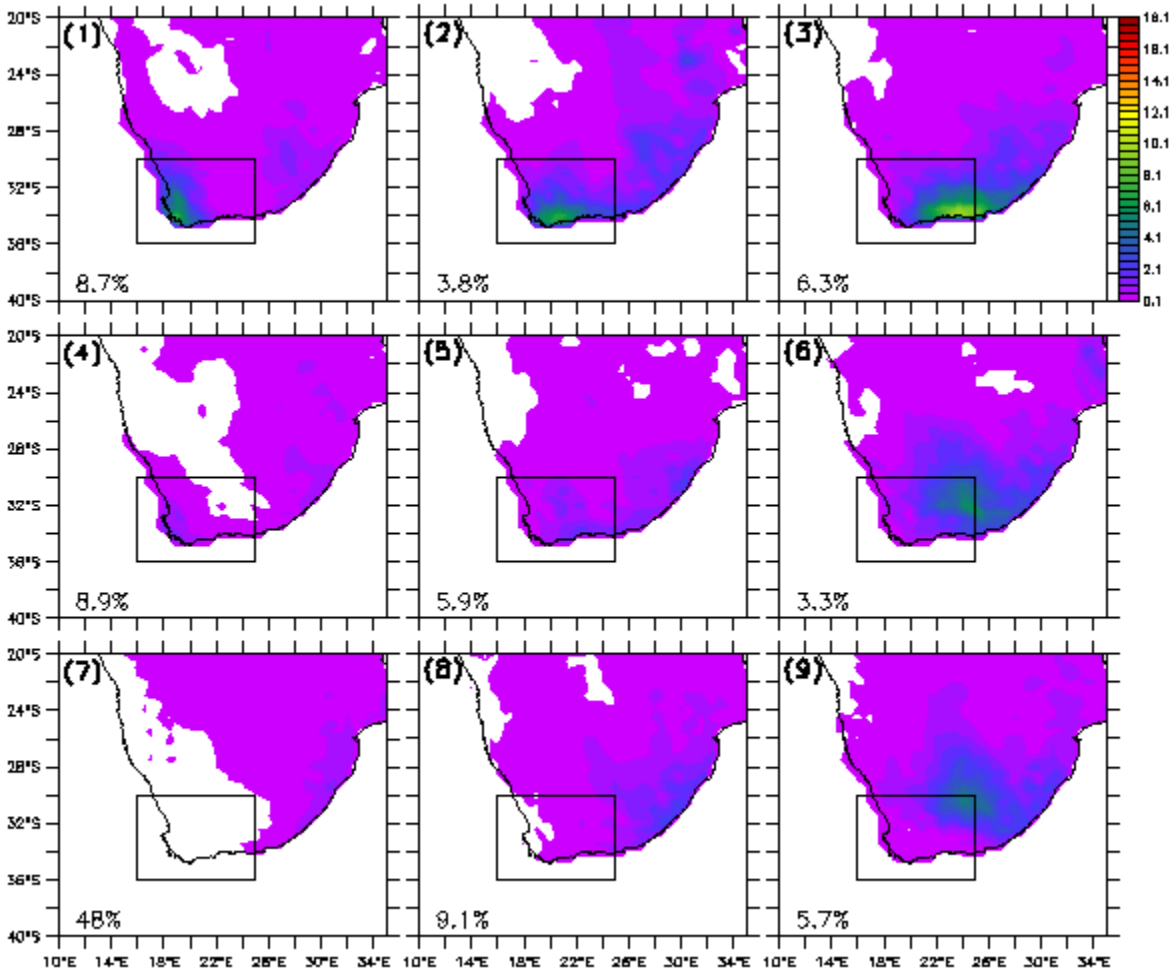

Figure A12: The same as Fig. A2 but for area 6

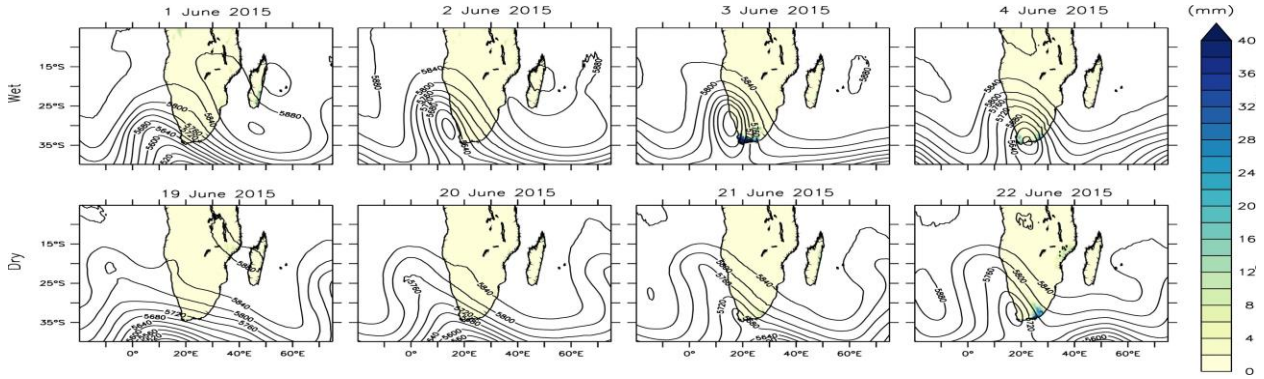

Figure A13: Evolution of COL over southern Africa during a wet COL case (upper panels) and a dry COL case (i.e. panels). The contours show the 500hPa geopotential height while shading indicates the associate precipitation.

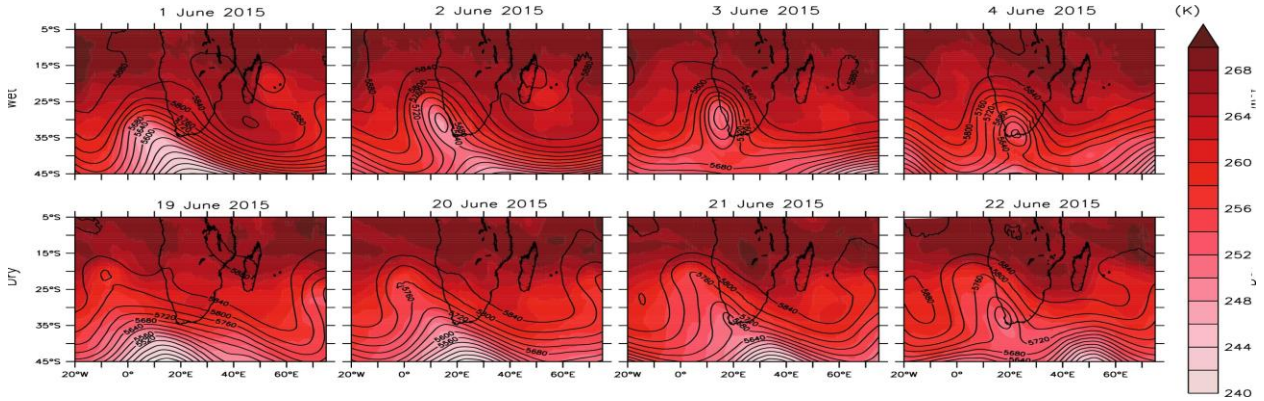

Figure A14: Same as Fig A13 but with shaded values showing temperature at 500hPa (K).